Hierarchically Structured Porous Materials for Energy Conversion and Storage

Yu Li, Zheng-Yi Fu, and Bao-Lian Su**

Materials with hierarchical porosity and structures have been heavily involved in newly developed energy storage and conversion systems. Because of meticulous design and ingenious hierarchical structuration of porosities through the mimicking of natural systems, hierarchically structured porous materials can provide large surface areas for reaction, interfacial transport, or dispersion of active sites at different length scales of pores and shorten diffusion paths or reduce diffusion effect. By the incorporation of macroporosity in materials, light harvesting can be enhanced, showing the importance of macrochannels in light related systems such as photocatalysis and photovoltaics. A state-of-the-art review of the applications of hierarchically structured porous materials in energy conversion and storage is presented. Their involvement in energy conversion such as in photosynthesis, photocatalytic H_2 production, photocatalysis, or in dye sensitized solar cells (DSSCs) and fuel cells (FCs) is discussed. Energy storage technologies such as Li-ions batteries, supercapacitors, hydrogen storage, and solar thermal storage developed based on hierarchically porous materials are then discussed. The links between the hierarchically porous structures and their performances in energy conversion and storage presented can promote the design of the novel structures with advanced properties.

1. Introduction

Natural materials developed the admirable and intriguing hierarchical structures using a basis of comparatively simple components such as polymers and brittle minerals with large variety of functions. They can act as mechanical support, providing protection and mobility to organisms, generate color (photonic structures), and help sense the environment. This hierarchy is one of main characteristics found in natural materials. More than being optimized and designed for durability, natural materials with hierarchical organization have the capability to adapt, to reshape their structure facing their environment, and even to self-repair for their survival, reproduction, and growth. Relationships between hierarchically organized living organisms and the environment are vectored by energy and material flows. All biological organisms and natural systems are maintained by the flow of energy through the systems. Therefore, natural materials developed in close relation with functions of energy conversion, capture, transport, and storage. The hierarchical structures in natural materials play a vital role in creating different functionalities and in energy related processes in nature. For example, the hierarchical structures of green leaves and certain photosynthetic plants are optimized for efficient light harvesting and sunlight conversion to chemical energy by photosynthesis[1] and certain photosynthetic micro-organisms containing the periodic hierarchical structures such as diatoms endow them with particular optical properties.[2] It is quite intriguing that the hierarchical micro-nanostructures present at the surface of different desert plants develop the capability to reflect a large zone of visible and UV light to protect against dryness whereas superhydrophobic surfaces can be used for energy conservation, which can reduce energy dissipation.[3]

As one step in learning from nature and toward largely man-made technologically hierarchical materials, which can not only mimic the functions of natural materials with a defined hierarchical structures, but also have new and superior properties, different natural structures have been used as biotemplates for the design of materials for the functions of energy conversion, capture, and storage. For example, plant leaves have been used as biotemplates to mimic part of photosynthetic process and the materials obtained contained well defined hierarchical structures including very fine replicas of chloroplaste structures, which showed enhanced light harvesting and photocatalytic H_2 evolution activity.[4–9] Butterfly wings also present a significant hierarchical structure with very interesting optical and photonic properties and have equally

Prof. Y. Li, Prof. B.-L. Su
Laboratory of Living Materials at the State Key Laboratory of Advanced Technology for Materials Synthesis and Processing
Wuhan University of Technology
122 Luoshi Road, 430070 Wuhan, Hubei, China
E-mail: yu.li@whut.edu.cn; baoliansu@whut.edu.cn
Prof. Z.-Y. Fu
State Key Laboratory of Advanced Technology for Materials Synthesis and Processing
Wuhan University of Technology
122 Luoshi Road, 430070 Wuhan, Hubei, China
Prof. B.-L. Su
Laboratory of Inorganic Materials Chemistry (CMI)
University of Namur (FUNDP)
61 rue de Bruxelles, B-5000 Namur, Belgium
E-mail: bao-lian.su@fundp.ac.be
Prof. B.-L. Su
Department of Chemistry
University of Cambridge
Lensfield Road, UK
E-mail: bls26@cam.ac.uk

DOI: 10.1002/adfm.201200591

been used to generate the replicas. Materials obtained showed very promising properties such as photoanodes for solar cells (SCs)[10–12] and dye sensitized solar cells (DSSCs).[13] Again inspired from the hierarchical structures of plant leaves, thylakoids, chloroplates, whole cells extracted from plant leaves, and other photosynthetic cells have been encapsulated into hierarchically porous SiO_2 hydrogels to form leaf-like materials to mimic the photosynthetic function of plant leaves.[14–30] The results are quite promising for sunlight conversion to chemical energy and the mitigation of CO_2 for environmental purposes. Diatoms with their beautiful hierarchical porous system have been used as a biosupport to coat a nanostructured TiO_2 layer to generate new hierarchically porous materials that could help triple the electrical output of experimental DSSCs.[31–34] The hierarchically porous carbon electrodes prepared using hierarchical wood structures and diatomaceous earth can improve the rate capabilities for lithiation and delithiation.[35–42] All these biotemplated hierarchically structured porous materials can serve as good models for the design of advanced man-made energy materials.

Materials with hierarchical porosity and structures have been heavily involved in newly developed energy storage and conversion systems. Owing to meticulous design and ingenious hierarchical structuration of porosities through the mimicking natural systems, hierarchically structured porous materials can provide large surface areas for reaction, interfacial transport, or dispersion of active sites at different length scales of pores and shorten diffusion paths or reduce the diffusion effect. By the fine hierarchization of the nanostructure and chemical composition at different scales, reactivity and light harvesting can be enhanced[43–45] since it has been found that in the macro- and mesoporous TiO_2 materials, the macrochannels acted as a light-transfer path for introducing incident photon flux onto the inner surface of mesoporous TiO_2. This allowed light waves to penetrate deep inside the photocatalyst, making it a more efficient light harvester.[43] Hierarchically porous structures can also act as host materials to stabilize or to incorporate other active components, or in the case of porous carbons, they can provide electrically conductive phases as well as intercalations sites. There are many examples of the use of hierarchically structured porous materials to provide more efficient energy conversion and storage. Hierarchically porous materials are already producing some very specific solutions in the field of rechargeable batteries. Electrolyte conductivity can be increased several times. Furthermore, novel hierarchical porous carbon nanofoams with high surface area as catalytic electrodes for fuel cell applications show good electrical conductivity, excellent chemical, mechanical, and thermal stabilities. The application of hierarchically structured porous materials in photovoltaic cells presented significant advantages to increase the efficiency/cost ratio by enhancing the effective optical path and significantly decreasing the probability of charge recombination. Hierarchization of materials in porosities and structures can provide us with superior materials that will unlock the tremendous potential of many energy technologies currently at the discovery phase. The importance of multifunctional 3D nanoarchitectures for energy storage and conversion has been recently reviewed by Rolison et al.[46] They indicated that the appropriate electronic, ionic, and electrochemical requirements

Yu Li received his B.S. from Xi'an Jiaotong University in 1999 and received his M.S. from Liaoning Shihua University in 2002. He obtained his Ph.D. from Zhejiang University in 2005. He worked in EMAT at the University of Antwerp with Prof. G. Van Tendeloo in 2005 and then in CMI at the University of Namur with Prof. Bao-Lian Su in 2006. Currently, he is a "Chutian" professor at Wuhan University of Technology. His research interests include nanomaterials design and synthesis, hierarchically porous materials synthesis, and their applications in the fundamental aspects of energy and environment.

Dr. Zhengyi Fu received his B.S. and M.S. from South China University of Technology in 1980 and 1987, and his Ph.D. from Wuhan University of Technology. He worked at the University of California, Davis, with Prof. Munir in 1990 and 1991. He is a chief professor at Wuhan University of Technology and Cheung Kong Scholar of Ministry of Education of China. His research interests are nanoceramics, multifunctional ceramics, bioinspired synthesis, and processing.

Bao-Lian Su is currently a Full Professor of Chemistry, Director of the Research Centre for Nanomaterials Chemistry and the Laboratory of Inorganic Materials Chemistry, Namur, Belgium. His is an "Expert of the State" in the framework of the Chinese Central Government program of "Thousands Talents" and "Changjiang Professor" at Wuhan University of Technology, China. His current research fields include the synthesis, property studies, and the molecular engineering of organized hierarchically porous and bioinspired materials, biomaterials, living materials, leaf-like materials, and nanostructures in addition to the immobilization of living organisms for artificial photosynthesis, nanotechnology, biotechnology, information technology, cell therapy, and biomedical applications.

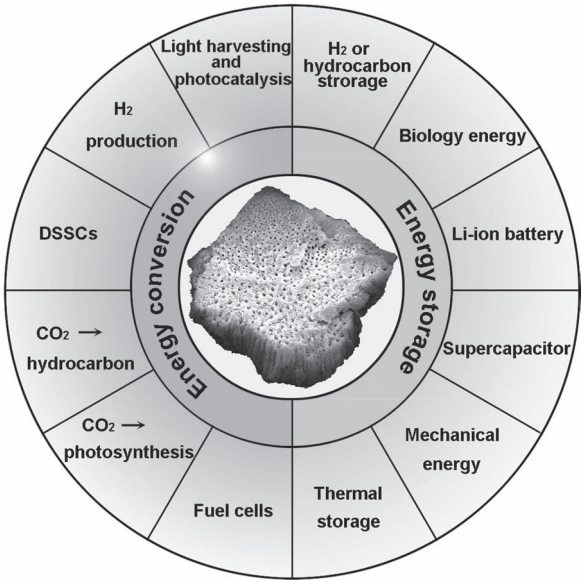

Scheme 1. Illustration of the potential application on energy convertion and storage of the hierarchically porous materials.

for devices that produce or store energy may be assembled within low density and ultraporous 3D nanoarchictectures on the bench-top that meld a high surface area for heterogeneous reactions with a continuous and hierarchical porous network for rapid molecular flux.

Here, the applications of hierarchically structured porous materials in energy conversion and storage (**Scheme 1**) are discussed. Their involvement in energy conversion, such as in photosynthesis, photocatalytic H_2 production, photocatalysis, or in dye sensitized solar cells (DSSCs) and fuel cells (FCs), is reviewed. Energy storage technologies such as Li-ions batteries, supercapacitors, hydrogen storage, and solar thermal storage developed based on hierarchically porous materials are then commented on.

2. Hierarchically Structured Porous Materials for Energy Conversion

Energy conversion concerns the transformation of energy from one form to another, for example, sun light to chemicals or electricity, electricity to thermal and mechanical energy, chemicals to thermal energy and electricity. Today the sense of energy conversion deals with the conversion of one form of energy to that we can use directly. Energy conversion is a very hot topic and essential for the development of humanity. In this section, we focus on sunlight conversion to chemicals and electricity and chemicals to electricity. First different conversion technologies using sun light as energy sources and hierarchically structured porous materials such as photocatalysis, photochemical H_2 production, dye-sensotized solar cells, photosynthesis, and CO_2 photochemical conversion are described. Then, hierarchically structured porous materials used in for Fuel cells (FCs) design are presented.

2.1. Sunlight Conversion to Chemicals and Electricity

The sun bathes the earth in more energy in an hour than humantiy uses in a year. If scientists could convert even a fraction of that surplus into a directly utilizable energy, our addiction to fossil fuels for daily life and the problems they cause can end. Chemical or other forms of energy would be the game changer if they could be made directly in an efficient and cost-free way from sunlight. Tremendous efforts have been devoted to the development of materials and devices for the conversion of sunlight to chemicals through photosynthesis and photocatalysis and of electricity through solar cells.

2.1.1. Hierarchically Structured Porous Materials for Light Harvesting and Photocatalysis Enhancement

Leaves constitute a hierarchical structure (**Figure 1**)[47] that strongly favors efficient light harvesting because of a series of evolutionarily optimized processes: 1) light focused by lens-like epidermal cells, 2) light multiple scattering and absorption within the venous porous architecture, 3) light propagation in the columnar cells in the palisade parenchyma acting as light guides, 4) effective light path length enhancement and light scattering by the less regularly arranged spongy mesophyll cells, and 5) efficient light-harvesting and fast charge separation in the high surface area 3D constructions of interconnected nanolayered thylakoid cylindrical stacks in the chloroplast.[4,5]

To better understand and use all these efficient natural processes to develop man-made materials, "artificial leaves", that can replicate similar processes, natural leaves have been used by Zhang and co-workers as biotemplates to replicate all the fine hierarchical structures of leaves using a pure inorganic structure of TiO_2 with same hierarchy as leaves by a two step procedure (**Figure 2**). It consists of the infiltration of inorganic precursors and then the calcination of the biotemplates. All the photosynthetic pigments were replaced by man-made catalysts such as Pt nanoparticles. The obtained leaf replica with catalyst components was used for efficient light-harvesting and photochemical hydrogen production.[4] Compared with TiO_2 nanoparticles prepared without biotemplates, the average absorbance intensities

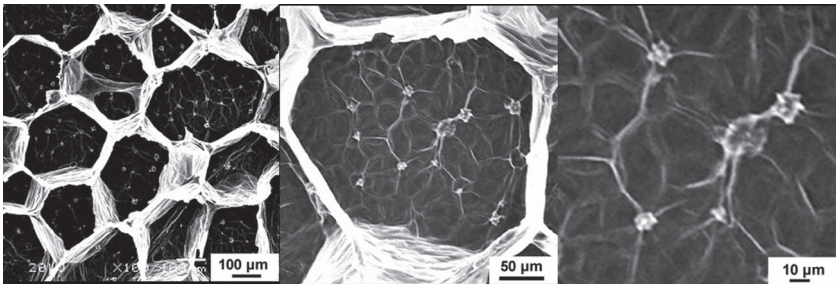

Figure 1. Scanning electron microscopy (SEM) image showing the hierarchical structure of a lotus leaf. Reproduced with permission.[47] Copyright 2008, American Institute Physics.

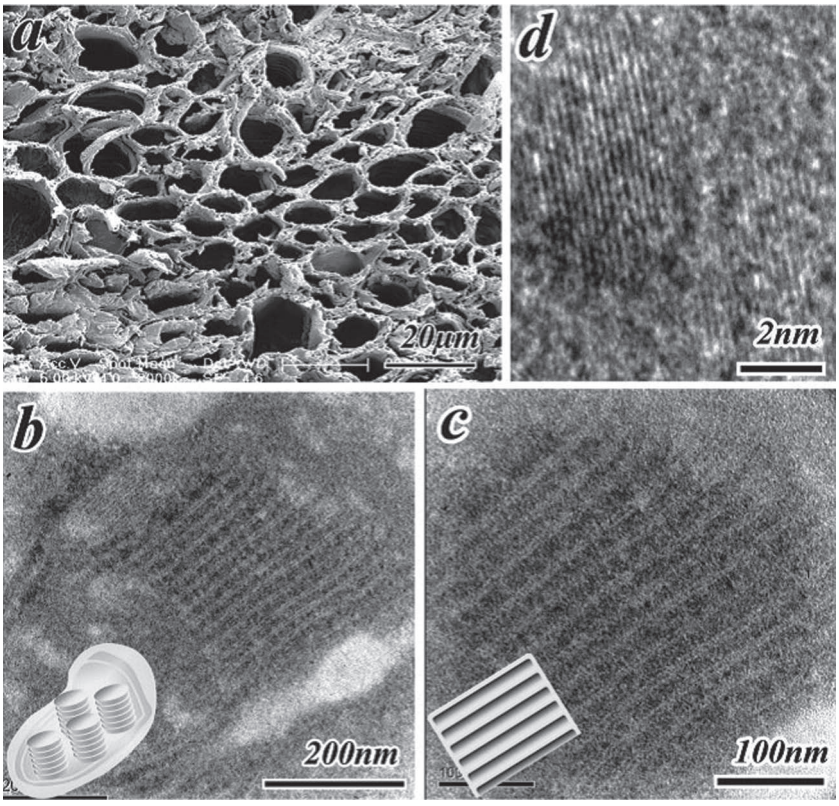

Figure 2. a) Field-emission SEM (FESEM) image of a cross-section of AIL-TiO_2 derived from *A. vitifolia Buch.* leaf. b) Transmission electron microscopy (TEM) image of a layered nanostructure in AIL1-TiO_2, with a corresponding illustration of the 3D structures. c) Magnified TEM image of layered nanostructures in AIL1-TiO_2; the inset is the corresponding illustration. d) High-resolution TEM (HRTEM) image of Pt nanoparticles deposited on TiO_2. Reproduced with permission.[4]

within visible range increased 200–234% for artificial leaves. This should certainly contribute to hierarchical architectures with all the fine structures of leaves imprinted in artificial leaves. The photocatalytic activity is much higher than that of TiO_2 nanoparticles prepared without biotemplates and commercial nanoparticulate P25.[4] This is discussed detail in the following section.

As TiO_2 has been expected to be the one of the most important potential photocatalysts given present energy and environmental concerns,[48,49] considerable effort has been devoted to improve the photocatalytic activity of TiO_2 nanostructures. TiO_2 photocatalysts with hierarchical structures (**Figure 3**) have been successfully replicated by Zhang and coworkers from a hierarchically structured biotemplate using a sonochemical method.[50] The biotemplates, cedarwoods(cedar leaves), were first irradiated under ultrasonic waves in $TiCl_4$ solutions and then calcined at temperatures between 450 and 600 °C. The fine replications of the hierarchically meso-macroporous structures of the biotemplates in TiO_2 down to the nanometer level were confirmed. The photocatalytic activities were assessed by measuring the percentage degradation of methylene blue using UV-vis spectroscopy. The replica obtained by calcination at 450 °C gives the best structural replication and the highest surface area of 55 m^2 g^{-1} and thus has the best photocatalytic properties. This method provides a simple, efficient, and versatile technique for fabricating TiO_2 with cedarwood (cedar leaf)-like hierarchical structures, and it has the potential to be applied to other systems for producing functional hierarchical materials for chemical sensors and nanodevices.

A hierarchically meso-microporous titania film has been synthesized by Zhu's group, showing increased catalytic activities of 30–40% and 60–70% for mineralizing gaseous acetaldehyde and liquid phase phenol, respectively.[51] This improvement is a result of the enhanced diffusion of the reactants within the photocatalyst, due to the hierarchical porous channels in the material.

The important role of meso-macroporous structures in light harvesting photocatalysis has been revealed by different research groups.[43–45,52–60] The preparation conditions, such as the synthesis time and calcination temperature significantly influence the photocatalytic activity of the meso-macroporous TiO_2. For instance, Yu and co-workers prepared bimodal meso-macroporous TiO_2 by a self-formation phenomenon process in the presence of surfactants (**Figure 4**).[43a] Ethylene photodegradation in gas-phase medium was employed as a probe reaction to evaluate the photocatalytic reactivity of the catalysts. The catalyst, which calcined at 350 °C, possessed an intact macro/mesoporous structure and showed photocatalytic reactivity about 60% higher than that of commercial P25. When the sample was calcined at 500 °C, the macroporous structure was retained but the mesoporous structure was partly destroyed. Further heating at temperatures above 600 °C destroyed both macro- and mesoporous structures, accompanied by a loss in photocatalytic activity. The existence of light-harvesting macrochannels that increase photoabsorption efficiency and allowed efficient diffusion of

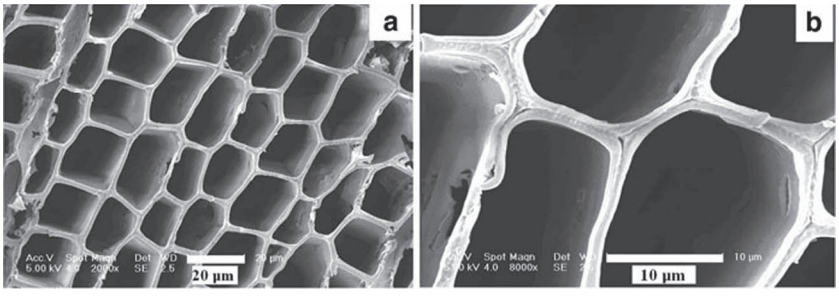

Figure 3. FESEM images at low (a) and high (b) magnification of replica TiO_2 obtained after applying ultrasonic waves process to cedar wood calcined at a,b) 450 °C in the radical direction. Reproduced with permission.[50] Copyright 2010, Springer.

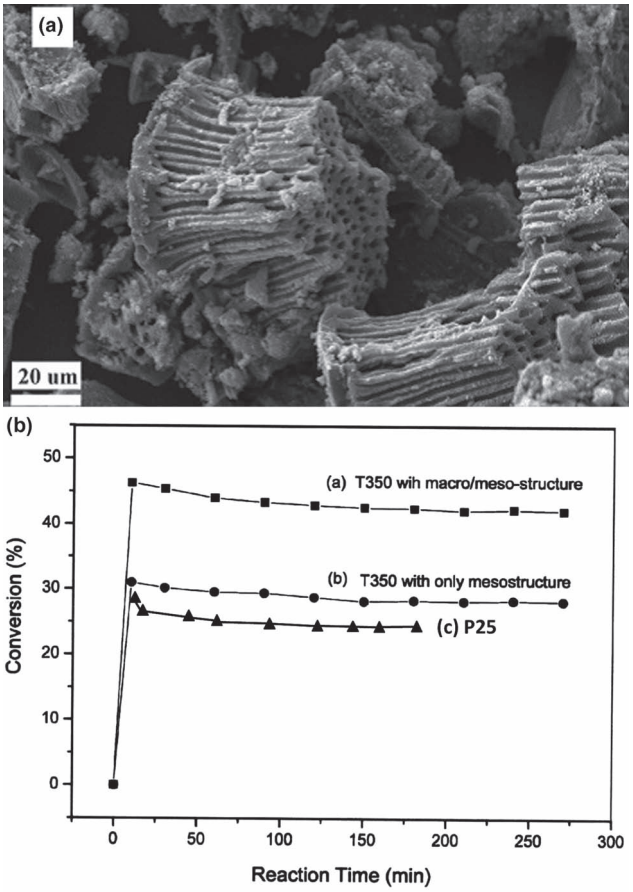

Figure 4. a) SEM images of the titanium dioxide monolithic particles calcined at 350 °C and b) its phototcatalytic activity (a) in comparison with that of T350 with only mesostructure (b) and P25 catalyst (c). Adapted with permission.[43a] Copyright 2005, American Chemical Society.

gaseous molecules was found to be the origin of the high photocatalytic performance of the intact macro-mesoporous TiO_2. In fact, in the macro-mesoporous TiO_2 photocatalyst, the macrochannels acted as a light-transfer path for introducing incident photon flux onto the inner surface of mesoporous TiO_2.[43b] This allowed light waves to penetrate deep inside the photocatalyst, making it a more efficient light harvester. It is known that a wavelength of 320 nm is reduced to 10% of its original intensity after penetrating a distance of only 8.5 μm on condensed TiO_2. The presence of macrochannels, however, makes it possible to illuminate even the core TiO_2 particles with the emission from the four surrounding UV sources. Considering the light absorption, reflection, and scattering within such a hierarchical porous system, the effective light-activated surface area can be significantly enhanced. Moreover, the interconnected TiO_2 nanoparticle arrays embedded in the mesoporous wall may allow highly efficient photogenerated electron transport through the macrochannel network. Another study by Yu and co-workers showed the same effect of the importance of the presence of macrochannels in hierarchical porous structures.[52] They found that the hierarchical macro-mesoporous TiO_2 calcinated under 300 °C exhibited a maximum photocatalytic activity for the oxidation of acetone in the gas phase (around twice that of Degussa P25). The activity then decreased as the calcination temperature increased, due to destruction of the macroporous structure and the decrease in surface area.

The beneficial effect and the importance of the hierarchical porosity in TiO_2 photocatalysts to improve the light harvesting were also confirmed by Ayral and co-workers, who studied TiO_2 anatase based layers with three levels of porosity: macropores, mesopores, and micropores.[45] The further confirmation of the role of macrochannels was provided by Su et al. In their study, different porous, nonporous, and hierarchically meso-macroporous structures were compared. The enhancement of the photocatalytic activity can be attributed to both the action of macrochannels as light harvester and the easy diffusion effect of organic molecules in hierarchically porous structures.[43b] A very recent study done by the same group supplied a new proof.[53] The action of macrochannels as light transport path for introducing photon flux onto the inner surface of mesoporous TiO_2 could be quite useful in the design of DSSCs and other photoelectrochemical devices. The application of hierarchically porous TiO_2 in DSSCs could provide important improvements in light harvesting, thus in the efficiency of DSSCs. Further study in this direction should be reinforced. We will discuss the importance of macrochannels as light harvester in the section concerning DSSCs.

To further improve the photocatalysis of hierarchically porous TiO_2, several strategies based on chemical and physical concepts have been adopted. On the one hand, metal doping of porous TiO_2 structures has been thought to be a good way to enhance photocatalyic activity.[61,62] The presence of metal nanoparticles can act as an electron sink and significantly reduces the life time of mobility of photogenerated electrons.[63] The electrons are then transferred to highly oxidative species to form reactive oxygen radicals that can decompose chemicals.[64,65] As the separation of the photogenerated electrons and holes increased, the photocatalytic activity was considerably increased after introducing metal NPs and therefore the quantum yield was improved.[66–72] For instance, Zhang and co-workers synthesized Pt/N-TiO_2 hierarchical porous structures using normal leaves as biotemplate. The obtained materials exhibit significantly improved photocatalytic hydrogen evolution activity.[5] Ozin's group used Pt nanocluster modified TiO_2 inverse opal to enhance the photodegradation of acid orange. By incorporating Pt nanoclusters on the surface of the inverse opal, more light is absorbed and the lifetimes of the UV-generated electrons and holes are extended because of the synergy of slow photon optical amplification with chemical enhancement.[57] However, the induced cations can also act as recombination centers and therefore the activity improvements are only possible at low concentrations of dopants.[62,73,74]

On the other hand, other elements doping hierarchically porous TiO_2 have been believed to increase its visible light absorption.[75,76] Currently, the most promising way may be the partial substitution of oxygen with B, C, N, F, S, and codoping of the above elements.[75–79] The origin of this photoresponse at higher wavelengths is the mixing of the 2p nitrogen level with the oxygen 2p orbitals to form the valence band, which results in a lower bandgap resulting in visible light absorption.[80] For example, Xu and co-workers reported a simple new route to the

synthesis of N-F codoped hierarchical macro-mesoporous TiO_2 inverse opal films.[78] Most recently, Zhang and co-workers used biosystems-templated materials to fabricate N and/or P self-doping hierarchically porous TiO_2 structures.[5,81,82] For instance, the N doped morph-TiO_2 products derived from different leaves have displayed absorbance intensities increase of 103–258% within the visible light range because of the self-doping of N and thus a higher photocatalytic degradation activity than that of some standard photocatalysts, such as Degussa P25, under UV irradiation.[5] The synthesized biogenic-TiO_2 with kelp as the biotemplate exhibits superior photocatalytic degradation activity of methylene blue under UV-visible light irradiation.[81] Moreover, they used crop seeds as templates to synthesize N-P-codoped hierarchically porous TiO_2, demonstrating enhanced light-harvesting and photocatalytic properties. This impressive method not only allows the mineralization of crop seeds but also leads to N and P contained in original crop seeds being simultaneously self-doped into the TiO_2 lattice.[82] In addition to TiO_2, the self-doping method could also be applied to other metal oxides, such as ZnO, In_2O_3, CeO_2, etc. The enhanced photocatalytic activity is a result of the synergy between their structures and components.

Additionally, element doping, incorporating electron-accepting and electron-transporting material, such as carbon nanotubes and graphene, is also a very useful route for photocatalysis enhancement.[79,83,84] Graphene-doped hierarchically ordered meso-macroporous TiO_2 films have been produced through a confinement self-assembly method within the regular voids of a colloidal crystal with 3D periodicity by Jiang's group.[79] Significant enhancement of photocatalytic activity for degrading methyl blue has been achieved. The apparent rate constants for macro-mesoporous titania films with and without graphene are up to 0.071 and 0.045 min^{-1}, respectively, almost 17 and 11 times higher than that for pure mesoporous titania films (0.0041 min^{-1}). Incorporating interconnected macropores in mesoporous films improves the mass transport through the film, reduces the length of the mesopore channel, and increases the accessible surface area of the thin film, whereas the introduction of graphene effectively suppresses the charge recombination.

Furthermore, doping with another semiconductor is a widely used method to improve the photocatalytic activity of hierarchically porous titania. If the electron bandgaps of the materials couple well, charge carriers become physically separated upon generation and therefore the recombination rate greatly decreases.[85–87] For instance, hierarchical macro-mesoporous TiO_2/SiO_2 and TiO_2/ZrO_2 nanocomposites have been synthesized.[44] The resulting porous TiO_2-based nanocomposites not only feature enhanced textural properties and improved thermal stability, but also show an improvement in photocatalytic activity over pure TiO_2. The introduction of a secondary phase imparts the additional functions of improved surface acidity and extra binding sites onto the porous structures. The favorable meso-macroporous textural properties, along with the improved surface functions, contribute to the high photocatalytic activity of catalysts calcined at high temperatures. Again, the macrochannels acted as a light-transfer path for introducing incident photon flux onto the inner surface of mesoporous TiO_2. This allowed light waves to penetrate deep inside the photocatalyst, making it a more efficient light harvester having higher photocatalytic activity. The hierarchical porous TiO_2-SiO_2-$TeO_2/Al_2O_3/TiO_2$ composite exhibited enhanced photocatalytic performance in decomposing acetaldehyde gas under UV illumination because of the combination of a large surface area, high porosities, and transparency.[88] In particular, the composite with 120 nm pores calcined at 500 °C showed the highest photocatalytic activity, 6–10 times higher than commercial P25 under the experimental conditions.

Although more than half of the published research has focused on hierarchically porous TiO_2 based photocatalysts, preparations of other hierarchically porous pohotocatalysts, such as ZnO, WO_3, CeO_2, In_2O_3, In_2S_3, and alkaline earth titanate materials, have also received attention.[82,89–95] Lee and co-workers synthesized hierarchically porous Bi_2WO_6 microspheres via the ultrasonic spray pyrolysis method.[91] The bandgap energy of hierarchical Bi_2WO_6 microspheres is 2.92 eV. It was found that the synthesis temperature was an important parameter controlling the morphology of the Bi_2WO_6 microspheres. As compared with the bulk Bi_2WO_6 sample, the hierarchically porous Bi_2WO_6 microspheres demonstrated superior photocatalytic activities on the removal of NO under either visible light or simulated solar light irradiation. The highest NO removal rates were 110 and 27 ppb/min for the porous Bi_2WO_6 sample under solar light and visible light ($\lambda > 400$ nm) irradiation, respectively. Wei and co-workers fabricated a hierarchically macro-mesoporous polycrystalline ZnO-Al_2O_3 framework by using legume as a biotemplate. This polycrystalline ZnO-Al_2O_3 framework has been demonstrated as an effective and recyclable photocatalyst for the decomposition of dyes in water, owing to its rather high specific surface area and hierarchical distribution of pore size (including mesopores and macropores).[95]

The utilization of TiO_2 inverse opal structures with macropores and interparticulate mesopores has become an important focus of recent research in the field of photocatalysis. Su and co-workers synthesized hierarchically porous TiO_2 an inverse opal structure exhibiting a greatly enhanced photocatalytic activity.[53] Sordello and co-workers also revealed that the photocatalytic activity of the TiO_2 inverse opal mainly comes from the structure rather than composition.[59] Zhao and co-workers fabricated TiO_2 binary inverse opal via a sandwich-vacuum infiltration of titania precursor. The synthesized material displays higher photocatalytic activity on degradation of benzoic acid compared to TiO_2 nanoparticles.[60] Ozin et al. clearly demonstrated that the amplified photochemical reaction can occur using inverse TiO_2 opals. They indicated that this amplification has been attributed to the slow-photon effect. In fact, highly ordered inverse opals behave as photonic crystals and thus have a periodic dielectric contrast that is in the length scale of the wavelength of light, coherent Bragg diffraction forbids light with certain energies to propagate through the material in a particular crystallographic direction. This gives rise to stop-band reflection and the range of energies that is reflected back depends on the periodicity and dielectric contrast of the photonic crystal. At the frequency edges of these stop bands, photons propagate with strongly reduced group velocity, hence, they are called slow photons. Slow photons can be observed in periodic photonic structures at energies just above and below the photonic stop band. If the energy of the slow photons overlaps with

the absorbance of the material, then an enhancement of the absorption can be expected as a result of the increased effective optical path length.[55–57] The work of Ozin et al. revealed that photocatalytic activity can be dramatically enhanced by utilizing slow photons with energies close to the electronic bandgap of the semiconductor.[55–57] The study using the slow-photon effect on the basis of photonic crystals to improve the photocatalytic activity by enhancing the light absorption could be an important future research direction. The slow-photon effect can be applied to all the fields related to light absorption for example solar cells. This beneficial effect will further be discussed in following section for DSSCs performance improvement.

2.1.2. Hierarchically Structured Porous Materials for Photochemical H_2 Production

Hydrogen has been considered the cleanest energy source because there is no pollutant emission. Dissociation of water to produce hydrogen has gathered more attention because of the energy crisis. However, applying this simple process is very difficult because of a considerable energy barrier seen in the equation below:

$$H_2O(l) \rightarrow H_2(g) + 1/2O_2(g) \quad \Delta G = +237 \text{ kJ mol}^{-1} \tag{1}$$

In 1972, Fujishima and Honda carried out a classic work on photoelectrochemical decomposition of water over TiO_2 electrodes.[96] The use of a photocatalyst reduces this activation energy and makes the process feasible with photons within the solar spectrum. The sunlight photons with wavelengths below 1100 nm can be used for photocatalytic water splitting and more than 800 W m^{-2} of the available solar energy could be potentially converted to H_2 energy.[97] As just a small percentage of the sunlight that reaches the earth's surface is capable of fulfilling the current energy needs of mankind, one of the important tasks for materials science and chemistry scientists is to find suitable materials and to design their structures to use sunlight for photoelectrochemical decomposition of water for H_2 production.[97–99]

As stated in above, hierarchically porous structures in nature such as leaves have shown their efficiency in light harvesting and mass transportation due to special structural properties. Again to design materials with improved photocatalytic water splitting performance, natural materials have been used as inspiration and as biotemplates. Zhang and co-workers demonstrated the use of artificial inorganic leaves composed of Pt/N-doped TiO_2 for efficient water splitting under UV-vis irradiation in the presence of sacrificial reagents by using leaves as natural biotemplates. The light harvesting performance and photocatalytic activity of such systems is higher than those prepared with the usual approaches.[4,5] The photocatalytic hydrogen production activity is 3.3 times higher than P25 and about eight times higher than that of TiO_2 nanoparticles prepared without biotemplates.[4]

Giordano and co-workers recently reported a one-step synthesis of hierarchical microstructures of magnetic iron carbide from leaf skeleton, which acts as both a template and a carbon source for formation of the iron or iron carbide material by carbothermal reduction of iron (II) precursor. The obtained materials, which are a perfect replica of a hierarchical leaf skeleton, have been used as electrodes for water splitting and the electrodeposition of Pt. This method has great promise for the synthesis of a variety of hierarchically microstructured objects for catalytic and electrochemical purposes and can be extended to other photocatalysts such as ZnO, Cu_2O, In_2O_3, CeO_2, WO_3, and peroskites including $SrTiO_3$, $BaTiO_3$, and $Sr_2Nb_2O_7$.[7]

Hierarchically porous structures can also been fabricated without a template with enhanced photocatalytic activity for H_2 production.[100,101] Peng and co-workers prepared hierarchically porous $ZnIn_2S_4$ microspheres using a facile template-free hydrothermal method.[100] The as-prepared $ZnIn_2S_4$ showed considerable photocatalytic H_2 production efficiency and the photocatalytic activity was further enhanced by the presence of a Pt cocatalyst under visible light irradiation. Specifically, the $ZnIn_2S_4$ prepared at 160 °C with pH = 1.0 showed the highest photoactivity of H_2 production with an apparent quantum yield of up to 34.3% under incident monochromatic light of 420 nm. Janek and co-workers compared the photoelectrochemical properties of two kinds of hierarchically porous TiO_2 films prepared by the prevalent methods.[101] The photoelectrochemical experiments clearly show that sol-gel derived hierarchically porous TiO_2 films demonstrated about 10 times higher efficiency for the water splitting reaction than their counterparts obtained from crystalline TiO_2 nanoparticles. In fact, the performance of nanoparticle-based TiO_2 films might suffer from insufficient electronic connectivity, yet the hierarchically porous TiO_2 films prepared from the $TiCl_4$ source through the sol-gel method can provide not only sufficient electronic connectivity but also hierarchically macro-mesopores for easy mass transport and high surface area during the photocatalytic process.

Significant progress has been achieved in recent years in the exploring and developing of novel structures for photocatalytic water splitting. Nevertheless, the performance of photocatalysts under visible light could be improved. Although around 140 different materials have been evaluated to produce H_2 efficiently by photocatalytic process,[97,102–106] the number of studies using hierarchically porous structures is still limited in spite of the important promise of hierarchically structured porous materials in light harvesting and mass diffusion. This is due to the lack of efficient and easy synthesis of pathways to and through desired porous materials with well defined three length scales (micro, meso, and macro). In this respect, the challenge is still great to develop a practical solar powered system for photocatalytic water splitting.

2.1.3. Hierarchically Structured Porous Materials for Dye-Sensitized Solar Cells (DSSCs)

Photovoltaic technology, commonly in the form of solar cells has received tremendous attention for its direct conversion of sunlight to electricity. Most of the existing solar cell technologies based on silicon is reaching the limits of what can be done with it. To increase solar/electricity conversion efficiency, quantum dot based solar cells (QDSCs), and, in particular, DSSCs have been developed.[107] The DSSCs are a photoelectrochemical system that incorporates a porous-structured oxide film with adsorbed dye molecules as the photosensitized anode. The

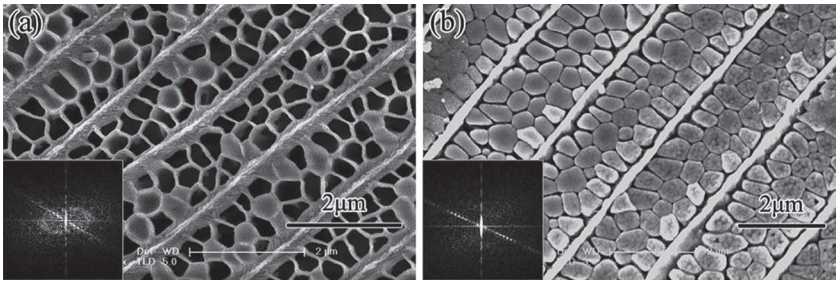

Figure 5. FESEM images of as-synthesized titania photoanodes templated from butterfly wings with different colors. a,b) Quasi-beehive structures synthesized under different conditions. Reproduced with permission.[109] Copyright 2009, American Chemical Society.

photoanode is crucial in light harvesting efficiency, which determines the overall cell efficiency. The ideal photoanode should have a high surface area nanostructure for dye adsorption. The presence of a hierarchical porous structure, as described in the previous section, can increase the optical path length and improves the light harvesting efficiency.

It has been reported that some butterfly wings contain photonic structures that are effective solar collectors.[108] The honeycomb-like structure found at the surface of butterfly wings takes advantage of refraction in trapping light. In fact, when light meets this kind of material, instead of crossing it, it is reflected back into the material. Nearly all the incident light can be adsorbed. This kind of structure can certainly improve the solar/electricity conversion efficiency in DSSCs since light harvesting is the first and essential step. To take the advantage of such structures and in order to improve the light harvesting efficiency, Zhang and co-workers have prepared hierarchically periodic microstructure titana film photoanode by using butterfly wing scales as biotemplates. The morphology of the photoanodes is an exact replica of the original butterfly wings with a natural photonic structure. The hierarchically porous titania film after calcinations is formed by the aggregation of crystalline nanoparticles (**Figure 5**).[109] The obtained quasi-honeycomb structure TiO_2 replica showed a higher light harvesting efficiency than the normal titania photoanode prepared without biotemplates. Choosing the appropriate structural model of butterfly wings may lead to enhanced photon-to-current efficiencies. This study demonstrated that the butterfly wing photonic structures are the best structural models in the design of photoanodes for DSSCs to improve light harvesting and solar/electricity conversion efficiency.

Recently a very exciting study showed diatom based DSSCs that may be up to three times as efficient as conventional solar cells. Diatoms are single-celled photosynthetic organisms that are abundant in marine and fresh water ecosystems. The creatures contain a silicon dioxide cell wall called a frustule, which possesses intricate periodic nanoscale patterning and is genetically controlled and unique to each species. These patternings, containing many naturally occurring nanometer sized pores throughout, hold great promise in applications as natural photonic structures that can control the flow of light within engineered devices and have high capacity for Dye molecules adsorption. To take advantage of such photonic structures in DSSCs, Rorrer and co-workers invented a quite ingenious process to coat hierarchically porous diatoms with a TiO_2 film. In the initial phase of the process, the diatoms are placed on a conductive glass surface. The organic components of the diatoms are then removed, leaving only the silica frustules, which forms a template for semiconducting materials. A biological agent is then used to precipitate soluble titanium into very tiny nanoparticles of TiO_2, creating a thin film on diatoms that acts as the semiconductor for the DSSC devices. It is known that in a conventional thin TiO_2 based film, photosynthesizing dyes generally take photons from sunlight and transfer them to TiO_2, thus creating electricity. In the system based on diatoms (**Figure 6**),[31–33] the photons bounce around more inside the pores of the diatoms frustules, making solar to current conversion more efficient. This efficiency can be attributed to the tiny hierarchical holes (pores) in diatoms frustules, which appear to increase the interaction between photons and the large quantity dye molecules loaded to promote the conversion of light to electricity and improve energy production in the process. Although the current efficiency of these DSSCs is still low (>1%), this research demonstrates the feasibility of device fabrication based solely on a biological process that is simple, environmentally benign, and takes place at room temperature.

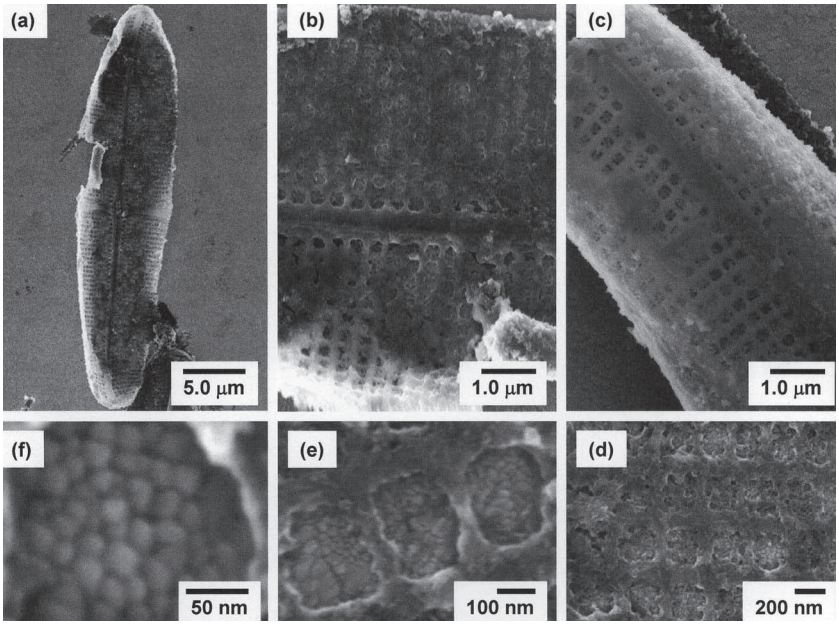

Figure 6. SEM images of *Pinnularia sp.* frustule biosilica after two successive layers of TiO_2 deposition. a–c) Microscale features of surface and d–f) nanoparticles packed into frustule pores. Reproduced with permission.[33] Copyright 2008, Materials Research Society.

As a promising high efficiency porous material, the inverse opal particles or films made from the hard templates have also provided good performance on the DSSCs. One of the most significant advantages of inverse opals, which are clearly distinct from traditional photoelectrodes, are hierarchical pore-channel networks that offer effective surface contact between the incident light and photoelectrodes. The highly periodic organization also results in the slow photon effect as discussed in Section 2.1.1. At present, the most typical method of preparation of TiO_2-IO films is based on a three step method: 1) deposition of opals on a substrate, such as fluorinated tin oxide (FTO) coated glass, by the self-assembly of submicrospheres (silica or polymeric) from a colloidal suspension; 2) infiltration of titanium precursor into the interstitial spaces of the opal by a sol-gel method; and 3) removal of the colloidal crystal template by solvent extraction or calcinations.[110–114] Lee and co-workers constructed TiO_2 inverse opal structures using non-aggregated TiO_2 NPs in a 3D colloidal array template as the photoelectrode of a DSSC. They prepared three inverse-opal structures of the different original sizes of the polystyrene (PS) micro-spheres and explored photoelectricity characteristics of inverse-opal cells made from different sized PS templates and showed the best conversion efficiency (3.47%) for a 1000-nm-diameter PS-templated cell.[111] Wang and co-workers found that the TiO_2 inverse opal demonstrated a photovoltaic conversion efficiency of 5.55% compared to the device using a bare P25 TiO_2 photoanode.[112] Moon and co-worker constructed bilayer inverse opal TiO_2 electrodes, which demonstrated a maximum photovoltaic conversion efficiency of 4.6%.[113]

When not using a sol-gel method, Tok and co-workers reported an atomic layer deposition (ALD) method leading to the fabrication TiO_2 inverse opal for DSSCs.[115] This method has the advantage to obtain high quality TiO_2 inverse opal because of a high filtration, which can make the inverse opal structure more stable under high temperature treatment.[116] However, this method also has a drawback for the crystalline grain size of the TiO_2 nanoparticles. Using ALD, the TiO_2 nanocrystalline grain size is larger than that of the sol-gel method resulting in a low surface area. For instance, the highest power conversion efficiency of the TiO_2 inverse opal obtained is only 2.22%, which is lower than that of the TiO_2 inverse opal prepared by sol-gel method. Nevertheless, the high infiltration of TiO_2 in this structure is helpful in enhancing the light harvesting.

Most recently, Moon and co-workers introduced a method to generate hierarchical macro-mesoporous electrodes using a dual templating method (**Figure 7**).[117] Mesoscale colloidal particles and lithographically patterned macropores were used as dual templates, with the colloidal particles assembled within the macropores. An infiltration of TiO_2 into the template and subsequent removal of the template produced hierarchical TiO_2 electrodes for DSSCs. Compared with previous methods using block copolymer organization or TiO_2 precursor reaction control for mesopore generation,[118,119] the colloidal particle assemblies are simplier, more controllable, and produce fully connected mesopores. Moreover, the lithographic method produces macroporous structures with controllable, high fidelity macroscale morphologies.[120] The photovoltaic performance of the dual templated electrodes showed a maximum efficiency of 5.00% with 50 nm pores and a 6 μm thickness, this was attributed to the strong scattering and suppression of charge recombination in hierarchically macro-mesoporous TiO_2 electrodes.

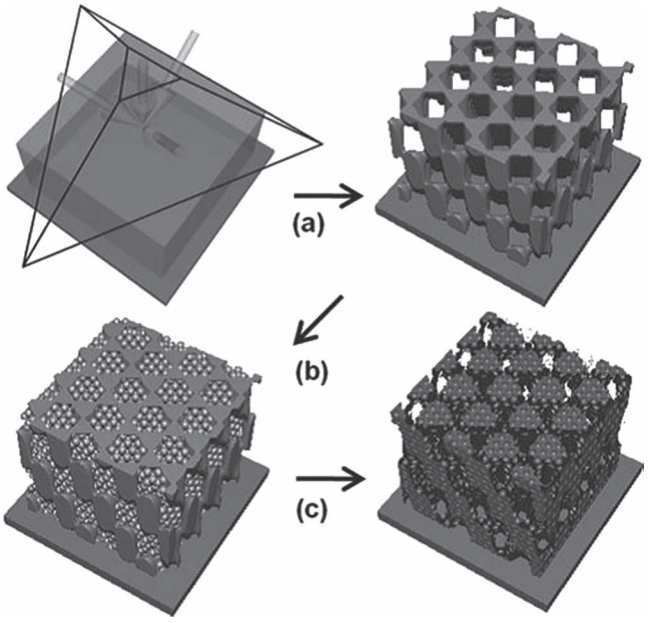

Figure 7. a) Scheme for formation of four-beam interference and the fabrication of the macroporous SU-8 structures, b) filling of the holographic patterns with mesoscale colloidal particles, and c) coating of precursors and removal of dual templates. Reproduced with permission.[117]

Recently, self-assembly of TiO_2 nanoparticles to form hierarchical pores for DSSCs application has been developed.[121,122] This method has the advantage to use the high surface area of nanoparticles and the formed hierarchical pores that can offer channels for mass transfer and light harvesting. For instance, Kim and co-workers prepared TiO_2 spheres with hierarchical pores via grafting polymerization and sol-gel synthesis.[121] DSSCs made from such TiO_2 nanospheres with hierarchical pores, exhibited improved photovoltaic efficiency compared to those from smoother TiO_2 nanoparticles, owing to the increased surface areas and light scattering. Although the report on this method for hierarchical pores formation is limited, it has demonstrated enhanced performance. In particular, this strategy provides an opportunity to assemble the TiO_2 nanostructures with exposed high surface energy to demonstrate high performance on DSSCs because of the high chemical activity.

ZnO is also a promising candidate for the photoanode of DSSCs, it has also been extensively studied due to the similar bandgap and the electron-injection process as that of TiO_2. At present, both TiO_2 and ZnO are the preferred choices for the production of hierarchically porous photoanodes for DSSCs. Compared to TiO_2, ZnO had higher electronic mobility that would favor photoinduced electron transport, this results in reduced recombination of photoexited electrons and holes, which can enhance the solar energy conversion when used in DSSCs. Furthermore, the ease of crystallization and anisotropic growth of ZnO make it a natural alternative to TiO_2. The effect of nanostructured ZnO on the performance of DSSCs was reviewed in detail by Cao and Zhang.[123] Here, we only focus on the performance of DSSCs created using hierarchically

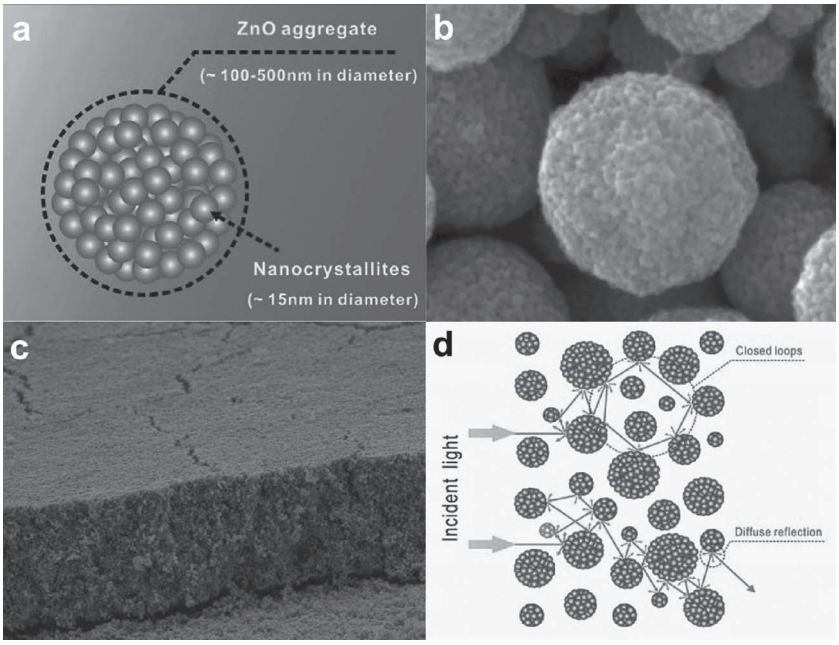

Figure 8. a) Schematic illustration of the submicrometer-sized aggregate consisting of closely packed ZnO nanocrystallites. SEM images of b) a submicrometer-sized aggregate of ZnO nanocrystallites and c) a photoelectrode film made of submicrometer-sized ZnO aggregates. d) Propagation and multiple scattering of light in a porous electrode consisting of submicrometer- or micrometersized aggregates. Reproduced with permission.[125,126]

porous ZnO structures. Hierarchically porous ZnO structures generated through aggregation of ZnO nanocrystals was successfully carried out by Cao and co-workers (**Figure 8**).[124–128] They achieved a significantly enhanced power conversion efficiency (PCEs) of 5.4% for hierarchically porous electrodes made of aggregates of ZnO nanocrystallites compared to the ordinary porous electrodes made of dispersed ZnO nanocrystallites using red N3 (Ruthenium 535) dyes.[124–126] After modifying the surface of ZnO with lithium, a PCE of 6.9% was achieved.[128] Cheng and Hsieh fabricated hierarchically structured ZnO, by self-assembly of secondary nanoparticles, as an effective photoelectrode for DSSCs. The hierarchical architecture, which manifested significant light scattering without sacrificing the specific surface area, can provide more photon harvesting. In addition, dye-molecule adsorption was sufficient due to enough internal surface area being provided by the primary single nanocrystallites. The enhancement of the open-circuit photovoltage (Voc) and the short-circuit photocurrent density (Jsc) of ZnO based DSSCs was ascribed to the effective suppression of electron recombination.[129]

In areas other than nanoparticle aggregation, hierarchically porous ZnO architectures assembled by other nanostructures have also drawn attention in recent years.[130–132] For instance, Wu and co-workers produced DSSCs with hierarchically porous ZnO based on the disk-like nanostructures and displayed an improved photovoltaic performance of an overall efficiency of 2.49%.[130] The annealing treatment was also found to further improve the fill factor of the DSSCs. Yang and co-workers fabricated hierarchically porous ZnO nanoplates for use in DSSCs, which demonstrated a decent energy conversion efficiency of 5.05% with the new type of photoanode.[131]

Though the PCE is still low for the DSSCs formed by hierarchically ZnO porous structures, the work above inspires not only rational preparation and hierarchical assembly of other novel porous single crystalline nanostructures, but also opens up new opportunities for the development of photoanodes for DSSCs. It is expected that the current best of 6.9% here can be improved to exceed the current record in the field of 11% for TiO_2 based DSSCs[133,134] by the optimization of the assembled films combining them with a variety of common treatments, modifications, or enhancement procedures.

A major drawback of TiO_2 and ZnO, which possess wide electronic bandgaps (3.2 eV), is that they absorb only the ultraviolet fraction of the solar spectrum; this limits their utilization efficiency for solar light. Consequently, the hierarchically porous structures made by the few metal oxides with narrower bandgaps, such as tungsten trioxide and fluorine- or antimony-doped tin oxide, have attracted attention for DSSCs application under visible light irradiation.[135–137] For instance, Ye and co-workers synthesized WO_3 inverse opal film used as a photoanode to enhance the incident photon to electron conversion efficiency (IPCE). A maximum of a 100% increase in photocurrent intensity was observed under visible light irradiation ($\lambda > 400$ nm) in comparison with a disordered porous WO_3 photoanode. When the red-edge of the stop-band was tuned well within the electronic absorption range of WO_3 (Eg = 2.6–2.8 eV), noticeable, but reduced, amplitude of enhancement in the photocurrent intensity was observed. The enhancement could be attributed to the fact discussed at the end of section 2.1.1, a longer photon-matter interaction length as a result of the slow-light effect at the photonic stop band edge, thus leading to a remarkable improvement in the light-harvesting efficiency.[135] Xu and co-workers reported template-assisted and solution chemistry-based synthesis of inverse opal fluorinated tin oxide (IO-FTO) electrodes. The photonic crystal structure possessed in the IO-FTO exhibits strong light trapping capabilities. Using atomic layer deposition (ALD) method, an ultrathin TiO_2 layer was coated on all surfaces of the IO-FTO electrodes. Cyclic voltammetry study indicated that the resulting TiO_2-coated IO-FTO showed excellent potential as electrodes for electrolyte-based photoelectrochemical solar cells.[137]

In DSSCs, the commonly used counter electrode material is FTO loaded with platinum; it demonstrates fast electrolyte regeneration kinetics and high efficiencies of the devices, but the high costs inhibits large scale applications. Therefore, it is highly desirable to develop alternative cheaper materials for the counter electrodes. Inexpensive and abundant carbon materials are a potential alternative to the Pt in DSSCs. However, energy conversion efficiency (η) is still lower than that of the Pt based DSSCs,[138] probably due to a higher charge transfer resistance of the carbon counter electrode toward the I^{3-}/I^- electrolyte and a retardation of the mass transfer of the electrolyte in

the carbon matrix.[139] Therefore, development of novel carbon materials with superior catalytic activity and highly porous structure is required to enhance charge transfer for the carbon counter electrode and the improvement of the electrolyte diffusion in the carbon layer. Most recently, the use of a multiple template approach for porous carbon with hierarchically porous structures and designed porosity has received considerable attention due to the interconnected pore structures providing low resistance and short diffusion pathway, which facilitate fast electron and mass transport to enhance the electrochemical performance.[140–143]

The typical fabrication of hierarchically porous carbon is similar to the preparation of TiO_2 inverse opal films: first the formation of a highly ordered opal structure and then the infiltration of carbon precursors into the voids in the opal structure to solidify the porous structure. For instance, ordered multimodal porous carbon (OMPC) having a unique nanostructure was explored as counter electrodes in I^{3-}/I^- based DSSCs by Yu and co-workers.[144] The unique structural characteristics, such as a large surface area and well-developed 3D interconnected ordered macroporous framework with open mesopores embedded in the macropore walls, make the OMPC electrodes have high catalytic activity and fast mass transfer kinetics toward both triiodide/iodide and polysulfide electrolytes. The efficiency (ca. 8.67%) of the OMPC based DSSC is close to that (ca. 9.34%) of the Pt base. Furthermore, they developed hollow macroporous core/mesoporous shell carbon (HCMSC) with a hierarchical nanostructure for a counter electrode in DSSCs. For comparison, ordered mesoporous carbon CMK-3 and commercially available activated carbon (AC) were also investigated. The DSSC electrode based on HCMSC demonstrated highly enhanced catalytic activity toward the reduction of I^{3-}, and accordingly considerably improved photovoltaic performance (a Voc of 0.74 V), which is 20 mV higher than that (i.e., 0.72 V) of Pt. It also displayed a fill factor of 0.67 and an energy conversion efficiency of 7.56%, which are markedly higher than those of its carbon counterparts and comparable to that of Pt (i.e., fill factor of 0.70 and conversion efficiency of 7.79%). In addition, the electrode made by HCMSC possesses excellent chemical stability in the liquid electrolyte containing I^-/I^{3-} redox couples. After 60 days of aging, ca. 87% of its initial efficiency is still achieved by the solar cell based on the HCMSC counter electrode.[145]

Dye-sensitized solar cells are much cheaper and easier to produce in bulk than their crystalline silicon counterparts, and have thus attracted significant research efforts to meet the long-term goal of manufacturing very low-cost and high-efficiency solar cells. However, the power conversion efficiency is still low for practical use. The highest power conversion efficiency is just over 11%.[133,134] To improve the solar cells photon to electron conversion efficiency, two methods can be separately or simultaneously considered to design the materials with high light harvesting and develop stable dyes suitable for long term solar irradiation. Hierarchically porous structures have already shown enhanced power conversion efficiency by the presence of light harvesting macrochannels and the increase in the dye molecules loading. The further challenge is the optimization of the light harvester and the stabilization of dye molecules in hierarchically porous materials.

2.1.4. Hierarchically Structured Porous Materials for Immobilization of Photosynthetic Species for CO_2 Conversion by Photosynthesis: Design of Leaf-Like Materials

In nature, a wide variety of eukaryotic algae, gymnosperms, angiosperms, bryophytes and ferns perform carbon dioxide and water conversion to chemicals by photosynthesis with great efficiency. The key sub-cellular component of this process is the chloroplast. This organelle, which encloses photosynthetic membranes (viz. thylakoids), is extremely efficient since the quantum yield of the primary process of the photochemical reactions is close to 100%.[146] However, these photosynthetic membranes and, more generally, natural materials (enzymes, DNA, antibodies, cells) isolated from their native superstructures are very fragile, making them difficult to exploit.[14,15,17,19–21,26] Leaves, which are climate-dependent biological systems, can not complete photosynthesis efficiently in winter. Other photosynthetic entities are also impaired in severe environments, which limits their photosynthetic efficiency. Moreover, the small size of individual cells poses a problem in their efficient application to processes.

To achieve the benefits of photosynthesis process of CO_2 and water conversion in useful chemical compounds under the action of sunlight, inspired by hierarchical leaf structures and diatom frustules, one can imagine an artificial system performing photosynthesis as leaves and other microorganisms do by encapsulating or immobilizing the biological photosynthetic matter, organells, and whole cells within an inert support that can offer protection by providing a stable microenvironment. Such system, called "leaf-like materials" can incorporate all the properties of biological systems for photosynthesis but remain independent of season change (**Figure 9**).[14–29] The host biocomposite material should ideally be mechanically and chemically resistant, inert both to its surroundings and the guest it encompasses, nontoxic, and phototransparent, and should eventually possess affinities with the cells.[147] To allow easy diffusion of nutrients, CO_2, water, and metabolits produced by photosynthesis, the microenvironment should contain the hierarchical

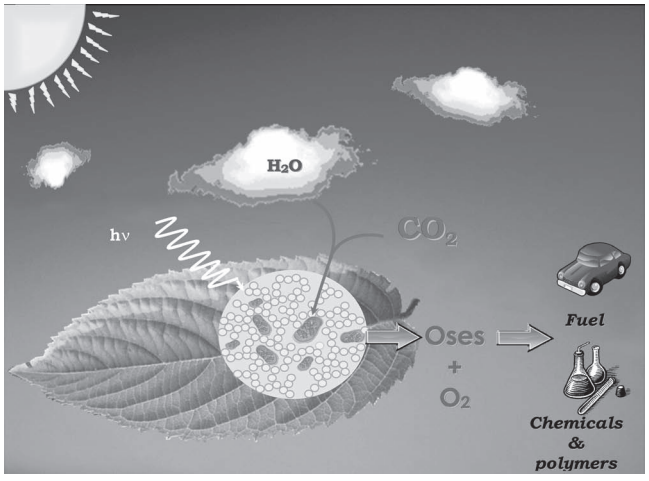

Figure 9. Schematic representation of life-like materials made by the immobilization of photosynthetic matters within the biocompatible hierarchically porous materials. Reproduced with permission.[21] Copyright 2009, The Royal Society of Chemistry.

porous systems found in leaves and diatoms. The hybrid material should additionally prolong the viability of the entity.

Inspired by diatoms, silica is the first choice owing to its easily generated and tuneable porosity, optical transparency, resistance to microbial attack, and mechanical, chemical,and thermal stability. Porosity and optical transparency are of prime importance as these parameters permit the diffusion of nutrients and light energy respectively throughout the bulk of the hybrid material to reach the cells encapsulated within. It is true that most porous silica samples are generally highly scattering and therefore not so transparent as bulky silica materials. However, hierarchically organized porous silicas such as diatoms show high transparency and allow the penetration of light into the core of diatoms. The filling in the pores with a fluid can further improve the transparency. If the refractive index of the fluid used matches that of silica, the materials can reach an almost complete transparency. Hierarchically structured porous silica materials can be targeted by so called "chimie douce" techniques. Such soft chemistry methods lend themselves to the synthesis of photochemical materials as they can enable the in situ immobilization of fragile living entities while posing minimal risk to their viability. Such photochemical materials would become the active component of a stationary phase bioreactor through which the media can be pumped and the metabolites harvested owing to the porosity of the encapsulating matrix. These hybrid materials can be produced by exploiting well known sol-gel chemistry reactions.

The earliest work was performed with thylakoids, which produce the light reaction (water splitting to produce O_2) of photosynthesis. The entrapped thylakoids, using alkoxides or H^+-exchanged silicate as precursors, can produce oxygen up to 40 days (**Figure 10**).[14,17,20,21,26] These quite exciting and promising results could allow the design of a photosynthetic H_2 generator and photosynthetic biofuel cells.[30] Chloroplates have also been immobilized. Unfortunately, the living hybrid materials obtained did not show significant photosynthetic efficiency.[14,15,17,20,26] Attention was then turned to the immobilisation of more complex biological systems: photoautotrophic plant

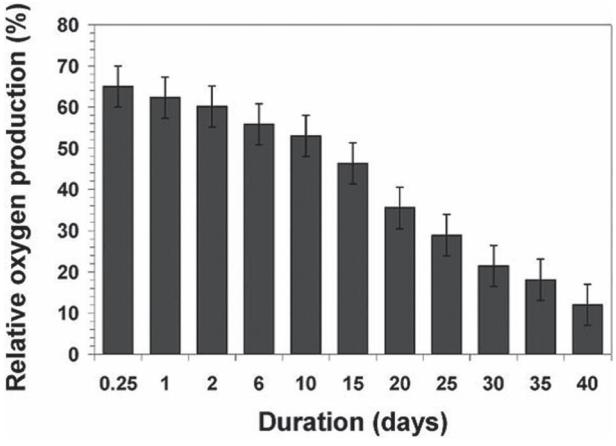

Figure 10. Photochemical production of O_2 by entrapped thylakoids within a biocompatible hierarchically porous silica matrix. Reproduced with permission.[17] Copyright 2010, The Royal Society of Chemistry.

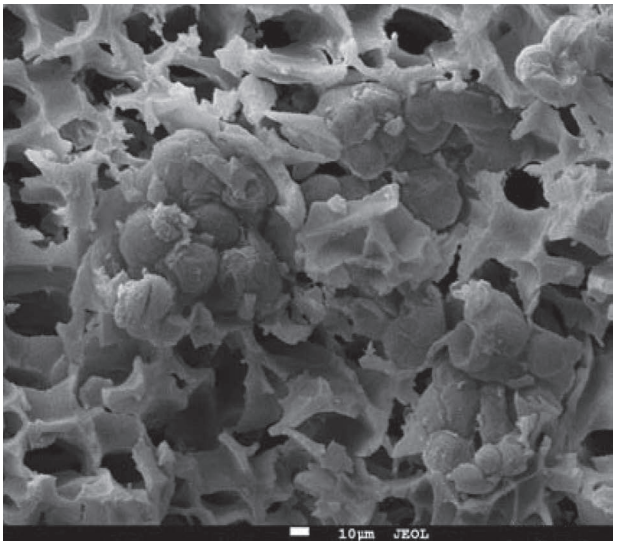

Figure 11. SEM picture of the immobilization of *A. thaliana* cells within a silica-based hierarchical porous matrix.

cells (**Figure 11**).[15,17,19,20,26] These new bioproduction platforms have a bright future in the development of new sustainable technologies. The metabolism of plant cells could be exploited advantageously to convert CO_2 and water to valuable (macro-) molecules and nanomaterials, and simultaneously reduce CO_2 emissions. The results showed that plant cells retain their photosynthetic activity during one month after their encapsulation into an organo-modified silica matrix (**Figure 12**a). The hybrid materials are able to reduce CO_2 into carbohydrates. The molecules excreted by the material were mainly polysaccharides composed of rhamnose, galactose, glucose, xylose, and mannose units (Figure 12b).[15,17,20,26] It was shown that the quantity of sugars increased as a function of time. This photosynthetic material holds much promise in the development of new and green chemical processes. These results present a significant advancement in the realization of a bioreactor based on photosynthetic cells immobilized in hierarchically porous silica.

The photosynthetic process is not limited to just plants and trees, there are many species of algae and bacteria that can harvest light energy to convert CO_2 and water by photosynthesis into chemical energy. The encapsulation of unicellular cyanobacteria and a series of algae into 3D hierarchically porous silica matrix for the conversion of water and CO_2 into biofuels by photosynthesis under the action of light was also a great success.[16,18,22–29] The immobilized species have shown survival times of up to 5 months with the photosynthetic production of oxygen recorded as much as 17 weeks post immobilization.[16,18,22–29] As a consequence, the immobilization of cells could allow the continuous exploitation of cells in a non-destructive way to produce metabolites as biofuels. Compared to well-known photocatalysts (e.g., TiO_2), which generally reduce CO_2 into hydrocarbons under UV irradiation, high temperature, and high pressure,[148] these photochemical materials operate at room temperature and atmospheric pressure. The environmental impact and energy required are lower. These photochemical materials could thus contribute towards future

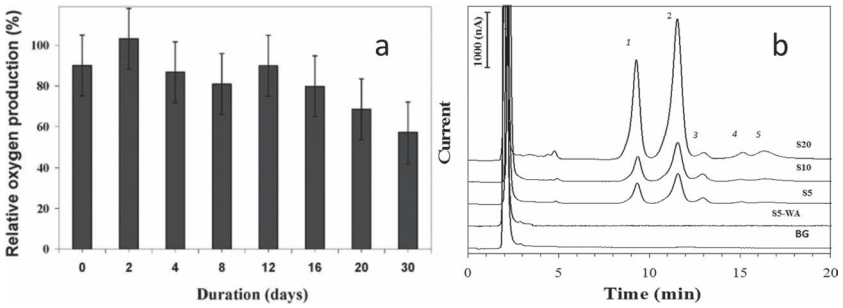

Figure 12. a) Photosynthetic production of oxygen by entrapped plant cells. 100% corresponds to the photosynthetic activity of free cells (13 mmol g^{-1} FW h^{-1}). b) HPAEC-PAD analysis of gel supernatants. Chromatograms showing the comparison between (BG) a blank gel and a hybrid gel after (S5) five days, (S10) ten days, and (S20) twenty days. (S5-WA) corresponds to the supernatant of the hybrid gels after five days without acid treatment. The peaks correspond to 1, rhamnose; 2, galactose; 3, glucose; 4, xylose; 5, mannose. Reproduced with permission.[15] Copyright 2010, The Royal Society of Chemistry.

initiatives in helping to mitigate the energy crisis and reduce CO_2 emissions. The exploitation of such systems for biofuel cells to convert sunlight or biological energy to electricity is a very important direction for future research.[30a,b] In future, genetic engineering of photosynthetic strains and modification of cell membranes can be used to improve the viability and biological activity of the cells or to control the products obtained via cellular metabolism, may thus pave the way to more efficient photobioreactors that can directly convert CO_2 and water under the action of sunlight through photosynthesis into other more valuable and desirable chemical products. Additionally, the chemical, morphological, and diffusion properties of the matrix have to be carefully controlled. Looking to natural systems we see that in many cases it is not only the photosynthetic cell itself that is the key to efficiency but the overall system such as the 3D architecture of a leaf. With this in mind, future work needs to focus on the design of the encapsulating matrix that encompasses structural features such as hierarchical porosity and targeted surface properties.

2.1.5. Hierarchically Structured Porous Materials for CO_2 Conversion to Hydrocarbons

Since CO_2 is considered as a major contributor to the greenhouse effect, the reduction of the thermodynamically stable CO_2 molecule into useful hydrocarbon products has turned into a research priority. The artificial photocatalysis of CO_2 to hydrocarbons can be traced back to ninety years ago. In 1921, Baly and co-workers studied the production of formaldehyde under visible light, using colloidal uranium and ferric hydroxides as catalysts.[149,150] After over sixty years, Halmann reported photoelectrochemical reduction of carbon dioxide by using single crystal p-type GaP as the photocatalyst in 1978.[151] In 1979, Fujishima, Honda and coworkers studied the use of several semiconductor powders, including TiO_2, ZnO, CdS, WO_3, and SiC, suspended in CO_2 saturated water by Xe lump irradiation.[152] Many kinds of products, such as formic acid, formaldehyde, methanol, and methane, were obtained. Based on the experiments, they suggested a multiple reduction process as follows:

$$H_2O + 2h^+ \rightarrow 1/2O_2 + 2H^+ \quad (2)$$

$$CO_2(aq.) + 2H^+ + 2e^- \rightarrow HCOOH \quad (3)$$

$$HCOOH + 2H^+ + 2e^- \rightarrow HCHO + H_2O \quad (4)$$

$$HCHO + 2H^+ + 2e^- \rightarrow CH_3OH \quad (5)$$

$$CH_3OH + 2H^+ + 2e^- \rightarrow CH_4 + H_2O \quad (6)$$

where h^+ and e^- represent the photogenerated holes and electrons, respectively. The band-edge positions of the semiconductors can significantly influence CO_2 photoreduction as illustrated in **Figure 13**. The SiC conduction band edge lies at a higher position (more negative) than the $HCHO/H_2CO_3$ redox potential, which is believed to be responsible for the high rates of product formation. When WO_3 was used as a catalyst, no

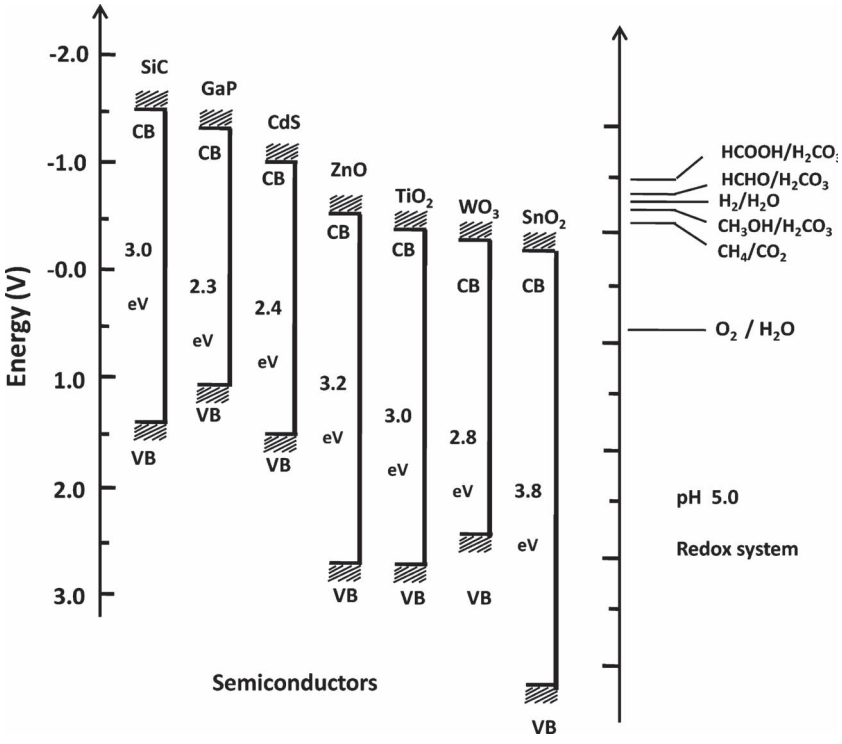

Figure 13. Conduction band and valence band potentials of semiconductor photocatalysts relative to energy levels of the redox couples in water. Reproduced with permission.[152] Copyright 1979, Macmillan Publisher Limited.

methanol was obtained due to the conduction band at a position lower than the $HCHO/H_2CO_3$ redox potential.

As mesoporous materials possess high surface area, the utilization of porous structures for CO_2 photocatalysis conversion has been attracting attention recently. For instance, Ti species incorporated mesoporous silicas exhibit a much higher activity than bulk TiO_2 in the photoreduction of CO_2 with water to generate methanol and methane under UV irradiation.[153] Lin and co-workers prepared a series of mesoporous TiO_2/SBA-15, Cu/TiO_2, and Cu/TiO_2/SBA-15 composite photocatalysts by the sol-gel method for photoreduction of CO_2 with H_2O to methanol.[154] The thermal stability and grain growth of anatase TiO_2 crystallite was confined when loading the titanium isopropoxide (TTIP) on SBA-15 support by sol-gel synthesis. The loading quantity of TiO_2 in mesoporous TiO_2/SBA-15 composite photocatalysts played a key role to control the crystallite size of the supported TiO_2 particles and the mesoporous structure of the catalyst. The optimum amount of titanium loading of TiO_2/SBA-15 was 45 wt%, which exhibited higher photoreduction activity than pure TiO_2. An addition of copper to TiO_2 or TiO_2/SBA-15 catalyst as co-catalyst was found to enhance the catalytic activity because copper serves as an electron trapper and prohibits the recombination of hole and electron. Li and co-workers synthesized mesoporous silica supported Cu/TiO_2 nanocomposites through a one-pot sol-gel method, and the photoreduction experiments were carried out in a continuous-flow reactor using CO_2 and water vapor as the reactants under the irradiation of a Xe lamp.[155] This significantly enhanced CO_2 photoreduction rates due to the synergistic combination of Cu deposition and high surface area SiO_2 support. CO was found to be the primary product of CO_2 reduction for TiO_2-SiO_2 catalysts without Cu. CH_4 was selectively produced when Cu species was deposited on TiO_2. The optimal Cu loading on the Cu/TiO_2-SiO_2 composite was found to be 0.5 wt%. The Cu species were identified to be Cu_2O, which was the active sites of electron traps, suppressing electron-hole recombination and enhancing multi-electron reactions. Cu(I) species may be reduced to Cu(0) during the photoreduction, and the Cu(0) species can be re-oxidized back to Cu(I) in an air environment. The rate limiting step for this reaction may be the desorption of the reaction intermediates from the active sites.

Because zeolites offer unique nanoscaled pore reaction fields, an unusual internal surface topology, and ion-exchange capacities as well as a molecular condensation effect, TiO_2 catalysts based on zeolites have been widely studied. For instance, high efficiency and high selectivity for methanol was obtained in the photoreduction of CO_2 with water under UV irradiation, over Ti-oxide/Y-zeolite catalysts containing highly dispersed isolated titanium oxide species. The charge-transfer excited state of these species is thought to play a key role in the high selectivity for CH_3OH, in contrast to the selectivity to CH_4 obtained on bulk TiO_2.[156] Anpo and co-workers investigated the effect of the hydrophilic-hydrophobic properties of the zeolite surface on the activity and selectivity of titanium oxide based β-zeolite photocatalysts in the photoreduction of CO_2 in water. The catalyst with hydrophilic properties demonstrated higher activity, whereas the catalyst with hydrophobic properties showed higher selectivity to methanol.[157] Frei and co-workers used a Ti silicalite molecular sieve (TS-1) as photocatalyst under UV light and using methanol as an electron donor could synthesize the main product of formic acid. IR spectroscopy was used to study the mediate product, indicating that CO originated from the secondary photolysis of HCO_2H, while HCO_2CH_3 was the result of a spontaneous Tishchenko reaction of CH_2=O.[158] They also used the bimetallic ZrCu(I)-MCM-41 silicate sieve for the CO_2 photoreduction. They found that CO_2 can be split to CO and O_2 at the excited metal-to-metal charge-transfer sites.[159]

At present, many of studies have already demonstrated that zeolites, mesoporous molecular sieves, porous silica thin films, and TiO_2 species, which are highly dispersed in their cavities and framework, are promising candidates as efficient photocatalysts compared to bulk TiO_2 powder for the photoreduction of CO_2 in H_2O.[160–164] TiO_2 based photocatalysts are at present widely used for CO_2 photoreduction, whereas they are not the only materials for CO_2 photoreduction processes. In fact, a large variety of photocatalysts have been reported for photocatalytic CO_2 conversion. These materials include semiconductors, such as TiO_2, ZnO, WO_3, NiO, ZrO_2, SiC, CdS, ZnS, p-type $CaFe_2O_4$, $K_2Ti_6O_{13}$, $SrTiO_3$, and organics such as transition-metal complexes.[97,102,165–174] Methanol was also selectively produced over a $NiO/InTaO_4$ photocatalyst under visible light irradiation.[173] More photocatalytic conversion of CO_2 into methanol in aqueous phase with high yield was obtained over NiO and ZnO than over TiO_2.[174]

On the basis of these very promising results obtained with microporous and mesoporous photocatalysts and considering the hierarchically porous structures that possess special optical properties and porous advantages,[43,44] the utilization of hierarchically porous structures for CO_2 photoreduction should enhance the efficiency and the selectivity of the products. However, currently there are almost no reports about the ultimate application of hierarchically porous materials for CO_2 photoreduction. The present rising concentration of CO_2 in the atmosphere has renewed interest in this process due to the environmental pressure. Recycling of carbon dioxide via photocatalysis provides an interesting route for CO_2 conversion to hydrocarbon which mimics photosynthesis in green plants. From this point of view, the hierarchically porous structures made from the biotemplates should be one of the most promising model materials as a guide for the rational design of new efficient and advanced materials for CO_2 photoreduction as suggested by Zhang and co-workers.[102]

2.2. Hierarchically Structured Porous Materials for Fuel Cells (FCs)

A fuel cell is an electrochemical cell that converts chemical energy from a fuel into electric energy in a constant temperature process. Electricity is generated from the reaction between a fuel supply and an oxidizing agent. The reactants flow into the cell, and the reaction products flow out of it, while the electrolyte remains within it. Fuel cells can operate continuously using wide range of fuels, including hydrogen, as long as the necessary reactant and oxidant flows are maintained. They are made up of three segments which are sandwiched together: the anode, the electrolyte, and the cathode. At the anode a catalyst

oxidizes the fuel, usually hydrogen, turning the fuel into a positively charged ion and a negatively charged electron. At the cathode, a catalyst turns the ions into the waste chemicals such as water or carbon dioxide. There are different kinds of fuel cells. The lower temperature systems including alkaline fuel cells (AFC), polymer electrolyte membrane fuel cells (PEMFC), and phosphoric acid fuel cells (PAFC), operate essentially on H_2 fuel, whereas the higher temperature systems, including molten carbonate fuel cells (MCFC) and solid oxide fuel cells (SOFC), can also electrochemically oxidize CO, which is advantageous when a hydrocarbon fuel is supplied to the fuel cell. For reasons of electrode activity, which translates into higher efficiency and greater fuel flexibility, higher temperature operation is preferred, but for portable (intermittent) power applications, lower temperature operation is typically favored as it enables rapid start-up and minimizes stress due to thermal cycling. In addition, solid electrolyte systems can avoid the need to contain corrosive liquids, thus solid oxide and polymer electrolyte fuel cells are preferred by many developers comparing to alkali, phosphoric acid, or molten carbonate fuel cells.[175,176]

Porous materials have largely been used in the design of high efficiency and high current density FCs since the configuration of FCs needs anodes and cathodes to be porous to facilitate the diffusion of the fuel and chemical wastes produced. The effect of porous structures on the performance of fuel cells is well reviewed in detail.[175–182] Here we only discuss the application of the hierarchically structured porous materials in the two promising PEMFCs and SOFCs technologies.

Generally, porous materials for electrodes in fuel cells play two roles. One is transporting gases to/from the fuel cell electrodes. The key component of PEMFCs is the membrane-electrode assembly (MEA), which is composed of a polymer electrolyte membrane, catalyst layers for the anode and cathode, and gas diffusion layers (GDLs). Porous GDLs play an important role in forming current collectors, which not only collect/inject current, but which also enable the transport of gaseous fuels to the fuel cell electrodes, while rejecting water, the reaction product. The presence of hierarchically structured porous layers will undoubtedly favor gas fuel diffusion to fuel cell electrodes.[176,179,180] In SOFCs, porous ceramics are commonly used to provide the mechanical support for thin and delicate ceramic oxide electrolytes. In many cases these porous materials also play an important role in current collection on the anode or cathode side (**Figure 14**).[176] This scheme shows clearly the importance of hierarchically porous structures in the design of anodes and cathodes. The second vital role of porous materials is within the fuel cell electrodes. In both PEMFCs and SOFCs, the electrodes play a crucial role in minimizing losses attributable to electrode kinetics, and in some cases mass transport. This is achieved by maximizing the length of the so-called triple phase or three-phase boundary (TPB), a term describing the conjunction of a pore space, an ionically conducting phase, and an electronically conducting phase.[176–183] The hierarchical structures with ionic and electronic conducting phases and porosities at different length scales incorporated in one solid body should be an ideal configuration for electrode materials.

The introduction of porosity to electrodes permits the flow of reactants, facilitates electrode reactions and permits the flow of products. The important pore structure characteristics

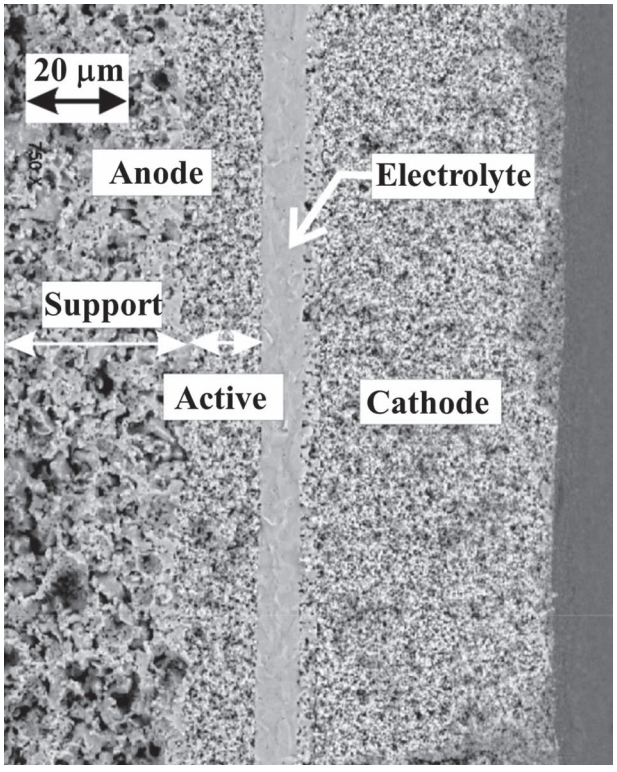

Figure 14. Example of the microstructure of an anode supported SOFC showing the cathode, electrolyte and an anode composed of an active catalyst region and anode support region. Reproduced with permission.[176] Copyright 2006, The Royal Society.

of electrodes are pore diameters, pore size distribution, pore surface area, and gas permeability. The development of hierarchically structured electrocatalysts and their supports can effectively address some of the current limitations of fuel cells. For example, to decrease the current cost of fuel cells, it is highly desirable to decrease Pt loading, while increasing the obtainable power densities and improve the durability of fuel cells. One way to increase the current density is through the design of the electrocatalyst with not only high surface area but also with a high number of accessible three-phase sites. Hierarchically porous structures owing to the presence of large pores and mesopores can effectively minimize transport limitations, thus increasing the accessibility of the active sites by gas and electrolyte phases. The GDL should be sufficiently porous to ensure effective reactant delivery but not so much as to compromise the through-plane electronic conductivity or mechanical properties; porosity values of 75% or higher are typical. Production of an effective GDL is largely a matter of controlling the structure and porosity of the material.[176,179,180] The vital role of GDL porosity in determining fuel cell performance has been studied by Chu and co-workers.[183] They found that it is important to consider the GDL as having a gradually dispersed porosity, owing to the spatially varying water content within the structure. As a consequence, hierarchically graded porosity of the GDL both in the thickness and laterally across the layer is expected to improve performance by assisting water removal and access of gas when reactant becomes depleted in the flow channel.

Recently, the direct methanol fuel cells (DMFC), based on the PEMFCs, has attracted great attention for its future potential as a clean and ideal power source. Challenges in anode electrocatalysis arise when the hydrocarbon fuel contains residual CO, or when methanol is to be directly electro-oxidized. Development of new catalysts with special structures is essential to increase the catalytic activity of methanol electro-oxidation. Hierarchically porous carbon materials, which possess high surface area, regulated pore volume, and structural integrity in the frameworks, has already demonstrated improvement on the methanol oxidation activity.[184–187] Yu and co-workers reported the use of the hierarchically porous carbons resulted in much improved catalytic activity for methanol oxidation in the fuel cell. Among the porous carbons studied in this work, the one with a mesoporosity of about 25 nm in pore diameter (Pt-Ru-C-25) showed the highest performance with power densities of ≈58 and ≈167 mW cm^{-2} at 30 and 70 °C, respectively. These values roughly correspond to ≈70 and ≈40% increase as compared to those of a commercially available Pt-Ru alloy catalyst (E-TEK), respectively. The structural integrity with good interconnectivity between different structures seems to be more important for the catalytic oxidation of methanol when the pore sizes get smaller.[185] Kim and Suslick used hierarchically porous carbon as catalyst supports for a DMFC catalyst and as pore formers in a membrane electrode assembly (MEA). The effect of these materials on unit cell performance was compared to traditional Vulcan XC-72 carbon nanoparticle powder. It has been demonstrated that the inclusion of these hierarchically organized porous carbon microspheres in electrodes is a simple, effective way to facilitate the mass transport of air and methanol during fuel cell operation due to the hierarchical porosity.[186] Wu and co-workers synthesized hierarchically ordered porous carbon via in situ self-assembly of colloidal polymer and silica spheres generating macropores and small interparticulate pores. The obtained hierarchically ordered porous carbons were used as the support of the Pt-Ru alloy catalyst and compared with the commercially available E-TEK catalysts with Pt-Ru alloy supported on carbon for methanol fuel cell applications. The cyclic voltammograms show that the specific mass current density at the same potential for the hierarchically porous carbon supported catalyst is considerably higher than that for the commercial catalyst in the forward as well as the reverse scan. This indicates that the Pt-Ru catalyst supported on their bimodal porous carbon has higher catalytic activity than the commercial E-TEK catalyst, due to the higher surface and more efficient diffusion of methanol and oxidized product in the 3D interconnected macropores and mesopores.[187]

Depending upon the fuel cell design, porous support materials for SOFCs can be fabricated either from the anode material and the cathode material. These materials are all characterized by a relatively coarse microstructure (particle size generally in the range of 1–20 mm) with porosity in the range of 30–40%. Hierarchically structured porous materials with high surface area are quite important for electrode materials in reducing the operating temperature of solid oxide fuel cells (SOFCs) by allowing easy diffusion of gaseous reactants and reducing the barrier for chemisorption by the electrode. For example, interesting oxygen ion and electron charge transport properties were observed in binary and ternary mesoporous yttria-stabilized-zirconia and metal (Pt, Ni)-yttria-zirconia solid solutions.[188–190]

By spontaneous assembly, mesoporous binary yttria-zirconia materials with an ordered channel-like macroporous structure have been synthesized. This thermally stable hierarchical structure provides large accessibility for gaseous reactants within the pores, enhancing the exchange rates of gaseous reactants by influencing adsorption equilibria and promoting overall charge-transfer reactions at the triple phase boundary that controls the efficiency of the SOFCs, which is thus applicable as a new SOFC electrode material.[191]

The SOFC is widely expected to play a major role in medium size electrical power generation, due to the possibility of operation using natural gas, zero emissions nitrogen and sulphur oxides, and very high cycle efficiencies when combined with a gas turbine. However, the production, transportation, and storage of hydrogen limit the use of fuel cells in commercial applications. A promising option is the reforming of natural gas, methanol, or other hydrocarbons. Nevertheless, the fast intrinsic kinetics of these reactions bring diffusion problems in the cell. Some theoretical calculations predict that the hierarchically macro-, meso-, and microporous structured catalysts can reduce the diffusion limitations.[192–195] Partial oxidation occurs at the anode and the products of this reaction are then consumed electrochemically, while oxygen is consumed electrochemically at the cathode. Because complications due to sealing are eliminated, the SOFC greatly simplifies system design and enhances thermal and mechanical shock resistance, thereby allowing rapid start up and cool down.[175]

3. Hierarchically Structured Porous Materials for Energy Storage

Energy storage is accomplished by devices or physical media that store some form of energy to perform some useful operation at a later time. Energy storage methods can be for example: 1) chemical H_2 or hydrocarbon storage, 2) biological storage such as glycogen or starch, 3) electrochemical storage such as batteries, 4) electrical storage for example capacitors or supercapacitors, 5) mechanical storage such as compressed air energy storage, and 6) thermal storage such as ice storage and stem accumulators, In this section, we concentrate on some most important research fields, such as Li ion batteries, supercapacitors, hydrogen storage, and solar thermal energy storage where hierarchically structured porous materials contribute to the important improvements in energy storage performance and efficiency.

3.1. Hierarchically Structured Porous Materials for Lithium Batteries

Lithium ion batteries are especially attractive because they can lead to an increase of 100–150% on storage capability per unit weight and volume compared with the more traditional aqueous batteries. Nevertheless, they still present a series of problems to be overcomed such as low energy and power density, large volume change on reaction, safety, and costs. All these challenges need new materials and new concepts.

A lithium-ion battery (sometimes Li-ion battery or LIB) is part of a family of rechargeable battery types in which lithium ions move from the negative electrode to the positive electrode during discharge, and back when charging. During discharge, lithium ions carry the current from the negative to the positive electrode, through the non-aqueous electrolyte and separator diaphragm. During charging, an external electrical power source (the charging circuit) applies a higher voltage (but of the same polarity) than that produced by the battery, forcing the current to pass in the reverse direction. The lithium ions then migrate from the positive to the negative electrode, where they become embedded in the porous electrode material in a process known as intercalation. Three primary functional components of a lithium-ion battery are the anode, cathode, and electrolyte. The anode of a conventional lithium-ion cell is made from insertion type materials such as carbon, the cathode is a Li containing metal oxide, and the electrolyte is a lithium salt in an organic solvent. The energy density of a battery is mainly determined by its output voltage and specific capacity, which are dependent on the electrochemical properties of electrode materials.

The diffusion of Li ions in electrolyte, electrodes, and at the electrolyte/electrode interface influences directly the electrochemical performance of LIBs, in particular the rate capability. Therefore, the pore structure of electrode materials is an important factor that largely determines the transport behavior of Li ions.

Hierarchically structured porous materials composed of well-interconnected pores and walls with a thickness of tens of nanometers can be readily used for enhancing the rate performance of LIBs since the solid-state diffusion length is much shorter and their relatively large surface area can also benefit the charge-transfer rate. In particular, hierarchically structured porous carbons provide several advantages for applications in LIBs and should be one of the most interesting materials to attract research attention.[196–201] Structured porous carbons can be prepared in a monolithic form and used as an active electrode without adding binders or conducting agents; their well-interconnected wall structure can provide a continuous electron pathway, yielding good electrical conductivity as Li ions in electrolytes can easily access the hierarchically porous surfaces.

A typical application of the hierarchically porous carbon in LIBs is shown by Stein and co-workers.[197] They prepared 3DOM (3D ordered macroporous) monoliths of hard carbon via a colloidal-crystal template method (**Figure 15**). They found that rate performance was significantly improved compared to similarly prepared non-templated carbon. A layer of SnO_2 coated on 3DOM carbon can further improve the rate performance and energy density. As a result, the first discharge capacity of 278 mAh g^{-1} was obtained, which is about 25% higher than that of pure 3D macroporous carbon. In a further study, they used a nanocasting method to produce hierarchically structured carbon (3DOM/m C) from silica templates with similar structural hierarchy. Then, monolithic carbon/carbon nanocomposites with a hierarchical macroporous structure were synthesized by filling a 3D ordered macro-/mesoporous carbon monolith with N-doped graphitic carbon via chemical vapor deposition (CVD) with acetonitrile as precursor (3DOM/m C/C). Depth-sensing indentation experiments revealed that the mechanical strength of a 3DOM/m C/C composite monolith was improved compared with 3DOM/m C, but 3DOM RFC monoliths prepared from resorcinol-formaldehyde precursors without templated mesopores in the wall were even stronger. Addition of a graphitic phase increased electronic conductivity of porous carbon, while lowering the capacity for lithium ions at low charge rates. Some advantages of the 3DOM/m C/C composite material in electrochemical experiments included a resistance toward forming a solid-electrolyte interface layer and greater lithium capacity at high charge and discharge rates, compared to 3DOM RFC with walls consisting only of amorphous carbon. Using carbon with hierarchical porosity as a basis for novel nanocomposites (including carbon and non-carbon guests within mesopores), leads to the possibility to fine-tune materials properties for a wide range of applications.[198]

Smarsly and co-workers prepared hierarchically porous carbon monoliths of macroscopic dimensions (several centimeters) and different shapes using meso-macroporous silica as a template. This porous carbon monolith with a mixed conducting 3D network shows a superior high rate performance when used as anode material in electrochemical lithium cells, due to the high porosity (providing ionic transport channels) and high electronic conductivity (ca. 0.1 S cm^{-1}).[199] Chen and co-workers used the hierachically porous carbon materials evaluated as Li ion battery anodes. It exhibits a giant first discharge capacity of 1704 mAh g^{-1} at a constant current density of 0.2 mA cm^{-2}, while the reversible capacity decreased to 200 mAh g^{-1}.[200]

On the basis of these studies, it can be concluded that there are several advantages to use hierarchical monolithic 3DOM carbon electrodes in Li-Ion (secondary) batteries: 1) solid state diffusion lengths for Li ions of the order of a few tens of nanometers, 2) a large number of active sites for charge-transfer reactions due to the high surface area of materials, 3) reasonable electrical conductivity due to a well-interconnected wall structure, 4) high ionic conductivity of the electrolyte within the 3DOM carbon matrix, and 5) no need for a binder and/or a conducting agent. They indicated that these factors can significantly improve rate performance compared to a similar but non-templated carbon electrode and compared to an electrode prepared from spherical carbon with binder.[197,198]

The metal oxide loaded in ordered macro-mesoporous carbon to enhance the capacity of the LIBs has recently attracted much attention. Zhao and co-workers synthesized ordered macroporous carbon with a 3D interconnected pore structure and a graphitic pore wall was prepared by CVD of benzene using inverse silica opal as the template and used this carbon material for LIBs application.[202] They found that the specific capacity was

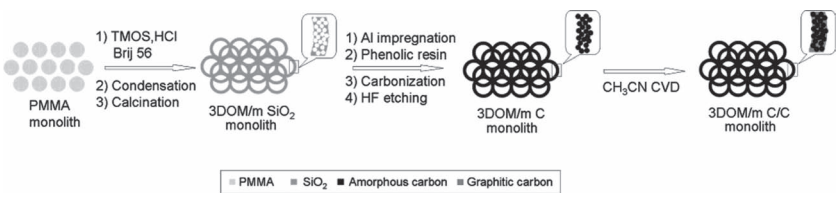

Figure 15. Diagram of the synthesis of 3DOM/m nanocomposite monoliths. Reproduced with permission.[198] Copyright 2006, American Chemical Society.

further improved when SnO_2 nanoparticles were supported on the hierarchically porous carbon, which is in agreement with the results of Stein and co-workers.[197] The hierarchically porous V_2O_5/carbon composites exhibited large capacity of more than 100 mAh g^{-1} and good rate capability of 80% at 5.0 A g^{-1}, due to large surface area and high rate lithium insertion to V_2O_5 gel. A calculation result indicates that a very high-power energy source with 177 mAh g^{-1} at 100 A g^{-1} is expected by using the nanoporous composite electrodes.[203] Long and co-workers prepared a flower-like Fe_3O_4/carbon nanocomposite with hierarchical nano/microporous structure. When used as the anode material for the lithium-ion batteries, the resultant nanocomposite shows high capacity and good cycle stability (1030 mAh g^{-1} at a current density of 0.2 C up to 150 cycles), as well as enhanced rate capability. The excellent electrochemical performance can be attributed to the high structural stability and high rate of ionic/electronic conduction arising from the synergetic effect of the unique hierarchical nano/microporous structure and conductive carbon coating.[204]

Due to the high theoretical capacity of 1675 mAh g^{-1}, the lithium-sulfur (Li-S) battery has been thought one of the great promising candidates for achieving the goal of large number of applications, such as electrical vehicles or high electrical vehicles.[205,206] However, there are two fatal factors that hinder their utilization for electrical vehicles: the low electrical conductivity of elemental sulfur and the solubility of the polysulfur formed during the electrochemical reaction process.[206–210] To solve the two key problems, it is necessary to introduce conductive additives and strong adsorbent agents with large surface areas to the system. In this sense, porous carbon materials, such as active carbon and carbon nanotubes, have been proved to be good candidates to improve the capacity and cycling stability of the sulfur electrodes due to large surface area, porous structure, and excellent conductivity.[211–213] In particular, recent reports demonstrated that the cathode made of sulfur on mesoporous carbon shows an excellent rate performance while retaining good cyclability of the cathode at low sulfur loading.[214] Therefore, the synthesis of the sulfur/porous carbon (S/PC) composite with highly developed porous structure and better electronic conductivity is a key issue for rechargeable Li-S batteries.[215–217] Liang and co-workers synthesized a hierarchical bimodal meso-microporous carbon material as a suitable substrate for the S/PC composite cathode material that possesses advantageous properties of high energy and high power over the cathodes made of monomodal mesoporous carbon or microporous carbon. The initial discharge capacity of the cells can be as high as 1584 mAh g^{-1} at a high current density of 2.5 A g^{-1}. The excellent performance of the hierachically bimodal porous carbon supported S/PC composite cathode is likely attributed to the synergetic effect of the hierarchically structured meso/microporosity: the microporosity gives high surface area and the micropore volume functions as a container that retains the sulfur species in the cathode region; the mesoporosity provides an avenue for the mass transport of Li ions and thus confers a high ionic conductivity to the cathode. Consequently, the cells can be discharged and charged at a high current density without compromising the cell capacity.[215] Gao and co-workers found that the sulfur/HPC (hierarchically porous carbon) composite with 57 wt% sulfur delivers the initial high specific capacity up to 1155 mAh g^{-1} and a stable capacity of 745 mAh g^{-1} after 84 cycles at the current density of 40 mA g^{-1}. In addition, it is demonstrated that the excellent cycling stability of the sulfur/HPC composite can be obtained at different current densities.[216]

$LiFePO_4$, a typical material for the lithium batteries, has been regarded as a good cathode material due to its appreciable capacity (a theoretical capacity of 170 mAh/$^{-1}$), moderate operating flat voltage, low cost, and low environmental impact. However, it has low electronic conductivity and low capacity, which severely limited its practical application at higher powers.[218–220] To overcome this problem, there have been numerous efforts of reducing the grain size of the samples and consequently the diminution of the diffusion length both for electrons and ions.[221] It has already been recognized that rate capability of $LiFePO_4$ was mainly controlled by its specific surface area and nanostructured electrodes could well improve the rate capability.[222,223] In fact, hierarchically structured porous electrodes which possess both macropores (>50 nm) and mesopores (2–50 nm) have a good potential to provide easy access of electrolyte ions to the electrode structure, where larger pores favor the mass transport of solvated ions into the smaller pores and thus reduce the transport limitation and the mesopores offer high surface areas while potentially avoiding the permanent trapping of lithium ions that is possible with micropores. The continuous macroporous network allows an efficient transport route for the solvated ions to get to the mesopores and thus may well improve the charge transport and power capacity.

Although hierarchically structured porous carbon monolith materials can be fabricated using the nanocasting of hard templates based on sol-gel method,[197–199] the preparation of a porous $LiFePO_4$ monolith directly using hard templates such as silica monolith is difficult because $LiFePO_4$ dissolves during removal of the template by reaction with HF or NaOH. In addition, $LiFePO_4$ could not be synthesized with a carbon monolith due to removal of the carbon template in the presence of oxygen causing the $LiFePO_4$ to oxidize into $Li_3Fe_2PO_4$ and other impurity phases. Using polymer colloids as a template to synthesize hierarchically porous $LiFePO_4$ shows its advantages, due to low calcination temperature. For example, Drummond and co-workers obtained macro- and mesoporous $LiFePO_4$ using poly(methyl methacrylate) (PMMA) colloidal crystal with different diameters and surfactant templates.[224] They found that the macropores produced using the 270 nm colloidal crystal template calcined at 700 °C offered both high surface areas and improved access to the active $LiFePO_4$ material, and hence this sample was able to obtain good discharge capacities of 160 mAh g^{-1}, which was close to the theoretical capacity. The hierachically structured meso-macroporous $LiFePO_4$ materials also performed better than monomodal macroporous $LiFePO_4$ at high discharge rates with capacities of 115 mAh g^{-1} reached at 5 C (**Figure 16**) confirming that a hierarchical porous structure can improve the rate capability.[224] For a better understanding of the link between hierarchically structured porous $LiFePO_4$ electrode materials and the electrochemical performance in Li-ion batteries, they further developed a $LiFePO_4$/carbon composite with hierarchically porous carbon monolith as an electrode material, which provides a robust, conductive framework into which the lithium iron phosphate can infiltrate. Electrochemical results showed discharge capacities for $LiFePO_4$ of

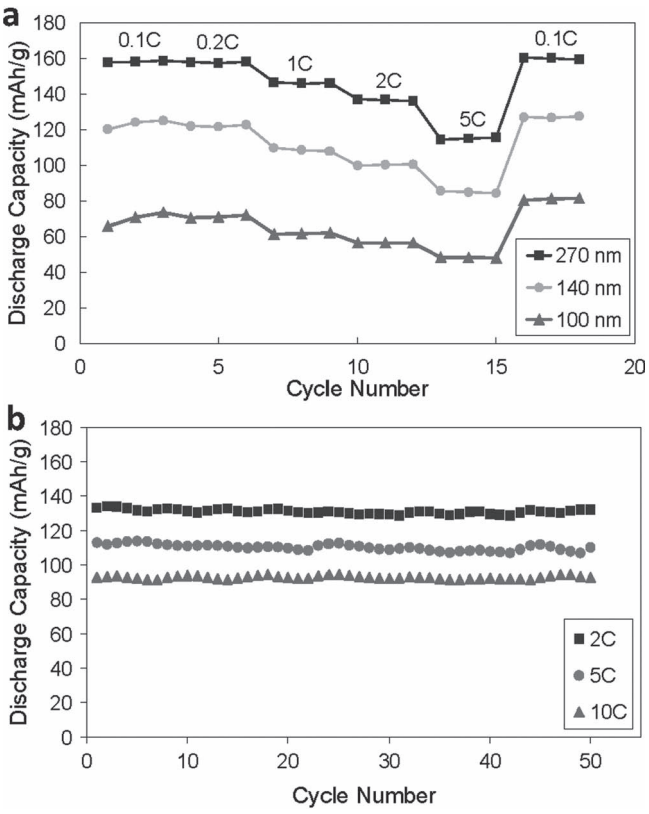

Figure 16. a) Comparison of discharge capacity for $LiFePO_4$ calcined at 700 °C and templated with different sized colloidal crystal templates and b) cyclability of $LiFePO_4$ sample templated with 270 nm colloidal crystal and calcined at 700 °C. Reproduced with permission.[224] Copyright 2009, American Chemical Society.

140 mAh g^{-1} at 0.1 C and 100 mAh g^{-1} at fast discharge rates of 5 C, showing again the importance of hierarchical porous structures for improving rate performance.[225]

The macro/mesoporous structures in hierarchically porous monolithic $LiFePO_4$/carbon composite potentially offer another benefit to enhance electrolyte access to the high interfacial areas and may improve the charge transport and power capability. This method of preparing electrodes provides a novel methodology of incorporating nanostructures into electrode materials. Instead of the traditional method of adhering nanoparticles/nanostructures to a flat current collector, the new collector becomes the nanostructured material onto which the electrode material is coated. This method could potentially avoid the addition of conductive and binding agents during the preparation of the electrodes, offering a significant advantage. Recently, more work on hierarchically porous $LiFePO_4$/carbon composite has been reported to enhance the capacity of the LIBs.[226–230] Stein and Vu[197,198] prepared three-dimensionally ordered macroporous and meso-/microporous (3DOM/m) $LiFePO_4$/C composite cathodes for lithium ion batteries by a multiconstituent, dual templating method. Millimeter-sized monolithic composite pieces were obtained in which $LiFePO_4$ was dispersed in a carbon phase around an interconnected network of ordered macropores. The composite walls themselves contained micropores or small mesopores. The carbon phase enhanced the electrical conductivity of the cathode and maintained $LiFePO_4$ in a highly dispersed phase during the synthesis and during electrochemical cycling. Monoliths containing 30 wt% carbon were electrochemically cycled in a three-electrode cell with lithium foil as counter and reference electrodes without additional binder or conductive agent. The capacity was as high as 150 mAh g^{-1} at a rate of 1/5 C, 123 mAh g^{-1} at 1C, 78 mAh g^{-1} at 8C, and 64 mAh g^{-1} at 16C, showing no capacity fading over 100 cycles. The macro-meso-microporous monolithic $LiFePO_4$/C composite was able to support current densities as high as 2720 mA g^{-1} in spite of the low electronic conductivity of bulk $LiFePO_4$ (10^{-9}–10^{-10} S cm^{-1}).[228] Munichandraiah and co-workers synthesized dual porous $LiFePO_4$/C composites. The composite prepared at 700 °C shows a better performance at all rates delivering discharge capacities of 156 and 56 mAh g^{-1} at 0.18 and 14.7 C rates, respectively, confirming the enhanced rate capability and stable capacity retention upon cycling with the bimodal porous $LiFePO_4$/C composites.[229] Richardson and co-workers obtained micrometer sized, 3D nanoporous spherical $LiFePO_4$/C composite by spray pyrolysis, which shows excellent cyclability (100% capacity retention in 100 cycles) and superior rate capability (106 mAh g^{-1} at 20 C).[230]

$LiMn_2O_4$ has also been extensively investigated for decades because with a theoretical energy density (150 mAh g^{-1}) comparable to that of $LiCoO_2$ (≈140 mAh g^{-1}) used commercially.[220,231] Most recently, mesoporous and hierarchically structured porous $LiMn_2O_4$ have been used for the lithium ion intercalation.[232–235] Bruce and co-workers synthesized mesoporous $LiMn_2O_4$ through a similar route by employing KIT-6 mesoporous material as template. The obtained mesoporous $LiMn_2O_4$ nearly doubled the capacity of bulk $LiMn_2O_4$ and possessed a much better cyclic stability than nanoparticulate $LiMn_2O_4$.[232] Xia and co-workers prepared well-ordered mesoporous spinel-structured $LiMn_2O_4$ by annealing the lithiated mesoporous MnO_2 at a low temperature of 350 °C. The lithiated MnO_2 was obtained by the chemical lithiation of LiI with mesoporous MnO_2. It was found that both low-temperature heat treatment and chemical lithiation processes could preserve the mesoporous structure of MnO_2. The ordered mesoporous $LiMn_2O_4$ showed high rate capability and excellent cycling ability as a cathode for lithium-ion batteries. It can maintain 94% of its initial capacity after 500 cycles and keeps 80% of its reversible capacity at 0.1 C rate, even at 5 C rate.[233] Tonti and co-workers prepared $LiMn_2O_4$ hierarchically macroporous inverse opal on conductive substrates and used as electrodes, showing fast and reversible lithium deinsertion over a large number of cycles without suffering significant morphological or electrochemical degradation. The original capacity is recovered if a lower rate is applied. Capacity loss over 30 discharge cycles at a rate of 20 μA is observed. Capacity stabilizes at 90% of the initial value, and no sign of any deterioration comparing SEM images before and after the electrochemical study. The open framework of an inverse opal sustains the volume changes produced very well during the insertion-deinsertion cycles.[234] Several other ordered macro-mesoporous structures, including $LiCoO_2$[236,237] and $LiNiO_2$,[238] have been prepared and explored for lithium ion batteries.

Spinel $Li_4Ti_5O_{12}$ has been considered as a promising anode material for LIB application, it has a good cyclic stability due to zero strain or volume change during charging and

discharging.[239–241] Furthermore, the spinel $Li_4Ti_5O_{12}$ possesses excellent reversibility, structural stability and excellent lithium ion mobility in the charge-discharge process. Therefore, it exhibits excellent cycling performance and great promise for high rate LIB applications.[242–244] However, similarly to $LiFePO_4$, it also suffered from poor rate capability due to low electronic conductivity.[245] Hierarchically porous structures have been designed to improve the performance of $Li_4Ti_5O_{12}$ at high powers.[246–248] For instance, Zhang and co-workers synthesized hierarchically porous $Li_4Ti_5O_{12}$ microspheres. The obtained $Li_4Ti_5O_{12}$ microspheres show outstanding rate and cycling performance. The specific discharge capacity is around 165.8 mAh g^{-1} obtained at a rate of 0.5 C, which is very close to the rate of 0.2 C. The specific discharge capacity was slightly reduced to 162.4, 156.8, 143.9, 134.6 and 116 mAh g^{-1} at rates of 1 C, 2 C, 3 C, 5 C and 10 C, respectively. At the high rate of 20 C, the specific charge capacity is still 92.3 mAh g^{-1}. Above 40 cycles, the $Li_4Ti_5O_{12}$ electrode was further charged-discharged at 2 C for another 200 cycles to investigate the cycling performance. The discharge capacity in the first cycle was 154.5 mAh g^{-1}, and after 200 charge-discharge cycles, the capacity remained at 147.4 mAh g^{-1}, which was less than 4.8% discharge capacity loss. The large surface area and rich and hierarchical diffusion channels ensure enough lithium ions to rapidly contact the much larger surfaces of the electroactive $Li_4Ti_5O_{12}$ microspheres and provide an easy and shorter diffusion pathway for ionic and electronic diffusion, resulting in extremely good power performance.[247] Chen and co-workers prepared $Li_4Ti_5O_{12}$ submicrospheres as anode materials of rechargeable lithium-ion batteries. The as-prepared $Li_4Ti_5O_{12}$ displayed excellent discharge/charge rate and cycling capability based on galvanostatical discharge/charge test and cyclic voltammetry (CV). A high discharge capacity of 174.3 mAh g^{-1} is obtained in the first discharge at 1 C rate. Meanwhile, there is only tiny capacity fading with nearly 100% columbic efficiency in the sequential 5–50 cycles. Moreover, calculated lithium-ion diffusion coefficient in $Li_4Ti_5O_{12}$ is 1.03×10^{-7} cm^2 s^{-1}, indicating that they are promising anode materials for rechargeable lithium-ion batteries for high power applications.[248]

Porous metal oxides have also been designed and used for the lithium ion batteries test. The mesoporous MnO_2 nanostructures have already displayed high lithium electrochemical activity because of the high surface area and larger pores compared to the conventional MnO_2 that is typical of electrochemical lithium inactivity.[249–251] For example, Bruce and co-workers used the mesoporous β-MnO_2 with a pore size centered at 3.65 nm, which exhibited a high capacity of 284 mAh g^{-1} and stabilized at 200 mAh g^{-1} after initial degradation at a current density of 15 mA g^{-1}, while bulk β-MnO_2 was for a long time assumed to be with extremely low intercalation capacity (below 60 mAh g^{-1}). This mesoporous electrode also possessed good rate capability by having 81% capacity remaining after the current density was increased to 300 mAh g^{-1}.[249] Recently, Guo and co-workers used hierarchically porous MnO_2 nanowall arrays on a platinum substrate for a lithium ion intercalation test to try to again improve the performance of mesoporous MnO_2. The experimental results revealed that both the discharge capacity and the cycle stability had been enhanced. When the film thickness was 0.5 μm, the initial capacity was as high as 256 mAh g^{-1} and after the thickness was increased to 2.5 μm, the initial capacity was still as high as 230 mAh g^{-1}. The cyclic stability improvement could be attributed to the hierarchically structured mesoporous MnO_2 nanowall arrays. As to the high discharge capacities at large deposition thickness, the macrostructure should play the key point. Besides the large surface area and shorter diffusion path provided for lithium-ion reaction, this honeycomb macroporous structure facilitated the penetration of electrolyte to the bottom of the array even when thickness was great, thus minimizing the adverse effect of high deposition thickness, i.e., difficulty of electrolyte penetration.[252]

Chen and co-workers prepared a hierarchically organized thin-film anode material composed of hollow porous spheres with a mean diameter of 5 μm. Each of the porous spheres consists of a multideck-cage structure, where the thickness of the "grids" ranges from around 60 to 100 nm (**Figure 17**a).[253]

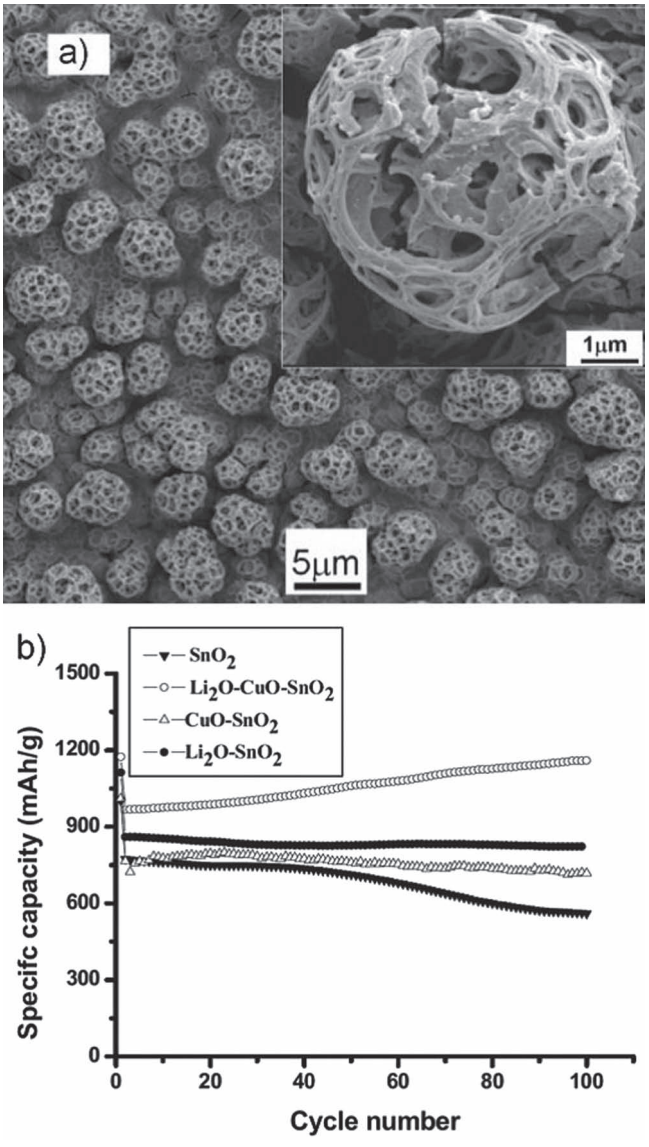

Figure 17. a) SEM image of the as-deposited thin film composed of a multideck-cage structured Li_2O-CuO-SnO_2. b) Capacity retention of the thin-film electrodes cycled between 0.01 and 3 V versus Li^+/Li at 0.5 C. Reproduced with permission.[253]

The morphology of the films was controlled to consist of special porous, spherical multideck-cage particles supported on a copper foil substrate. The Li_2O was introduced to suppress the aggregation of the Li-Sn alloy. The CuO was introduced to combine more Li per Sn metal and to improve the discharge capacity by enlarging the voltage range. These novel composites display outstanding cyclability when tested for Li storage in the voltage window 0.01–3.0 V. The ternary Li_2O-CuO-SnO_2 composite (molar ratio Li/Cu/Sn¼1:1:1) thin-film electrode shows a high reversible capacity of 1185.5 mAh g^{-1}, a low initial irreversible capacity loss of 17.6%, and nearly 100% capacity retention after 100 cycles at 0.5C (Figure 17b). Excellent rate capability is also demonstrated with an 8 C rate capacity of 525 mAh g^{-1}. The outstanding electrochemical performance of the Li_2O-CuO-SnO_2 electrode is attributed to its special hierarchically organized multideck-cage morphology and the ternary composition. In addition, the nanostructured particles shorten the transport lengths of Li ions, while the unique hierarchically porous structure ensures a large electrode-electrolyte contact area and confers the ability to accommodate the volume change during charge/discharge processes.[253]

In addition to the porous materials mentioned above, several ordered macro-mesoporous oxides or their based composite oxides, including SnO_2,[254–256] V_2O_5,[257–259] Co_3O_4,[260] NiO,[261–264] and TiO_2,[265–268] have been used for LIBs applications. The important improvements using hierarchically structured porous materials in Li-ions batteries has been superbly reviewed by several groups.[102,269,270] However, a challenge for future research as to its applicability in batteries is the improvement of the reversibility capacity.

3.2. Hierarchically Structured Porous Materials for Supercapacitors

Supercapacitors, also known as ultracapacitors, electronic, or electrochemical double layer capacitors (EDLC), pseudocapacitors, or supercondensers, are electrochemical capacitors with relatively high energy density. Compared to conventional electrolytic capacitors the energy density is typically on the order of hundreds of times greater. EDLCs also have a much higher power density over conventional batteries or fuel cells and do not have a conventional dielectric. Rather than two plates separated by an intervening substance, these capacitors use "plates" that are in fact two layers of the same substrate, and their electrical properties, the so-called "electrical double layer", result in the effective separation of charge despite the vanishingly thin (on the order of nanometers) physical separation of the layers. The lack of need for a bulky layer of dielectric permits the packing of plates with much larger surface area into a given size, resulting in high capacitances in practical-sized packages. In an electrical double layer, each layer by itself is quite conductive, but the physics at the interface where the layers are effectively in contact means that no significant current can flow between the layers. However, the double layer can withstand only a low voltage, which means that electric double-layer capacitors rated for higher voltages must be made of matched series-connected individual EDLCs, much like series-connected cells in higher-voltage batteries.

Research on supercapacitors is presently divided into two main areas that are based primarily on their mode of energy storage, namely: i) the electrochemical double layer capacitor (EDLC) and ii) the redox supercapacitor. The EDLC stores energy in much the same way as a traditional capacitor, by means of charge separation. By comparison, in redox supercapacitors (also referred to as pseudocapacitors), a reversible Faradaic-type charge transfer occurs and the resulting capacitance, while often large, is not electrostatic in origin (hence the pseudo prefix to provide differentiation from electrostatic capacitance).

The double layer capacitance can be described by Helmholtz equation:

$$C = \varepsilon_r \varepsilon_0 A/d \quad (7)$$

where ε_r is the dielectric constant of the electrolyte double-layer region, ε_0 is the dielectric constant of the vacuum, A is the surface area of the electrode, and d is the effective thickness of the electrical double layer (charge separation distance).[271] In double-layer capacitors, it is the combination of high surface-area with extremely small charge separation (Angstroms) that is responsible for their extremely high capacitance.[272] For a given EDLC, highly reversible charging/discharging and hundreds of thousands of cycles are typically attainable. However, as a consequence of electrostatic surface charging mechanism, these devices suffer from a limited energy density.[273]

In general, the use of a nanoporous material, typically activated charcoal, in place of the conventional insulating barrier can improve storage density of EDLCs. Activated charcoal is a powder made up of extremely small and very rough particles, which, in bulk, form a low-density heap with many holes that resembles a sponge. The overall surface area of even a thin layer of such a material is many times greater than a traditional material like aluminum, allowing many more charge carriers (ions or radicals from the electrolyte) to be stored in any given volume. The charcoal, which is not a good insulator, replaces the excellent insulators used in conventional devices, so in general EDLCs can only use low potentials at the order of 2 to 3 V. Activated charcoal is not the perfect material for this application. The charge carriers are actually (in effect) quite large especially when surrounded by molecules and are often larger than the holes left in the charcoal, which are too small to accept them, limiting the storage.

Research in EDLCs focuses on improved materials that offer higher usable surface areas. For this purpose, porous carbon materials are the first choice. A number of reviews have discussed the science and technology of surpercapacitors using carbon based materials, such as graphene, carbon nanotubes, carbon aerogel, solid activated carbon, and carbide-derived carbons.[274–279]

Applications in electrochemical capacitors of hierarchically structured porous carbon based composites such as ordered mesoporous carbon composites have recently been reviewed.[280] Previous studies provide some guidance to develop porous materials with controlled macro- and mesopores and to match the pore size with the ion size of electrolyte.[281,282] Today's EDLC research is largely focused on the increasing their energy performance and temperature limit. Here, we focus on how

to enhance the energy performance of the supercapacitors by using hierarchically structured porous materials.

HPCs are the most investigated materials. In fact, it has been predicted theoretically that hierarchically porous structures may lead to a better rate performance of supercapacitors compared to other kinds of porous carbons.[283,284] Considerable progress has been made to design and construct such HPCs and characterize their promising electrochemical capacitive properties. This high performance can be attributed to the generated pore surfaces that play a very important role in the formation of double-layer capacitance and to their unique hierarchical porous structures that favors the fast diffusion of electrolyte ions into the pores.[285–298] The hierarchical porous structure design is based on the different behaviors of electrolyte in pores with different sizes. Electrolyte in macropores, which maintains its bulk phase behavior, can reduce the transport length of ions inside a porous particle. Electrolyte ions have a smaller probability to crash against pore walls of large mesopores and hence reduce ion transport resistance. Macropores and mesopores can synergistically minimize the pore aspect ratio, while the strong electric potential in micropores can effectively trap ions and enhance the charge storage density. Therefore, a combination of macro-, meso-, micropores can result in high-performance electrode materials with short ion transport distance, low resistance, and large charge storage density. The use of hierarchically porous carbons in the design of supercapacitors was demonstrated and reviewed by Cheng and co-workers.[270]

Cheng and co-workers synthesized a 3D aperiodic hierarchically porous carbon. Different pore structures with macropores, mesoporous walls and micropores integrated in one carbon material as can be viewed in **Figure 18** and **Figure 19**.[288] This structure showed fast electron and ion transport and small equivalent series resistance (80 mΩ). The power density can be as high as 25 kW kg^{-1} and the energy density can even be

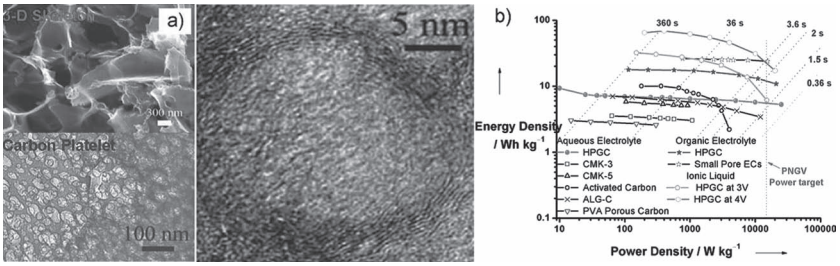

Figure 19. a) SEM and TEM images of the synthesized HPC. b) Ragone plot of the HPC in aqueous solution, organic electrolyte, and ionic liquid in comparison with other typical porous materials reported. Reproduced with permission.[288,289]

increased as high voltage electrolytes were used to, for example, 10 Wh kg^{-1} for 1 V electrolyst, 18 Wh kg^{-1} for 2.3 electrolyte, and 69 Wh kg^{-1} for a 4 V electrolyte (Figure 19b).[289]

Gao and co-workers reported an interesting hierarchical porous carbon with controlled micropores and mesopores. As supercapacitor electrode materials, they found the best electrochemical behavior with a specific gravimetric capacitance of 223 F g^{-1} and volumetric capacitance of 54 F cm^{-3} at a scan rate of 2 mV s^{-1} and 73% retained ratio at 50 mV s^{-1}. The good capacitive behavior may be attributed to the hierarchical pore structure (abundant micropores and interconnected mesopores with the size of 3–4 nm), high surface area (2749 m^2 g^{-1}), large pore volume (2.09 cm^3 g^{-1}), as well as well balanced micro- and mesoporosity.[290] In another study, Gao and co-workers confirmed the high performance of hierarchically porous carbons that the abondance of micropores and small mesopores increases the capacitance and make the electrolyte ions diffuse faster into the pores. These hierarchical porous carbons show high performance for supercapacitors possessing the optimized capacitance of 234 F g^{-1} in aqueous electrolyte and 137 F g^{-1} in organic electrolyte with high capacitive retention.[291] Further, they prepared hierarchical porous carbons taking alkaline-treated β-zeolite as the template by a two-step casting process. The carbon samples starting from alkaline-treated β-zeolite exhibit higher capacitance retentions than the sample started from β-zeolite due to the different pore structures. In aqueous electrolyte, the carbon sample replicated from alkaline treated β-zeolite presents the best electrochemical performance which could be attributed to the highest accessible specific surface area. In organic electrolyte, however, carbon samples replicated from pure β-zeolite showed the highest capacitance at low scan rate (or current load) consistant with the highest pseudocapacitance.[292]

As mentioned above, some electrochemical capacitors use fast reversible redox reaction at the surface of active materials, thus defining what is called the pseudocapacitors. The specific pseudo-capacitance exceeds that of carbon materials using double layer charge storage, justifying interest in these systems. But because redox reactions are used, pseudocapacitors, such as batteries, often suffer from a lack of stability during cycling. Ruthenium oxide or hydroxide,[299–302] is a typical classic metal oxide for pseudocapacitors due to highly conductivity and possesses three distinct oxidation states accessible within 1.2 V. A ruthenium hydroxide in aqueous H_2SO_4 possesses a high specific capacitance of 760 F g^{-1} and an excellent cycle-life stability.[303] However, ruthenium oxide is too expensive for

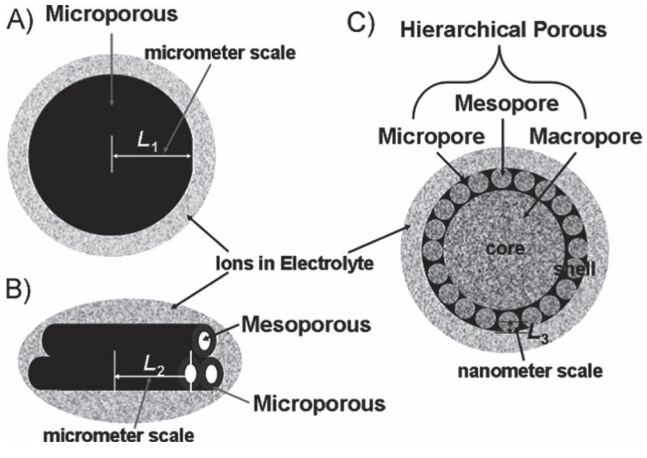

Figure 18. Illustration of the pore structures of a) AC, b) mesoporous carbon, and c) HPC. Reproduced with permission.[288]

commercialization. Most of the attention is, therefore, focused on alternative electrode materials that are inexpensive and exhibit capacitive behavior similar to that of ruthenium oxide.

In the alternative metal oxides, manganese, cobalt, nickel and iron oxides are the promising candidate transition metal oxides being studied for pseudocapacitor applications. In fact, cobalt oxide or hydroxide,[304–310] manganese oxide or hydroxide,[311–316] nickel oxide or hydroxide[317–325] have been extensively studied. Among such oxides and hydroxides, nickel oxide is of particular interest owing to its high theoretical specific capacitance of 2573 F g^{-1},[326,327] high chemical/thermal stability, ready availability, environmentally benign nature, and lower cost as compared to the state-of-the-art supercapacitor material RuO_2. However, the specific capacitances reported are still much lower than the corresponding theoretical value, which limited electrochemical utilization of nickel hydroxide/oxide. Improvement on its specific capacitance is becoming a challenge. Hierarchically porous nickel oxide film is a promising potential candidate to solve such a problem owing to its high surface area and easy ion infiltration. However, the report on the hierarchically porous nickel film for pseudocapacitor is limited partly due to the difficult preparation. Tu and co-workers prepared hierarchically porous NiO film by chemical bath deposition through a monolayer polystyrene sphere template. The film possesses a substructure of NiO monolayer hollow-sphere array and a superstructure of porous net-like NiO nanoflakes. The pseudocapacitive behavior of the NiO film is investigated by CV and galvanostatic charge-discharge tests in 1 M KOH. The hierarchically porous NiO film exhibits weaker polarization, better cycling performance and higher specific capacitance in comparison with the dense NiO film. The specific capacitance of the hierarchically porous NiO film is 309 F g^{-1} at 1 A g^{-1} and 221 F g^{-1} at 40 A g^{-1}, respectively, much higher than that of the dense NiO film (121 F g^{-1} at 1 A g^{-1} and 99 F g^{-1} at 40 A g^{-1}). The hierarchically porous architecture is responsible for the enhancement of electrochemical properties.[328]

Many kinds of electronically conducting polymers, such as polyaniline, polypyrrole, polythiophene and their derivatives, have also been used for pseudocapacitor applications in the past decades.[329–331] They have shown high gravimetric and volumetric pseudocapacitance in various non-aqueous electrolytes at operating voltages of about 3 V. However, conducting polymers suffer from a limited stability during cycling that reduces the initial performance.[273,275] Currently, research efforts with conducting polymers for supercapacitor applications are directed towards hybrid systems. For instance, Fu and co-workers prepared a polyacrylonitrile-based carbon material with a 3D continuous mesopore structure by using silica gel as a template. When used for a pseudocapacitor test, the sample carbonized at 800 °C demonstrated the highest specific capacitance of 210 F g^{-1} at the current density of 0.1 A g^{-1}, which could still stay over 90% when the current density increased by ten-fold. The combination of nitrogen functionalities, 3D continuous pore structure and the enhanced wettability should contribute to the good electrochemical properties.[332] Zhang and co-workers synthesized a porous and mat-like polyaniline/sodium alginate (PANI/SA) composite in an aqueous solution with sodium sulfate as a template. Cyclic voltammetry and galvanostatic charge/discharge tests were carried out to investigate the electrochemical properties. The PANI/SA nanostructure electrode exhibits an excellent specific capacitance as high as 2093 F g^{-1}, long cycle life, and fast reflect of oxidation/reduction on high current changes. The remarkable electrochemical characteristic is attributed to the hierarchically nanostructured porous electrode materials, which generates a high electrode/electrolyte contact area and short path lengths for electronic transport and electrolyte ion.[333] Fan and co-workers prepared a high-performance polyaniline electrode by potentiostatic deposition of aniline on a hierarchically porous carbon monolith, which was carbonized from the mesophase pitch. The obtained material demonstrated high pseudocapacitance values and high stability. A capacitance value as high as 2200 F g^{-1} (per weight of polyaniline) is obtained at a power density of 0.47 kW kg^{-1} and an energy density of 300 Wh kg^{-1}. These properties can be essentially attributed to the backbone role of HPCM, which has the advantage for the increase of ionic conductivity and power density.[334]

A hybrid surpercapacitor, combination of both Faradaic and non-Faradaic, offers an attractive alternative to EDLCs or conventional pseudocapacitors by combining a battery-like electrode (energy source) with a capacitor-like electrode (power source) in the same cell. Currently, two different approaches to hybrid systems have emerged: i) pseudo-capacitive metal oxides with a capacitive carbon electrode and ii) lithium-insertion electrodes with a capacitive carbon electrode. The improvement and development on the performance of supercapacitor has been reviewed in detail by Simon and Gogotsi.[275] Although most work has been done on the porous metal oxides/carbon electrode and lithium-insertion/carbon electrode,[335–338] the utilization of hierarchically structured porous materials for such a supercapacitor is still rare.[339,340] Cheng and co-workers prepared hierarchical porous nickel oxide and carbon as electrode materials for the construction of asymmetric supercapacitors. It was found that the capacitance, energy density, and power density of the asymmetric supercapacitor can be improved by elevating the supercapacitor voltage, and its cycling stability decays at high voltage, but the columbic efficiency stays close to 100%.[339] Kong and co-workers synthesized hierarchically porous composite materials consisting of nanoflake-like nickel hydroxide and mesoporous carbon, which shows the highest specific capacitance of 2570 F g^{-1} owing to the unique structure design in nickel hydroxide/mesoporous carbon composite in terms of its nanostructure, large specific surface area and good electrical conductance.[340] For automobile applications, the faradiac electrode led to an increase in the energy density at the cost of cyclability (for balanced positive and negative electrode capacities). This is the main drawback of the hybride devices, compared with EDLCs, and it is important to avoid transforming a good surpercapacitor into a mediocre battery.[275,341]

3.3. Hierarchically Structured Porous Materials for Hydrogen Storage

Hydrogen is considered the cleanest energy in the world and has great potential as an energy source, which makes hydrogen storage crucial for hydrogen cells or hydrogen-driven combustion engines. The research on hydrogen storage is focused on

the development of a safe, cheap, simple, and efficient storage method for practical utilization, such as mobile applications. To date, typical methods of storing hydrogen have involved storage of compressed gas, liquefied hydrogen, chemisorptions in the form of metal hydrides or physisorption using high surface adsorbents. Metal hydrides are the typical media for hydrogen storage. This method uses an alloy that can absorb and hold large amounts of hydrogen by bonding with hydrogen and forming hydrides. There are several problems regarding the metal hybrids for hydrogen storage. For example, the commercialized AB_5 type alloys, such as $LaNi_5$, can release hydrogen at room temperature, but have low gravimetric storage density.[342] High capacity metal hydrides, such as magnesium-based alloy and intermetallic compound Li_3Be_2 (theoretically ca. 7 wt% and 9 wt% of hydrogen storage capacity, respectively), cannot release hydrogen completely unless they are heated to a moderately high temperature.[343]

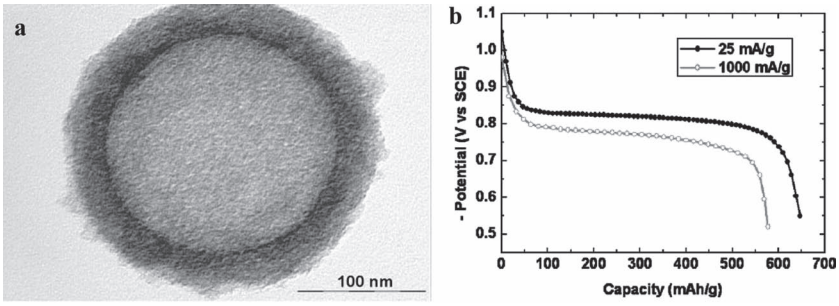

Figure 20. a) Representative TEM images for the HN-HCMSC $C_{180/40}$ and b) the first galvanostatic discharge curves at 25 and 1000 mA g^{-1} for the HN-HCMS $C_{180/40}$ electrode in 6 M KOH. Reproduced with permission.[355] Copyright 2008, American Chemical Society.

As compared to conventional low temperature-high pressure hydrogen storage technology, electrochemical hydrogen storage has been proved as elegant and more efficient at ambient pressure and temperature. Recently, lots of research has been conducted on electrochemical hydrogen storage in nanostructured materials, such as MoS_2 nanotubes,[344] $Cu(OH)_2$ nanoribbon,[345] and single walled carbon nanotubes (SWNTs).[346] In particular, nanostructured porous carbon materials with high specific surface area and highly developed micro-mesoporosity, such as activated carbon[347,348] and ordered mesoporous carbon (OMC),[349–352] have shown relatively high hydrogen storage capacities.

Recently, the hierarchically nanostructured porous materials have gradually attracted attention for hydrogen storage applications.[353–355] Ye and co-workers reported an electrochemical hydrogen uptake of 375 mAh g^{-1} at 50 mA g^{-1} for MoS_2 hierarchical hollow cubic cages,[353] which is ca. 44% larger than that (ca. 260 mAh g^{-1}) of MoS_2 nanotubes,[344] implying that the hierarchical nanostructure favors electrochemical hydrogen storage. Liang and co-workers reported that the hierarchically hollow palladium nanostructures exhibit enhanced activity for proton/hydrogen sensing compared to solid palladium nanoparticles, palladium microparticles, and bulk palladium electrode, indicating that the hierarchical structures have more advantages for hydrogen storage.[354] Yu and co-workers fabricated hierarchically nanostructured hollow macroporous core/mesomicroporous shell carbons (HN-HCMSCs) with various core sizes or shell thicknesses and explored this for the first time for electrochemical hydrogen storage (**Figure 20**a).[355] After the subtraction of the contributions of the electrical double layer (EDL) and the Ni current collector, a hydrogen desorption capacity of 586 mAh g^{-1} (corresponding to 2.17 wt% hydrogen uptake) has been achieved for the HN-HCMSC$_{180/40}$ at a discharge rate of 25 mA g^{-1}, which is larger than that (ca. 527 mAh g^{-1}) reported for the OMC,[351] strongly suggesting the advantage of hierarchically nanostructured porous networks over ordered mesoporous structure for electrochemical hydrogen storage. It is also found that the influence from the mass transport is smaller as compared to the contribution from the ohmic drop. Hydrogen desorption capacity of the HN-HCMSC$_{180/40}$ at 1000 mA g^{-1} decreased slightly by ca. 65 mAh g^{-1}, confirming that the HN-HCMSC$_{180/40}$ has an excellent rate capability, delivering the adsorbed hydrogen quickly at a high discharge rate. The hydrogen uptake (521 mAh g^{-1}) of the HN-HCMSC$_{180/40}$ at a discharge rate of 1000 mA g^{-1} is much larger than that (380 mAh g^{-1}) of purified multiwall nanotubes (MWNTs) at 100 mA g^{-1}[356] (Figure 20b).

Large hydrogen storage capacity, excellent capacity retainability, and rate capability are mainly attributable to the superb structural characteristics of the HN-HCMSCs including large specific surface area and micropore volume, and a particularly well-developed three-dimensionally interconnected hierarchical nanostructure. A large surface area and a large quantity of micropores are desirable for efficient hydrogen storage due to the enhanced electrochemical catalytic activity of the highly developed nanoporous structure. The macroporous hollow core can be used as an electrolyte solution buffering reservoir to minimize the diffusion distance to the interior surface of the mesoporous shell, while the mesoporous channels open to the macroporous core in the shell form fast mass transport networks around the micropores in the shell, which provides sites for the generation of hydrogen through electrochemical decomposition of water and the subsequent diffusion and adsorption of hydrogen. With this hierarchical nanostructure design, three electrochemical processes (i.e., buffering electrolyte species in the macroporous core, transporting electrolyte species through the mesoporous shell, and adsorptive hydrogen species in the micropores) involved in electrochemical hydrogen storage can take place very quickly and efficiently even at a high charging-discharging rate.[355]

More recently, the preparation of nanoporous carbon and of nanoporous carbon based hierarchical porous structures for hydrogen storage has been reported.[357–360] Vajo and co-workers found that the hierarchical structures formed by incorporating $LiBH_4$ within nanoporous carbon scaffolds can enhance hydrogen storage kinetics of $LiBH_4$. Their dehydrogenation rates up to 50 times faster than those in the bulk material are found at 300 °C. Furthermore, the activation energy for hydrogen desorption is reduced from 146 kJ mol^{-1} for bulk $LiBH_4$ to 103 kJ mol^{-1} for hierarchically nanostructured $LiBH_4$, and the faster kinetics result in desorption temperature reduction by up to 75 °C. In addition, the hierarchically

nanostructured hydrides exhibit increased cycling capacity over multiple sorption cycles.[359] Gao and co-workers synthesized nanoporous carbon materials with the presence of large pores and interparticulate pores by a two-steps casting process using zeolite 13X as template, which has an excellent performance on hydrogen storage at low temperature. A large hydrogen uptake capacity of 6.30 wt% has been achieved at 77 K and 20 bar. This good performance is because of the high surface area and high pore volume.[360] This demonstrated that the nanoporous carbons were a potential basic material for hydrogen storage.

Ordered porous carbons with tailored pore size, having ordered interconnected meso- and micropores for fast transportation of mass and highly developed ultramicropores for efficient adsorption of hydrogen, are expected to have higher hydrogen storage capacity than other nanostructured materials. Furthermore, for electrochemical hydrogen storage applications, in addition to interconnected macro- and mesopores as fast mass transportation pathways, highly developed micropores (<2 nm), especially ultramicropores (<0.7 nm), are mandatory for efficient hydrogen storage.[350,361–364] Since hierarchically carbonaceous materials offer benefits of low mass density and easy integration with hydrogen-active metals, investigations on hydrogen storage in hierarchically structured porous carbons are worth continuing unless a practical solution for large scale hydrogen storage comes out elsewhere. In these cases, the presence of macro-, meso-, and micropores in one porous carbon would be advantageous.

3.4. Hierarchically Structured Porous Materials for Solar Thermal Storage

New and renewable energy sources are being investigated all over the world. Nowadays, CO_2, produced mainly by the burning of fossil fuels, is considered to be responsible for more than 50% of the man-made greenhouse effect. Solar thermal power involves hardly any of the polluting emissions or environmental safety concerns associated with conventional, fossil or nuclear-based power generation. Utilization of solar thermal power offers a lot of benefits for both human life and the environment owing to very little pollution in the form of exhaust gases, dust, or fumes. Most importantly, in terms of the global environment, there are no emissions of carbon dioxide. In solar thermal generation, for practical reasons and ease of utilization, the storage of this kind of energy is indispensable since it can balance the energy demand between day and night. There are three methods to storage thermal energy: sensible heat, latent thermal energy, and chemical reactions. Among them, latent heat storage systems have the potential of storing a large amount of energy per unit mass. At present, the substances used for latent heat storage system are called phase change materials (PCMs). The PCM is solidified when cooling and melted when heating. PCMs can store a large amount of thermal energy with a constant temperature due to their high fusion heat (latent heat) during the phase transition, which offers a useful method for the appropriate utilization of solar energy.[365] PCMs allow large amounts of energy to be stored in relatively small volume, resulting in some of the lowest storage media costs. Unfortunately, most of the PCMs possess a low

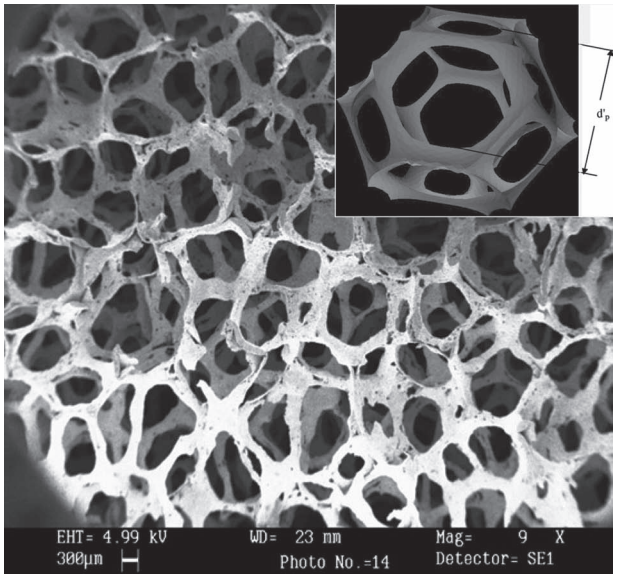

Figure 21. Typical cellular morphology open-celled metal foam. The inset is a representative unit cell. Reproduced with permission.[387] Copyright 2008, Elsevier B. V.

thermal conductivity (around 1 W mK^{-1}), which limits their deployment in large scale applications such as thermal solar power plants.[366]

To enhance the heat transfer for PCMs, several techniques have been used including adding high-conductivity particles,[367,368] carbon-fiber brushes,[369] finned tubes,[370–374] and metal matrix structure.[375–383] These techniques indeed have a great effect on increasing the PCMs' thermal conductivities. Among these techniques, the use of porous materials to enhance the heat transfer rates has been investigated.[384–391] A 3D porous network based PCM also offers a large heat storage density. Zhao and co-workers have extensively studied the porous metal foams with hierarchical structure for improving the thermal energy storage systems at high temperature (**Figure 21**).[384–390] They studied the effect of the copper and steel alloy based porous cellular foams with open cells with the addition of the $NaNO_3$ to the PCMs. All the data showed that the heat transfer was enhanced due to the high thermal conductivity of metal struts. The steel alloy demonstrated even better performance than that of copper. The heat transfer can also be enhanced by reducing the cell size because of the high contact surface area. However, the main problem of metal foam at high temperature is the corrosion in salty environments, which will reduce the positive effect of the metal foam.[390]

Another typical utilization of hierarchically structured porous material in solar thermal storage is the utilization of natural stone. The objective is to increase energy savings potentials and energy storage capacity of natural stone by improving its thermal properties by means of latent heat storage materials (PCMs). The treatment of natural stone with PCMs can supply the adjustment of porous systems and provides innovative products with thermal energy storage properties. This allows the storage and release of thermal energy during day/night cycles, contributing to reduced energy demands in buildings, and consequently to

CO_2 emission reduction. Additionally, health and human comfort indoors can be improved by the reduction of day/night temperature fluctuations. Therefore, treated natural stone can be used as construction materials to be able to store thermal energy and have materials with higher thermal inertia. Energy consumption in buildings (cooling/heating systems) is decreased and negative effects and damage to the environment are reduced. Hierarchically structured granular phase change composites (PCCs) have been prepared by the incorporation of PCM in porous materials. Nomura et al.[391] have prepared a series of PCCs by using expanded perlite (EP, a lightweight material with a high surface area and largely dispersed porosity due to the escape of trapped water), hierarchically bimodal porous diatoms (HPD), and monomodal mesoporous γ-Al_2O_3 (PA) using erythritol as PCM. It was found that both EP and HPD have much better latent heat performance than monomodal PA. In the cyclic test of heating and cooling, the EP based PCCs maintained 75 mass% of the initial latent heat after the test was repeated four times. This study demonstrated clearly that hierarchically packed granular PCCs prepared using porous natural stones are promising for conserving latent heat with high thermal density and provide no corrosion, enable quick heat transfer and offer a larger heat storage density if porous media with high porosity is selected. Results have shown that these new products based on natural stone have the ability to store energy.[392,393] Several good reviews have summarized the development of the PCMs for thermal storage.[394–397] The same strategy has been applied in a patent[398] for PCMs with hierarchically porous structures for construction material design. The macoporous pellets with porosity to account for volumic expansion have been prepared by a finely spreading by impregnation method of the PCM onto the surface of the porous materials. After which the porous materials are exposed to microwave energy to melt the PCM. The melted material is spontaneously absorbed into the pores generating a porous hierarchical structure with a layer of PCM on the surface of pores. The obtained construction materials with porous hierarchical structures are better able to absorb thermal energy and exhibit increased heat storage capacity.

One of the difficulties in the development of the highly efficient thermal storage materials containing PCMs is the incorporation in an efficient way and in a sufficient quantity of PCMs in matrix materials. A hierarchically porous media will be the best candidate to overcome this issue since large pores can ensure the heat transfer rates, large heat storage density and enough quantity of the PCMs whereas the small pores can lower the melting point of PCMs owing to the nanosize effect.[391] Another challenge to develop efficient thermal energy storage systems is low conductivity. Since porous materials can offer high thermal conductivity and high surface area, they can be used to form composites with PCMs to significantly enhance heat transfer. The light harvestor properties described in Section 2.1.1 could also provide an important guideline to design effecient solar thermal energy storage materials.

4. Conclusion and Outlook

Hierarchically structured porous materials prepared using natural materials as biotemplates to take advantage of their structures related to light harvesting and energy functions can be a good inspiration to develop new highly efficient materials. These materials have shown high potential in the development of highly efficient photocatalysts for photochemical H_2 production and are good models for the design of highly efficient DSSCs, FCs, light harvesters, LIBs, and supercapacitors. The immobilization of photosynthetic species holds great promise in future development of sunlight to chemical energy conversion by photosynthesis. The newly synthesized hierarchically structured porous materials open an exciting avenue to reduce the cost by greatly improving the performance of current DSSCs, FCs, photocatalysts, Li-ion batteries, and supercapacitors. **Table 1** summarizes the materials and their potential applications in energy conversion and storage. This review shows that important achievements can be made by using hierarchically structured porous materials.

However, present biotemplating methods are far from industrial being industrial processes. The scaling-up of biotemplating methods is still a wide gap to overcome. The lack of a sufficient number of biotemplates, in some case, renders the idea unrealizable. Nevertheless, materials obtained by biotemplates can be used as models due to their high efficiency. The leaf-like materials show a bright future while the extension of photosynthetic production for up to 6 months longer will be the key point for their industrialization. Rational design is still a heavy task if we want to reduce the current costs and to improve the performance of DSSCs, FCs, LIBs, and supercapacitors and render production processes more environmentally friendly with less waste by using more "green" materials.

Applications of hierarchically structured porous materials in CO_2 photoreduction will be a new and emerging research field considering their special optical properties and the benefits of a porous hierarchy. The foreseen improvements in CO_2 photoconversion efficiency, the selection of desired chemicals, and process cost will make the CO_2 photoreduction by water a reliable and sustainable energy technology that which not only mitigates CO_2 emission but also provides an efficient route of solar energy utilization.

The slow-photon effect found in hierarchically organized porous opaline photonic structures will also be an important phenomenon to explore, in spite of the few, but quite relevant, results demonstrating the enhancement in photocatalysis by using this kind of structure. The application of photonic structures holds important promise in all the fields relating to light, for examples photocatalysis, DSSCs, artificial photosynthesis, solar thermal storage, etc.

Although first studies using hierarchically structured porous materials in Li-ions batteries demonstrated great successes, a challenge for future research as to its applicability in batteries is the improvement of the reversibility capacity and their mechanical strength. The utilization of hierarchically structured porous materials in supercapacitor design is still rare. We are convinced that with the particular characteristics of hierarchically structured porous materials, the performance of supercapacitors can be further improved as described here. This domain still remains vierge. In the field of hydrogen storage, hierarchically structured porous materials have not been well explored. This could be another new research direction for scientists in this field.

Table 1. Summary of the hierarchically structured porous materials (HSPM) and their applications in energy conversion and storage.

Structures	Preparation method	Materials	Properties and applications	References
Hierarchical macro-mesopores	Biotemplates, such as leaves	Pt-/N-TiO_2	Enhanced light harvesting	[4,5]
	Brij56	TiO_2,	Enhanced light harvesting and ethylene photodegradation in gas-phase medium	[43]
	Biotemplates, polystyrene (PS), P123, etc.	TiO_2	Enhanced photodegradation dyes	[50,52–56]
	Metal doping, such as Au, Ag, Pt, etc.	Metal/TiO_2	Enhanced photodegradation dyes	[10,66–72]
	Element doping, such as B, C, N, etc.	Elements/TiO_2	Enhanced photocatalysis	[5,78,81,82]
	Carbon nanotubes, grapheme doping	CNTs/TiO_2, Graphene/TiO_2	Enhanced photocatalysis	[79]
	Semiconductors doping, such as ZrO_2, TeO_2, etc.	TiO_2/SiO_2, TiO_2/ZrO_2, etc.	Enhanced light harvesting and photodegradation	[44,88]
	Soft templates, hard templates	ZnO, WO_3, CeO_2, In_2O_3, Bi_2WO_6, etc.	Enhanced photocatalysis	[82,89–95]
Hierarchical meso-micropores	Electro-hydrodynamic	TiO_2	Enhanced photocatalysis	[51]
Hierarchical macro-meso-micropores	PS sphere, P123, F127	TiO_2	Enhanced light harvesting and photodegradation dyes	[45]
Hierarchical macro-mesopores	Biotemplates, such as leaves	Pt-/N-TiO_2, Fe_3C	Enhanced photochemical H_2 production	[4,5,7]
	Without template	$ZnIn_2S_4$,TiO_2	Enhanced photocatalytic H_2 production	[100,101]
Hierarchical macro-mesopores	Biotemplates, such as butterfly wings, diatoms	TiO_2	Enhanced light harvesting and DSSCs property	[31–33,109]
	Hard templates, such as silica, PS, PMMA, etc.	TiO_2	Enhanced power conversion efficiency for DSSCs	[111–114]
	Atomic layer decomposition (ALD)	TiO_2	low power conversion efficiency for DSSCs	[115]
	Hard template combining with lithography	TiO_2	Enhanced power conversion efficiency for DSSCs	[117]
	Self-assembly of nanoparticles	TiO_2	Improved photovoltaic efficiency for DSSCs	[121,122]
	Aggregation of nanocrystals	ZnO	Improved power conversion efficiency or photovoltaic efficiency for DSSCs	[124–126,128–132]
	Hard templates, soft templates	WO_3, FTO, etc.	Improved power conversion efficiency for DSSCs	[135–137]
	Hard templates, such as silica, etc.	Porous carbon (PC)	Improved power conversion efficiency or photovoltaic efficiency for DSSCs	[144,145]
Hierarchical macro-mesopores	Silica sol-gel immobilization cells	Whole cells or part of cell's	Photosynthesis for CO_2 capture or potential for biofuel cells	[14–30]
Mesopores	Sol-gel	TIO_2/SBA-15, Cu/TiO_2/SBA-15	Enhanced photoreduction of CO_2 to methanol and/or methane	[153,154]
	Sol-gel	Cu/TiO_2, Cu/TiO_2-SiO_2	Enhanced photoreduction of CO_2 to methane and CO	[155]
Micropores	Sol-gel	TiO_2/Y-Zeolites, TiO_2/β-Zeolites	Enhanced photoreduction of CO_2 to methanol	[156,157]
	Sol-gel	Ti silicate molecular sieve	Enhanced photoreduction of CO_2 to formic acid	[158]
	Sol-gel	ZrCu(I)-MCM-41 silicate sieve	Enhanced photoreduction of CO_2 to CO	[159]
Hierarchical macro-mesopores	Hard template and sol-gel	Pt-Ru/Carbon	Enhanced performances with power densities for FCs	[184–187]
Hierarchical mesopores	Hard templates	Y_2O_3-ZrO_2, (Pt, Ni)- Y_2O_3 -ZrO_2	Enhanced performances of oxygen ions and electron charges transport for FCs	[188–190]
Hierarchical macro-mesopores	Hard template, such as silica, PS, etc.	Porous carbon (PC)	Cathode for LIBs with enhanced capacity and recycles	[196–202]
	Silica template	SnO_2/PC, Fe_3O_4/PC	Anode for LIBs with enhanced capacity and recycles	[196,202,204]
	Silica template	V_2O_5/PC	Cathode for LIBs with enhanced capacity	[203]
	Silica template	S/PC	Cathode for LIBs with high energy and high power	[215–217]
	PMMA colloid crystal	$LiFePO_4$	Cathode for LIBs with high capacity and high discharge rate	[224]
	Silica template	$LiFePO_4$/PC	Cathode for LIBs with high capacity and high discharge rate	[225–230]

Table 1. (continued)

Structures	Preparation method	Materials	Properties and applications	References
Mesopores	KIT-6 template, Annealing MnO_2 as template	$LiMn_2O_4$	Cathode for LIBs with enhanced capacity and cycling stability	[232,233]
Hierarchical macro-mesopores	PS-MAA template	$LiMn_2O_4$	Cathode for LIBs with enhanced capacity and cycling stability	[234]
	Hard template	$LiCoO_2$	Cathode for LIBs with enhanced capacity	[236,237]
	Hard template	$LiNiO_2$	Cathode for LIBs with enhanced capacity	[238]
	Self assembly method	$Li_4Ti_5O_{12}$	Anode for LIBs with enhanced power and cycling performance	[207–248]
Mesopores	Hard templates	MnO_2	Anode for LIBs with high lithium electrochemical activity	[249–251]
Hierarchical macro-mesopores	Potentiostatic deposition method	MnO_2	Anode for LIBs with high capacity and cyclic stability	[252]
	Electrostatic spray deposition	Li_2O-CuO-SnO_2	Anode for LIBs with high capacity, reversibility and cyclic stability	[253]
	Hard template	SnO_2	Anode for LIBs with enhanced capacity	[254–256]
	Hard template	V_2O_5	Anode for LIBs with enhanced capacity	[257–259]
	Hard template	Co_3O_4	Anode for LIBs with enhanced capacity and cyclic stability	[260]
	Hard template	NiO	Anode for LIBs with enhanced capacity and cyclic stability	[261–264]
	Hard template	TiO_2	Anode for LIBs with enhanced capacity and cyclic stability	[265–268]
Hierarchical macro-meso-micropores	Phenolic resin and NiO as template	Porous carbon (PC)	Enhanced energy density for EDLCs	[288,289]
Hierarchical meso-micropores	CMK-1 and CMK-3 as template	PC	Enhanced capacitance for EDLCs	[290,291]
	Hard templates	PC	Enhanced capacitance for EDLCs	[293–298]
	alkaline-treated β-zeolite as template	PC	Enhanced capacitance for pseudocapacitors	[292]
	PS template	NiO	Enhanced capacitance for pseudocapacitors	[328]
	Silica nanoparticles template	PAN/PC	Enhanced capacitance for pseudocapacitors	[332]
	Sodium sulfate template	PANI/SA	Excellent capacitance for pseudocapacitors	[333]
	Potentiostatic deposition method	PANI/PC	Enhanced capacitance for pseudocapacitors	[334]
	P123 and Phenolic resin as template	NiO and PC	Enhanced capacitance for asymmetric capacitors	[339]
	CMK-3	NiO/PC	Enhanced capacitance for asymmetric capacitors	[340]
Hierarchical nanostructured pores	Sol-gel	MoS_2	Enhanced hydrogen uptake for H_2 storage	[353]
	Sol-gel	Pd	Enhanced activity for H_2 storage	[354]
	Silica template	PC	Enhanced capacity and discharge rate for H_2 storage	[355]
	Silica template	$LiBH_4$/PC	Enhanced low temperature storage for H_2 storage	[359]
	Zeolite 13X template	PC	Enhanced low temperature storage for H_2 storage	[360]
Mesopores	N/A	Copper, steel alloy in $NaNO_3$, etc.	Enhanced heat transfer rate for thermal storage	[384–390]
Hierarchical macro-mesopores	N/A	Nature stone	Construction materials for thermal storage	[392,393]

Research on hierarchically structured porous materials becomes a rapidly evolving field of current interest owing to their practical potential in different areas from nanoscience to catalysis, separation, electronics, optics, optoelectronics, energy, environmental, and life science.[399] This article illustrates only some examples of their application in energy storage and conversion. In spite of the great challenges in the fabrication of such materials, the recent important discovery of the self-formation phenomenon of porous hierarchy[43,399,400] provides foreseeable promise in their intelligent use and ease of synthesis of new advanced materials with tunable chemical compositions, excellent mechanical and chemical resistance, controllable micro-, meso-, and macroporosities at different length scales, and desired multifunctionalities for a determined application.

Acknowledgements

This work was realized in the frame of a "Changjiang" Innovative group program (IRT1169) financially supported by the Chinese Ministry of Education. B.L.S. thanks the Chinese Central Government for an "Expert

of the State" position in the program of "Thousand talents", the Chinese Ministry of Education for a "Changjiang" Chair Professor position located at the Wuhan University of Technology and the Clare Hall College and the Department of Chemistry at the University of Cambridge for a Clare Hall visiting fellow and financial support. Y.L. acknowledges Hubei Provincial Department of Education for the "Chutian Scholar" program. The authors would like to thank the graduate students, Miss Jing Liu, Miss Nan Jiang, Mr. Jun Jin, Mr. Shaozhuang Huang, Mr. Chao Wang, Mr. Li Wang, Mr. Zhiyi Hu, Mr. Yi Lu, and Mr. Wei Geng, for their very useful references collection. This work was also financially supported by "the Fundamental Research Funds for the Central Universities" (2011-IV-031), Hubei Provincial Natural Science Foundation (2011CDB425) and Self-determined and Innovative Research Funds of SKLWUT (2011-PY-2 and 2011-PY-3).

Received: February 29, 2012
Published online: July 5, 2012

[1] E. Shimoni, O. Rav-Hon, I. Ohad, V. Brumfeld, Z. Reich, *Plant Cell* **2005**, *17*, 2580.
[2] T. Fuhrmann, S. Landwehr, M. El Rharbi-Kucki, M. Sumper, *Appl. Phys. B* **2004**, *78*, 257.
[3] K. Koch, B. Bhushan, W. Barthlott, *Prog. Mater. Sci.* **2009**, *54*, 137.
[4] H. Zhou, X. Li, T. Fan, F. E. Osterloh, J. Ding, E. M. Sabio, D. Zhang, Q. Guo, *Adv. Mater.* **2010**, *22*, 951.
[5] X. F. Li, T. X. Fan, H. Zhou, S. K. Chow, W. Zhang, D. Zhang, Q. X. Guo, H. Ogawa, *Adv. Funct. Mater.* **2009**, *19*, 45.
[6] J. L. Gole, J. D. Stout, C. Burda, Y. B. Lou, X. B. Chen, *J. Phys. Chem. B* **2004**, *108*, 1230.
[7] Z. Schnepp, W. Yang, M. Antonietti, C. Giordano, *Angew. Chem. Int. Ed.* **2010**, *49*, 6564.
[8] C. Chen, W. Ma, J. Zhao, *Chem. Soc. Rev.* **2010**, *39*, 4206.
[9] J. H. Pan, H. Dou, Z. Xiong, C. Xu, J. Ma, X. S. Zhao, *J. Mater. Chem.* **2010**, *20*, 4512.
[10] J. Huang, X. Wang, Z. L. Wang, *Nano Lett.* **2006**, *6*, 2325.
[11] W. Zhang, D. Zhang, T. Fan, J. Ding, Q. Guo, H. Ogawa, *Micropor. Mesopor. Mater.* **2006**, *92*, 227.
[12] W. Zhang, D. Zhang, T. Fan, J. Ding, J. Gu, Q. Guo, H. Ogawa, *Bioinsp. Biomim.* **2006**, *1*, 89.
[13] J. I. L. Chen, G. Freymann, S. Y. Choi, V. Kitaev, G. A. Ozin, *J. Mater. Chem.* **2008**, *18*, 369.
[14] C. F. Meunier, P. V. Cambier, Y. U. Kwon, B. L. Su, *J. Mater. Chem.* **2009**, *19*, 4131.
[15] C. F. Meunier, J. C. Rooke, A. Leonard, P. V. Cutsem, B. L. Su, *J. Mater. Chem.* **2010**, *20*, 929.
[16] A. Leonard, J. C. Rooke, C. F. Meunier, H. Sarmento, J. P. Descy, B. L. Su, *Energy Environ. Sci.* **2010**, *3*, 370.
[17] C. F. Meunier, J. C. Rooke, A. Leonard, H. Xie, B. L. Su, *Chem. Commun.* **2010**, *46*, 3843.
[18] J. C. Rooke, A. Léonard, C. F. Meunier, H. Sarmento, J. P. Descy, B. L. Su, *J. Colloid Interface Sci.* **2010**, *344*, 348.
[19] C. F. Meunier, J. C. Rooke, K. Hajdu, P. V. Cutsem, P. Cambier, A. Leonard, B. L. Su, *Langmuir* **2010**, *26*, 6568.
[20] C. F. Meunier, P. Dandoy, B. L. Su, *J. Colloid Interface Sci.* **2010**, *342*, 211.
[21] C. F. Meunier, P. V. Cambier, Y. U. Kwon, B. L. Su, *J. Mater. Chem.* **2009**, *19*, 1535.
[22] J. C. Rooke, C. Meunier, A. Léonard, B. L. Su, *Pure Appl. Chem.* **2008**, *80*, 2345.
[23] J. C. Rooke, A. Léonard, H. Sarmento, J. P. Descy, B. L. Su, *J. Mater. Chem.* **2008**, *18*, 2833.
[24] J. C. Rooke, A. Léonard, B. L. Su, *J. Mater. Chem.* **2008**, *18*, 1333.
[25] J. C. Rooke, A. Léonard, C. F. Meunier, H. Sarmento, J. P. Descy, B. L. Su, *J. Colloid Interface Sci.* **2010**, *344*, 348.
[26] A. Léonard, Ph. Dandoy, E. Danloy, G. Leroux, C. F. Meunier, J. C. Rooke, B. L. Su, *Chem. Soc. Rev.* **2011**, *40*, 860.
[27] J. C. Rooke, A. Léonard, H. Sarmento, C. F. Meunier, J. P. Descy, B. L. Su, *J. Mater. Chem.* **2011**, *21*, 951.
[28] J. C. Rooke, B. Vandoorne, A. Léonard, C. F. Meunier, P. Cambier, H. Sarmento, J. P. Descy, B. L. Su, *J. Colloid. Interface Sci.* **2011**, *356*, 159.
[29] J. C. Rooke, A. Léonard, C. F. Meunier, B. L. Su, *ChemSusChem* **2011**, *4*, 1249.
[30] a) C. F. Meunier, X. Y. Yang, J. C. Rooke, B. L. Su, *ChemCatChem* **2011**, *3*, 376; b) X. Y. Yang, G. Tian, N. Jiang, B. L. Su, *Energy Environ. Sci.* **2012**, *5*, 5540.
[31] C. Jeffryes, T. Gutu, J. Jiao, G. L. Rorrer, *Mater. Sci. Eng. C-Biomimetic Supramol. Syst.* **2008**, *28*, 107.
[32] C. Jeffryes, T. Gutu, J. Jiao, G. L. Rorrer, *ACS Nano* **2008**, *2*, 2103.
[33] C. Jeffryes, T. Gutu, J. Jiao, G. L. Rorrer, *J. Mater. Res.* **2008**, *23*, 3255.
[34] D. Losic, P. J. Evans, A. Atanacio, J. G. Mitchell, N. H. Voelcker, *J. Mater. Chem.* **2006**, *16*, 4029.
[35] Z. Liu, T. Fan, W. Zhang, D. Zhang, *Micropor. Mesopor. Mater.* **2005**, *85*, 82.
[36] Z. Liu, T. Fan, D. Zhang, *J. Am. Ceram. Soc.* **2006**, *89*, 662.
[37] X. Li, T. Fan, Z. Liu, J. Ding, Q. Guo, D. Zhang, *J. Eur. Ceram. Soc.* **2006**, *26*, 3657.
[38] T. Fan, X. Li, Z. Liu, J. Gu, D. Zhang, Q. Guo, *J. Am. Ceram. Soc.* **2006**, *89*, 3511.
[39] T. Ota, M. Imaeda, H. Takase, M. Kobayashi, N. Kinoshita, T. Hirashita, H. Miyazaki, Y. Hikichi, *J. Am. Ceram. Soc.* **2000**, *83*, 1521.
[40] J. Cao, H. Sieber, *J. Porous Mater.* **2004**, *11*, 163.
[41] S. M. Holmes, P. Foran, P. Hill, E. P. L. Roberts, B. H. Sakakini, J. M. Newton, *Chem. Commun.* **2006**, *25*, 2662.
[42] Z. Bao, M. R. Weatherspoon, S. Shian, Y. Cai, P. D. Graham, S. M. Allan, G. Ahmad, M. B. Dickerson, B. C. Church, Z. Kang, H. W. Abernathy III, C. J. Summers, M. Liu, K. H. Sandhage, *Nature* **2007**, *446*, 172.
[43] a) X. C. Wang, J. C. Yu, C. M. Ho, Y. D. Hou, X. Z. Fu, *Langmuir* **2005**, *21*, 2552; b) *X. Y. Li, L. H. Chen, Y. Li, J. C. Rooke, C. Wang, Y. Lu, A. Krief, X. Y. Yang, B. L. Su, J.Colloid Interface Sci.* **2012**, *368*, 128; c) Y. Li, X. Y. Yang, G. Tian, A. Vantomme, J. G. Yu, G. Van Tendeloo, B. L. Su, *Chem. Mater.* **2010**, *22*, 3251; d) L. H. Chen, X. Y. Li, G. Tian, Y. Li, J. C. Rooke, G. S. Zhu, S. L. Qiu, X. Y. Yang, B. L. Su, *Angew. Chem. Int. Ed.* **2011**, *50*, 11156; e) L. H. Chen, X. Y. Li, G. Tian, Y. Li, H. Y. Tan, G. Van Tendeloo, G. S. Zhu, S. L. Qiu, X. Y. Yang, B. L. Su, *ChemSusChem* **2011**, *4*, 1452; f) X. Y. Yang, G. Tian, L. H. Chen, Y. Li, J. C. Rooke, Y. X. Wei, Z. M. Liu, Z. Deng, G. Van Tendeloo, B. L. Su, *Chem. Eur. J.* **2011**, *17*, 14987; g) X. Y. Yang, A. Leonard, A. Lemaire, G. Tian, B. L. Su, *Chem. Commun.* **2011**, *47*, 2763; h) X. Y. Yang, Y. Li, G. Van Tendeloo, F. S. Xiao, B. L. Su, *Adv. Mater.* **2009**, *21*, 1368; i) X. Y. Yang, Y. Li, A. Lemaire, J. G. Yu, B. L. Su, *Pure Appl. Chem.* **2009**, *81*, 2265; j) Z. Y. Yuan, T. Z. Ren, A. Azioune, J. J. Pireaux, B. L. Su, *Chem. Mater.* **2006**, *18*, 1753; k) B. L. Su, A. Vantomme, L. Surahy, R. Pirard, J. P. Pirard, *Chem. Mater.* **2007**, *19*, 3325.
[44] X. F. Chen, X. C. Wang, X. Z. Fu, *Energy Environ. Sci.* **2009**, *2*, 872.
[45] F. Bosc, P. Lacroix-Desmazes, A. Ayral, *J. Colloid Interface Sci.* **2006**, *304*, 545.
[46] D. R. Rolison, J. W. Long, J. C. Lythe, A. F. Fischer, Ch. P. Rhodes, T. M. Mc Evoy, M. E. Bourg, A. M. Lubers, *Chem. Soc. Rev.* **2009**, *38*, 226.
[47] Z. G. Guo, W. M. Liu, B. L. Su, *Appl. Phys. Lett.* **2008**, *93*, 201909.
[48] Y. Li, X. Y. Yang, Y. Feng, Z. Y. Yuan, B. L. Su, *Crit. Rev. Solid State Mater. Sci.* **2012**, *37*, 1.
[49] X. B. Chen, S. S. Mao, *Chem. Rev.* **2007**, *107*, 2891.
[50] S. M. Zhu, D. Zhang, Z. X. Chen, G. Zhou, H. B. Jiang, J. L. Li, *J. Nanopart. Res.* **2010**, *12*, 2445.

[51] Y. Zhao, X. T. Zhang, J. Zhai, J. L. He, L. Jiang, Z. Y. Liu, S. Nishimoto, T. Murakami, A. Fujishima, D. B. Zhu, *Appl. Catal. B* **2008**, *83*, 24.
[52] J. G. Yu, Y. R. Su, B. Cheng, *Adv. Funct. Mater.* **2007**, *17*, 1984.
[53] M. Wu, Y. Li, Z. Deng, B. L. Su, *ChemSusChem.* **2011**, *4*, 1481.
[54] J. I. L. Chen, G. Von Freymann, S. Y. Choi, V. Kitaev, G. A. Ozin, *Adv. Mater.* **2006**, *18*, 1915.
[55] J. I. L. Chen, G. A. Ozin, *J. Mater. Chem.* **2009**, *19*, 2675.
[56] J. I. L. Chen, G. Von Freymann, V. Kitaev, G. A. Ozin, *J. Am. Chem. Soc.* **2007**, *129*, 1196.
[57] J. I. L. Chen, E. Loso, N. Ebrahin, G. A. Ozin, *J. Am. Chem. Soc.* **2008**, *130*, 5420.
[58] Y. Z. Li, T. Kunitake, S. Fujikawa, *J. Phys. Chem. B* **2006**, *110*, 13000.
[59] F. Sordello, C. Duc, V. Maurino, C. Minero, *Chem. Commun.* **2011**, *47*, 6147.
[60] Z. Cai, J. Teng, Z. Xiong, Y. Li, Q. Li, X. Lu, X. S. Zhao, *Langmuir* **2011**, *27*, 5157.
[61] M. N. Patel, R. D. Williams, R. A. May, H. Uchida, K. J. Stevenson, K. P. Johnston, *Chem. Mater.* **2008**, *20*, 6029.
[62] X. Wang, R. A. Caruso, *J. Mater. Chem.* **2011**, *21*, 20.
[63] J. T. Carneiro, T. J. Savenije, G. Mul, *Phys. Chem. Chem. Phys.* **2009**, *11*, 2708.
[64] C. J. Liu, T. Y. Yang, C. H. Wang, C. C. Chien, S. T. Chen, C. L. Wang, W. H. Leng, Y. Hwu, H. M. Lin, Y. C. Lee, C. L. Cheng, J. H. Je, G. Margaritondo, *Mater. Chem. Phys.* **2009**, *117*, 74.
[65] A. V. Rupa, D. Divakar, T. Sivakumar, *Catal. Lett.* **2009**, *132*, 259.
[66] V. Iliev, D. Tomova, L. Bilyarska, G. Tyuliev, *J. Mol. Catal. A: Chem.* **2007**, *263*, 32.
[67] Y. Mizukoshi, Y. Makise, T. Shuto, J. W. Hu, A. Tominaga, S. Shironita, S. Tanabe, *Ultrason. Sonochem.* **2007**, *14*, 387.
[68] J. Xu, Y. Sun, Y. M. Zhao, J. J. Huang, C. M. Chen, Z. Y. Jiang, *Int. J. Photoenergy* **2007**, 1, article ID: 97308.
[69] J. C. Yu, X. Wang, X. Fu, *Chem. Mater.* **2004**, *16*, 1523.
[70] J. Disdier, J. M. Herrmann, P. Pichat, *J. Chem. Soc. Faraday Trans.* **1983**, *79*, 651.
[71] J. S. Curran, D. Lamouche, *J. Phys. Chem.* **1983**, *87*, 5405.
[72] A. Wood, M. Giersig, P. Mulvaney, *J. Phys. Chem. B* **2001**, *105*, 8810.
[73] J. Lukáč, M. Klementová, P. Bezdička, S. Bakardjieva, J. Šubrt, L. Szatmáry, Z. Bastl, J. Jirkovský, *Appl. Catal. B* **2007**, *74*, 83.
[74] C. Adán, A. Bahamonde, M. Fernández-García, A. Martínez-Arias, *Appl. Catal. B* **2007**, *72*, 11.
[75] R. Asahi, T. Morikawa, T. Ohwaki, K. Aoki, Y. Taga, *Science* **2001**, *293*, 269.
[76] S. U. M. Khan, M. Al-Shahry, W. B. Ingler Jr, *Science* **2002**, *297*, 2243.
[77] D. Li, H. Haneda, S. Hishita, N. Ohashi, *Chem. Mater.* **2005**, *17*, 2596.
[78] J. Xu, B. Yang, M. Wu, Z. Fu, Y. Lv, Y. Zhao, *J. Phys. Chem. C* **2010**, *114*, 15251.
[79] J. Du, X. Lai, N. Yang, J. Zhai, D. Kisailus, F. Su, D. Wang, L. Jiang, *ACS Nano* **2010**, *5*, 590.
[80] T. L. Thompson, J. T. Yates, *Chem. Rev.* **2006**, *106*, 4428.
[81] N. Shi, X. Li, T. X. Fan, H. Zhou, J. Ding, D. Zhang, H. Zhu, *Energy Environ. Sci.* **2011**, *4*, 172.
[82] T. Han, T. Fan, S. K. Chow, D. Zhang, *Bioresour. Technol.* **2010**, *101*, 6829.
[83] S. Wang, Q. M.Gong, J. Liang, *Ultrason. Sonochem.* **2009**, *16*, 205.
[84] H. Zhang, X. J. Lv, Y. M. Li, Y. Wang, J. H. Li, *ACS Nano* **2010**, *4*, 380.
[85] M. R. Hoffmann, S. T. Martin, W. Choi, D. W. Bahnemann, *Chem. Rev.* **1995**, *95*, 69.
[86] A. L. Linsebigler, G. Lu, J. T. Yates, *Chem. Rev.* **1995**, *95*, 735.
[87] O. Carp, C. L. Huisman, A. Reller, *Prog. Solid State Chem.* **2004**, *32*, 33.
[88] S.-Z. Chu, S. Inoue, K. Wada, D. Li, H. Haneda, S. Awatsu, *J. Phys. Chem. B* **2003**, *107*, 6586.
[89] F. Xu, P. Zhang, A. Navrotsky, Z. Y. Yuan, T. Z. Ren, M. Halasa, B. L. Su, *Chem. Mater.* **2007**, *19*, 5680.
[90] G. Xi, B. Yue, J. Cao, J. Ye, *Chem. Eur. J.* **2011**, *17*, 5145.
[91] Y. Huang, Z. Ai, W. Ho, M. Chen, S. Lee, *J. Phys. Chem. C* **2010**, *114*, 6342.
[92] S. Rengaraj, S. Venkataraj, C.-W Tai, Y. Kim, E. Repo, M. Sillanpää, *Langmuir* **2011**, *27*, 5534.
[93] O. Ruzimuradov, G. Hasegawa, K. Kanamori, K. Nakanishi, *J. Am. Ceram. Soc.* **2011**, *94*, 3335.
[94] F. Lu, W. P. Cai, Y. G. Zhang. *Adv. Funct. Mater.* **2008**, *18*, 1047.
[95] Y. Zhao, M. Wei, J. Lu, Z. L. Wang, X. Duan. *ACS Nano* **2009**, *3*, 4009.
[96] A. Fujishima, K. Honda, *Nature* **1972**, *238*, 37.
[97] M. D. Hernández-Alonso, F. Fresno, S. Suárez, J. M. Coronado, *Energy Environ. Sci.* **2009**, *2*, 1231.
[98] N. Serpone, D. Lawless, R. Terzian, *Sol. Energy* **1992**, *49*, 221.
[99] T. Kodama, N. Gokon, *Chem. Rev.* **2007**, *107*, 4048.
[100] B. Chai, T. Peng, P. Zeng, X. Zhang, X. Liu, *J. Phys. Chem. C* **2011**, *115*, 6149.
[101] P. Hartmann, D. -K. Lee, B. M. Smarsly, J. Janek, *ACS Nano* **2010**, *4*, 3147.
[102] H. Zhou, T. Fan, D. Zhang, *ChemSusChem* **2011**, *4*, 1344.
[103] F. E. Osterloh, *Chem. Mater.* **2008**, *20*, 35.
[104] K. Maeda, K. Domen, *J. Phys. Chem. C* **2007**, *111*, 7851.
[105] M. A. Bizeto, A. L. Shiguihara, V. R. L. Constantino. *J. Mater. Chem.* **2009**, *19*, 2512.
[106] A. Kudo, Y. Miseki, *Chem. Soc. Rev.* **2009**, *38*, 253.
[107] M. Grätzel, *Nature* **2001**, *414*, 338.
[108] B. D. Heilman, I. N. Miaoulis, *Appl. Opt.* **1994**, *33*, 6642.
[109] W. Zhang, D. Zhang, T. J. Fan, J. J. Gu, J. Ding, H. Wang, Q. X. Guo, H. Ogawa, *Chem. Mater.* **2009**, *21*, 33.
[110] Y. Li, F. Piret, T. Léonard, B. L. Su, *J. Colloid Interface Sci.* **2010**, *348*, 43 .
[111] E. Kwak, W. Lee, N. -G. Park, J. Kim, H. Lee, *Adv. Funct. Mater.* **2009**, *19*, 1093.
[112] J. Du, X. Y. Lai, J. E. Halpert, Y. Yang, D. Wang, *Sci. China Chem.* **2011**, *54*, 930.
[113] J.-H. Shin, J. H. Moon, *Langmuir* **2011**, *27*, 6311.
[114] J. Lei, X. Li, W. Li, F. Sun, D. Lu, J. Yi, *Inter. J. Hydrog. Energy* **2011**, *36*, 8167.
[115] L. Liu, S. K. Karuturi, L. T. Su, A. I. Y. Tok, *Energy Environ. Sci.* **2011**, *4*, 209–215.
[116] J. S. King, E. Graugnard, C. J. Summers, *Adv. Mater.* **2005**, *17*, 1010.
[117] C.-Y. Cho, J. H. Moon, *Adv. Mater.* **2011**, *23*, 2971.
[118] E. J. W. Crossland, M. Nedelcu, C. Ducati, S. Ludwigs, M. A. Hillmyer, U. Steiner, H. J. Snaith, *Nano Lett.* **2009**, *9*, 2813.
[119] D. H. Chen, F. Z. Huang, Y. B. Cheng, R. A. Caruso, *Adv. Mater.* **2009**, *21*, 2206.
[120] J. H. Moon, J. Ford, S. Yang, *Polym. Adv. Technol.* **2006**, *17*, 83.
[121] J. T. Park, D. Y. Roh, R. Patel, E. Kim, D. Y. Ryu, J. H. Kim, *J. Mater. Chem.* **2010**, *20*, 8521.
[122] D. Hwang, H. Lee, S.-Y. Jang, S. M. Jo, D. Kim, Y. Seo, D. Y. Kim, *ACS Appl. Mater. Interface* **2011**, *3*, 2719.
[123] Q. Zhang, C. S. Dandeneau, X. Zhou, G. Cao, *Adv. Mater.* **2009**, *21*, 4087.
[124] T. P. Chou, Q. F. Zhang, G. E. Fryxell, G. Z. Cao, *Adv. Mater.* **2007**, *19*, 2588.
[125] Q. F. Zhang, T. P. Chou, B. Russo, G. E. Fryxell, S. A. Jenekhe, G. Z. Cao, *Angew. Chem. Int. Ed.* **2008**, *47*, 2402.

[126] Q. F. Zhang, T. P. Chou, B. Russo, S. A. Jenekhe, G. Z. Cao, *Adv. Funct. Mater.* **2008**, *18*, 1654.
[127] G. Z. Cao, *SPIE Newsroom.* **2008**, DOI: 10.1117/2.1200809.1266.
[128] Q. F. Zhang, C. S. Dandeneau, S. Candelaria, D. W. Liu, B. B. Garcia, X. Y. Zhou, Y. H. Jeong, G. Z. Cao, *Chem. Mater.* **2010**, *22*, 2427.
[129] H. M. Cheng, W. F. Hsieh, *Energy Environ. Sci.* **2010**, *3*, 442.
[130] J. X. Wang, C. M. L. Wu, W. S. Cheung, L. B. Luo, Z. B. He, G. D. Yuan, W. J. Zhang, C. S. Lee, S. T. Lee, *J. Phys. Chem. C* **2010**, *114*, 13157.
[131] Y. Qiu, W. Chen, S. Yang, *J. Mater. Chem.* **2010**, *20*, 1001.
[132] V. M. Guerin, C. Magne, Th. Pauporté, T. Le Behers, J. Rachousky, *ACS Appl. Mater. Interface* **2010**, *2*, 3677.
[133] M. Grätzel, *Inorg. Chem.* **2005**, *44*, 6841.
[134] M. K. Nazeeruddin, F. D. Angelis, S. Fantacci, A. Selloin, G. Viscardi, P. Liska, S. Ito, B. Takeru, M. Grätzel, *J. Am. Chem. Soc.* **2005**, *127*, 16835.
[135] X. Chen, J. Ye, S. Ouyang, T. Kako, Z. Li, Z. Zou, *ACS Nano* **2011**, *5*, 4310.
[136] E. Arsenault, N. Soheilnia, G. A. Ozin, *ACS Nano* **2011**, *5*, 2984.
[137] Z. Yang, S. Gao, W. Li, V. Vlasko-Vlasov, U. Welp, W.-K. Kwok, Tao Xu, *ACS Appl. Mater. Interface* **2011**, *3*, 1101.
[138] G. Wang, W. Xing, S. Zhuo, *J. Power Sources* **2009**, *194*, 568.
[139] J. G. Nam, Y. J. Park, B. S. Kim, J. S. Lee, *Scr. Mater.* **2010**, *62*, 148.
[140] Y. H. Deng, C. Liu, T. Yu, F. Liu, F. Q. Zhang, Y. Wan, L. Zhang, C. Wang, B. Tu, P. A. Webley, H. Wang, D. Zhao, *Chem. Mater.* **2007**, *19*, 3271.
[141] Z. Y. Wang, E. R. Kiesel, A. Stein, *J. Mater. Chem.* **2008**, *18*, 2194.
[142] J. Z. Zhao, F. Y. Cheng, C. H. Yi, J. Liang, Z. L. Tao, J. Chen, *J. Mater. Chem.* **2009**, *19*, 4108.
[143] X. B. Lu, Y. Xiao, Z. B. Lei, J. P. Chen, *Biosens. Bioelectron.* **2009**, *25*, 244.
[144] S.-Q. Fan, B. Fang, J. H. Kim, B. Jeong, C. Kim, J.-S. Yu, J. Ko, *Langmuir* **2010**, *26*, 13644.
[145] B. Fang, S.-Q. Fan, J. H. Kim, M.-S. Kim, M. Kim, N. K. Chaudhari, J. Ko, J.-S. Yu, *Langmuir* **2010**, *26*, 11238.
[146] T. Hiyama, *Physiol. Veg.* **1985**, *23*, 605.
[147] N. Mallick, *Biometals* **2002**, *15*, 377.
[148] S. S. Tan, L. Zhou, E. Hu. *Catal. Today* **2006**, *115*, 269.
[149] E. C. C. Baly, I. M. Heilbron, W. F. Barker, *J. Chem. Soc. Trans.* **1921**, *119*, 1025.
[150] E. C. C. Baly, I. M. Heilbron, D. P. Hudson, *J. Chem. Soc. Trans.* **1922**, *121*, 1078.
[151] M. Halmann, *Nature* **1978**, *275*, 115.
[152] T. Inoue, A. Fujishima, S. Konishi, K. Honda, *Nature* **1979**, *277*, 637
[153] J.-S. Hwang, J.-S. Chang, S.-E. Park, K. Ikeue, M. Anpo, *Top. Catal.* **2005**, *35*, 311.
[154] H.-C. Yang, H.-Y. Lin, Y.-S. Chien, J. C.-S. Wu, H.-H. Wu, *Catal. Lett.* **2009**, *131*, 381.
[155] Y. Li, W.-N. Wang, Z. Zhan, M.-H. Woo, C.-Y. Wu, P. Biswas, *Appl. Catal. B* **2010**, *100*, 386.
[156] M. Anpo, H. Yamashita, Y. Ichihashi, Y. Fujii, M. Honda, *J. Phys. Chem. B* **1997**, *101*, 2632.
[157] K. Ikeue, H. Yamashita, M. Anpo, *J. Phys. Chem. B* **2001**, *105*, 8350.
[158] N. Ulagappan, H. Frei, *J. Phys. Chem. A* **2000**, *104*, 7834.
[159] W. Lin, H. Frei, *J. Am. Chem. Soc.* **2005**, *127*, 1610.
[160] M. Anpo, H. Yamashita, K. Ikeue, Y. Fujii, S. G. Zhang, Y. Ichihashi, D. R. Park, Y. Suzuki, K. Koyano, T. Tatsumi, *Catal. Today* **1998**, *44*, 327.
[161] R. Obert, B. C. Dave, *J. Am. Chem. Soc.* **1999**, *121*, 12192.
[162] K. Ikeue, S. Nozaki, M. Ogawa, M. Anpo, *Catal. Today* **2002**, *74*, 241.
[163] K. Ikeue, S. Nozaki, M. Ogawa, M. Anpo, *Catal. Lett.* **2002**, *80*, 111.
[164] Y. Li, W. N. Wang, Z. Zhan, M. H. Woo, C. Y. Wu, P. Biswas, *Appl. Catal. B* **2010**, *100*, 386.
[165] P. Usubharatana, D. McMartin, A. Veawab, P. Tontiwachwuthikul, *Ind. Eng. Chem. Res.* **2006**, *45*, 2558.
[166] S. C. Roy, O. K. Varghese, M. Paulose, C. A. Grimes, *ACS Nano* **2010**, *4*, 1259.
[167] H. Takeda, O. Ishitani, *Coord. Chem. Rev.* **2010**, *254*, 346.
[168] H. Fujiwara, H. Hosokawa, K. Murakoshi, Y. Wada, S. Yanagida, *Langmuir* **1998**, *14*, 5154.
[169] Y. Kohno, T. Tanaka, T. Funabiki, S. Yoshida, *Chem. Lett.* **1997**, *993*, 285
[170] Y. Kohno, T. Tanaka, T. Funabiki, S. Yoshida, *Phys. Chem. Chem. Phys.* **2000**, *2*, 2635.
[171] Y. Kohno, T. Tanaka, T. Funabiki, S. Yoshida, *Phys. Chem. Chem. Phys.* **2000**, *2*, 5302.
[172] Y. Kohno, H. Ishikawa, T. Tanaka, T. Funabiki, S. Yoshida, *Phys. Chem. Chem. Phys.* **2001**, *3*, 1108.
[173] P. -W. Pan, Y. -W. Chen, *Catal. Commun.* **2007**, *8*, 1546.
[174] A. H. Yahaya, M. A. Gondal, A. Hameed, *Chem. Phys. Lett.* **2004**, *400*, 206.
[175] S. M. Haile, *Acta Mater.* **2003**, *51*, 5981.
[176] N. P. Brandon, D. J. Brett, *Phil. Trans. R. Soc. A* **2006**, *364*, 147.
[177] N. Q. Minh, *J. Am. Ceram. Soc.* **1993**, *78*, 563.
[178] L. Carrette, K. A. Friedrich, U. Stimming, *ChemPhysChem* **2000**, *1*, 162.
[179] P. Costamagna, S. Sri nivasan, *J. Power Sources* **2001**, *102*, 242.
[180] P. Costamagna, S. Srinivasan, *J. Power Sources* **2001**,*102*, 253.
[181] R. M. Ormerod, *Chem. Soc. Rev.* **2003**, *32*, 17.
[182] S. C. Singhal, *Solid State Ionics* **2002**, *405*, 152.
[183] H. S. Chu, C. Yeh, F. Chen, *J. Power Sources* **2003**, *123*, 1.
[184] J.-S. Yu, S. K. Kang, S. B. Yoon, G. S. Chai, *J. Am. Chem. Soc.* **2002**, *124*, 9382.
[185] G. S. Chai, S. B. Yoon, J.-S. Yu, J.-H. Choi, Y.-E. Sung, *J. Phys. Chem. B* **2004**, *108*, 7074.
[186] J. H. Bang, K. Han, S. E. Skrabalak, H. Kim, K. S. Suslick, *J. Phys. Chem. C* **2007**, *111*, 10959.
[187] S Zhang, L. Chen, S. Zhou, D. Zhao, L. Wu, *Chem. Mater.* **2010**, *22*, 3433.
[188] M. Mamak, N. Coombs, G. A. Ozin, *Adv. Mater.* **2000**, *12*, 198.
[189] M. Mamak, N. Coombs, G. A. Ozin, *J. Am. Chem. Soc.* **2000**, *122*, 8932.
[190] M. Mamak, N. Coombs, G. A. Ozin, *Adv. Funct. Mater.* **2001**, *11*, 59.
[191] S. Somacescu, J. M. Calderon Moreno, P. Osiceanu, B. L. Su, V. Parvulescu, *J. Phys. Chem. C* **2010**, *114*, 19365.
[192] G. Wang, E. Johannessen, C. R. Kleijn, S. W. de Leeuw, M.-O. Coppens, *Chem. Eng. Sci.* **2007**, *62*, 5110.
[193] G. Wang, M. -O. Coppens, *Ind. Eng. Chem. Res.* **2008**, *47*, 3847.
[194] G. Wang, M. -O. Coppens, *Chem. Eng. Sci.* **2010**, *65*, 2344.
[195] B. A. Haberman, J. B. Young, *Inter. J. Heat Mass Transfer* **2004**, *47*, 3617.
[196] H. S. Zhou, S. M. Zhu, M. Hibino, I. Honma, M. Ichihara, *Adv. Mater.* **2003**, *15*, 2107.
[197] K. T. Lee, J. C. Lytle, N. S. Ergang, S. M. Oh, A. Stein, *Adv. Funct. Mater.* **2005**, *15*, 547.
[198] Z. Y. Wang, F. Li, N. S. Ergang, A. Stein, *Chem. Mater.* **2006**, *18*, 5543.
[199] Y. S. Hu, P. Adelhelm, B. M. Smarsly, S. Hore, M. Antonietti, J. Maier, *Adv. Funct. Mater.* **2007**, *17*, 1873.
[200] L. Wei, Q. Chen, X. Kong, *J. Am. Ceram. Soc.* **2011**, *94*, 3078.
[201] G.-P. Hao, W.-C. Li, S. Wang, G.-H. Wang, L. Qi, A.-H. Lu, *Carbon* **2011**, *49*, 3762.
[202] F. Su, X. S. Zhao, Y. Wang, J. Zeng, Z. Zhou, J. Y. Lee, *J. Phys. Chem. B* **2005**, *109*, 20206.
[203] H. Yamada, K. Tagawa, M. Komatsu, I. Moriguchi, T. Kudo, *J. Phys. Chem. C* **2007**, *111*, 8397.

[204] S. Jin, H. Deng, D. Long, X. Liu, L. Zhan, X. Liang, W. Qiao, L. Ling, *J. Power Sources* **2011**, *196*, 3887.
[205] B. Jin, J. U. Kim, H. B. Gu, *J. Power Sources* **2003**, *117*, 148.
[206] E. Peled, A. Gorenshtein, M. Segal, Y. Sternberg, *J. Power Sources* **1989**, *26*, 269.
[207] S. E. Cheon, K. S. Ko, J. H. Cho, S. W. Kim, E. Y. Chin, H. T. Kim, *J. Electrochem. Soc.* **2003**, *150*, A796.
[208] H. S. Ryu, H. J. Ahn, K. W. Kim, J. H. Ahn, J. Y. Lee, *J. Power Sources* **2006**, *153*, 360.
[209] Y. J. Jung, S. Kim, *Electrochem. Commun.* **2007**, *9*, 249.
[210] J. Wang, S. Y. Chew, Z. W. Zhao, S. Ashraf, D. Wexler, J. Chen, S. H. Ng, S. L. Chou, H. K. Liu, *Carbon* **2008**, *46*, 229.
[211] J. L. Wang, J. Yang, J. Y. Xie, N. X. Xu, Y. Li, *Electrochem. Commun.* **2002**, *4*, 499.
[212] J. L. Wang, L. Liu, Z. J. Ling, J. Yang, C. R. Wan, C. Y. Jiang, *Electrochim. Acta* **2003**, *48*, 1861.
[213] W. Zheng, Y. W. Liu, X. G. Hu, C. F. Zhang, *Electrochim. Acta* **2006**, *51*, 1330.
[214] X. L. Ji, K. T. Lee, L. F. Nazar, *Nat. Mater.* **2009**, *8*, 500.
[215] C. Liang, N. J. Dudney, J. Y. Howe, *Chem. Mater.* **2009**, *21*, 4724.
[216] C. Lai, X. P. Gao, B. Zhang, T. Y. Yan, Z. Zhou, *J. Phys. Chem. C* **2009**, *113*, 4712.
[217] S. R. Chen, Y. P. Zhai, G. L. Xu, Y. X. Jiang, D. Y. Zhao, J. T. Li, L. Huang, S. G. Sun, *Electrochim. Acta* **2011**, *56*, 9549.
[218] A. K. Padhi, K. S. Nanjundaswamy, J. B. Goodenough, *J. Electrochem. Soc.* **1997**, *144*, 1188.
[219] A. K. Padhi, K. S. Nanjundaswamy, C. Masquelier, S. Okada, J. B. Goodenough, *J. Electrochem. Soc.* **1997**, *144*, 1609.
[220] J. B. Goodenough, *J. Power Sources* **2007**, *174*, 996.
[221] P. S. Herle, B. Ellis, N. Coombs, L. F. Nazar, *Nat. Mater.* **2004**, *3*, 147.
[222] N. J. Yun, H. W. Ha, K. H. Jeong, H. Y. Park, K. Kim, *J. Power Sources* **2001**, *97–98*, 508.
[223] Y. Xia, M. Yoshio, H. Noguchi, *Electrochim. Acta* **2006**, *52*, 240.
[224] C. M. Dohetry, R. A. Caruso, B. M. Smarsly, C. J. Drummond, *Chem. Mater.* **2009**, *21*, 2895.
[225] C. M. Dohetry, R. A. Caruso, B. M. Smarsly, P. Adellhelm, C. J. Drummond, *Chem. Mater.* **2009**, *21*, 5300.
[226] C. M. Doherty, R. A. Caruso, C. J. Drummond, *Energy Environ. Sci.* **2010**, *3*, 813.
[227] G. Wang, H. Liu, J. Liu, S. Qiao, G. M. Lu, P. Munro, H. Ahn, *Adv. Mater.* **2010**, *22*, 4944.
[228] A. Vu, A. Stein, *Chem. Mater.* **2011**, *23*, 3237.
[229] N. N. Sinha, C. Shivakumara, N. Munichandraiah, *ACS Appl. Mater. Interface* **2010**, *2*, 2031.
[230] J. Liu, T. E. Conry, X. Song, M. M. Doeff, T. J. Richardson, *Energy Environ. Sci.* **2011**, *4*, 885.
[231] M. J. Zou, M. Yoshio, S. Gopukumar, J. I. Yamaki, *Chem. Mater.* **2003**, *15*, 4699.
[232] F. Jiao, J. L. Bao, A. H. Hill, P. G. Bruce, *Angew. Chem. Int. Ed.* **2008**, *47*, 9711.
[233] J. Y. Luo, Y. G. Wang, H. M. Xiong, Y. Y. Xia, *Chem. Mater.* **2007**, *19*, 4791.
[234] D. Tonti, M. J. Torralvo, E. Enciso, I. Sobrados, J. Sanz, *Chem. Mater.* **2008**, *20*, 4783.
[235] T. Sri Devi Kumari, T. Prem Kumar, *Ionics* **2010**, *16*, 61.
[236] N. S. Ergang, J. C. Lytle, H. W. Yan, A. Stein, *J. Electrochem. Soc.* **2005**, *152*, A1989.
[237] F. Jiao, K. M. Shaju, P. G. Bruce, *Angew. Chem. Int. Ed.* **2005**, *44*, 6550.
[238] H. W. Yan, S. Sokolov, J. C. Lytle, A. Stein, F. Zhang, W. H. Smyrl, *J. Electrochem. Soc.* **2003**, *150*, A1102.
[239] T. Ohzuku, A. Ueda, N. Yamamota, *J. Electrochem. Soc.* **1995**, *142*, 1431.
[240] K. M. Colbow, J. R. Dahn, R. R. Haering, *J. Power Sources* **1989**, *26*, 397.
[241] S. Y. Yin, L. Song, X. Y. Wang, M. F. Zhang, K. L. Zhang, Y. X. Zhang, *Electrochim. Acta* **2009**, *54*, 5629.
[242] L. Cheng, H. J. Liu, J. J. Zhang, H. M. Xiong, Y. Y. Xia, *J. Electrochem. Soc.* **2006**, *153*, A1472.
[243] J. Kim, J. Cho, *Electrochem. Solid-State Lett.* **2007**, *10*, A81.
[244] S. C. Lee, S. M. Lee, J. W. Lee, J. B. Lee, S. M. Lee, S. S. Han, H. C. Lee, H. J. Kim, *J. Phys. Chem. C* **2009**, *113*, 18420.
[245] D. Peramunage, K. M. Abraham, *J. Electrochem. Soc.* **1998**, *145*, 2609.
[246] E. M. Sorensen, S. J. Barry, H. Jung, J. R. Rondinelli, J. T. Vaughey, K. R. Poeppelmeier, *Chem. Mater.* **2006**, *18*, 482.
[247] L. Shen, C. Yuan, H. Luo, X. Zhang, K. Xua, Y. Xia, *J. Mater. Chem.* **2010**, *20*, 6998.
[248] A. Zhang, Z. M. Zheng, F. Y. Cheng, Z. L. Tao, J. Chen, *Sci. China Chem.* **2011**, *54*, 936.
[249] F. Jiao, P. G. Bruce, *Adv. Mater.* **2007**, *19*, 657.
[250] J. Y. Baek, H.-W. Ha, I.-Y. Kim, S.-J. Hwang, *J. Phys. Chem. C* **2009**, *113*, 17392.
[251] T. X. T. Sayle, R. R. Maphanga, P. E. Ngoepe, D. C. Sayle, *J. Am. Chem. Soc.* **2009**, *131*, 6161.
[252] D. W. Liu, B. B. Garcia, Q. F. Zhang, Q. Guo, Y. H. Zhang, S. Sepehri, G. Z. Cao, *Adv. Funct. Mater.* **2009**, *19*, 1015.
[253] Y. Yu, C. H. Chen, Y. Shi, *Adv. Mater.* **2007**, *19*, 993.
[254] J. C. Lytle, H. W. Yan, N. S. Ergang, W. H. Smyrl, A. Stein, *J. Mater. Chem.* **2004**, *14*, 1616.
[255] Z. H. Wen, Q. Wang, Q. Zhang, J. H. Li, *Adv. Funct. Mater.* **2007**, *17*, 2772.
[256] Q. Wang, Z. Wen, J. Li, *J. Power Sources* **2008**, *182*, 334.
[257] P. Liu, S. H. Lee, C. E. Tracy, Y. Yan, J. A. Turner, *Adv. Mater.* **2002**, *14*, 27.
[258] J. S. Sakamoto, B. Dunn, *J. Mater. Chem.* **2002**, *12*, 2859.
[259] S. Wang, S. Li, Y. Sun, X. Feng, C. Chen, *Energy Environ. Sci.* **2011**, *4*, 2854.
[260] X. H. Xia, J. P. Tu, J. Y. Xiang, X. H. Huang, X. L. Wang, X. B. Zhao, *J. Power Sources* **2010**, *195*, 2014.
[261] X. H. Huang, J. P. Tu, Z. Y. Zeng, J. Y. Xiang, X. B. Zhao, *J. Electrochem. Soc.* **2008**, *155*, A438.
[262] X. H. Huang, J. P. Tu, X. H. Xia, X. L. Wang, J. Y. Xiang, L. Zhang, Y. Zhou, *J. Power Sources* **2009**, *188*, 588.
[263] X. H. Huang, J. P. Tu, X. H. Xia, X. L. Wang, J. Y. Xiang, L. Zhang, *J. Power Sources* **2010**, *195*, 1207.
[264] Y. F. Yuan, X. H. Xia, J. B. Wu, J. L. Yang, Y. B. Chen, S. Y. Guo, *Electrochem. Commun.* **2010**, *12*, 890.
[265] J. Yi, D. Lu, X. Li, S. Hu, W. Li, J. Lei, Y. Wang, *J. Solid State Electrochem.* **2011**, 1351.
[266] H.-G. Jung, S. W. Oh, J. Ce, N. Jayaprakash, Y.-K. Sun, *Electrochem. Commun.* **2009**, *11*, 756.
[267] I. Moriguchi, Y. Shono, H. Yamada, T. Kudo, *J. Phys. Chem. B* **2008**, *112*, 14560.
[268] Y.-G. Guo, Y.-S. Hu, J. Maier, *Chem. Commun.* **2006**, 2783.
[269] D. W. Liu, G. Z. Cao, *Energy Environ. Sci.* **2010**, *3*, 1218.
[270] C. Liu, F. Li, L. P. Ma, H. M. Cheng, *Adv. Mater.* **2010**, *22*, E28.
[271] H. V. Helmholtz, *Ann. Phys.* **1853**, *89*, 211.
[272] A. K. Shukla, S. Sampath, K. Vijayamohanan, *Curr. Sci.* **2000**, *79*, 1656.
[273] R. Kötz, M. Carlen, *Electrochim. Acta* **2000**, *45*, 2483.
[274] A. G. Pandolfo, A. F. Hollenkamp, *J. Power Sources* **2006**, *157*, 11.
[275] P. Simon, Y.Gogotsi, *Nat. Mater.* **2008**, *7*, 845.
[276] V. V. N. Obreja, *Physica E* **2008**, *40*, 2596.
[277] L. C. Liu, Z. N. Yu, D. Neff, A. Zhamu, B. Z. Jang, *Nano Lett.* **2010**, *10*, 4863.
[278] A. C. Dillon, *Chem. Rev.* **2010**, *110*, 6856.
[279] G. Lota, K. Fic, E. Frackowiak, *Energy Environ. Sci.* **2011**, *4*, 1592.
[280] C. Z. Yuan, B. Gao, L. F. Shen, S. D. Yang, L. Hao, X. J. Lu, F. Zhang, L. J. Zhang, X. G. Zhang, *Nanoscale* **2011**, *3*, 529.

[281] J. Chmiola, C. Largeot, P.-L. Taberna, P. Simon, Y. Gogotsi, *Angew. Chem. Int. Ed.* **2008**, *47*, 3392.
[282] C. Largeot, C. Portet, J. Chmiola, P.-L. Taberna, Y. Gogotsi, Patrice Simon, *J. Am. Chem. Soc.* **2008**, *130*, 2730.
[283] H. K. Song, Y. H. Jung, K. H. Lee, L. H. Dao, *Electrochim. Acta* **1999**, *44*, 3513.
[284] G. J. Lee, S. I. Pyun, *Langmuir* **2006**, *22*, 10659.
[285] W. C. Li, G. Reichenauerc, J. Frickeb, *Carbon* **2002**, *40*, 2955.
[286] H. K. Song, Y. H. Jung, K. H. Lee, L. H. Dao, *Electrochim. Acta* **1999**, *44*, 3513.
[287] T. Horikawa, J. Hayashi, K. Muroyama, *Carbon* **2004**, *42*, 1625.
[288] D. W. Wang, F. Li, M. Liu, G. Q. Lu, H. M. Cheng, *Angew. Chem. Int. Ed.* **2008**, *47*, 373.
[289] D. W. Wang, F. Li, M. Liu, G. Q. Lu, H. M. Cheng, *Angew. Chem. Int. Ed.* **2009**, *48*, 1525.
[290] K. S. Xia, Q. M. Gao, J. H. Jiang, J. Hu, *Carbon* **2008**, *46*, 1718.
[291] Z. J. Zheng, Q. M. Gao, *J. Power Sources* **2011**, *196*, 1615.
[292] H. Xu, Q. Gao, H. Guo, H. Wang, *Micropor. Mesopor. Mater.* **2010**, *133*, 106.
[293] W. Xing, C. C. Huang, S. P. Zhuoa, X. Yuana, G. Q. Wang, D. Hulicova-Jurcakovac, Z. F. Yan, G. Q. Lu, *Carbon* **2009**, *47*, 1715.
[294] D. Carriazo, F. Picó, M. C. Gutiérrez, F. Rubio, J. M. Rojo, F. del Monte, *J. Mater. Chem.* **2010**, *20*, 773.
[295] M. C. Gutierrez, F. Pico, F. Rubio, J. M. Amarilla, F. J. Palomares, M. L. Ferrer, F. del Monte, J. M. Rojo, *J. Mater. Chem.* **2009**, *19*, 1236.
[296] M. Rose, Y. Korenblit, E. Kockrick, L. Borchardt, M. Oschatz, S. Kaskel, G. Yushin, *Small* **2011**, *7*, 1108.
[297] F. Xu, R. J. Cai, Q. C. Zeng, C. Zou, D. C. Wu, F. Li, X. Lu, Y. Liang, R. Fu, *J. Mater. Chem.* **2011**, *21*, 1970.
[298] K. Zhang, B. T. Ang, L. L. Zhang, X. S. Zhao, J. Wu, *J. Mater. Chem.* **2011**, *21*, 2663.
[299] J. P. Zheng, P. J. Cygan, T. R. Jow, *J. Electrochem. Soc.* **1995**, *142*, 2699.
[300] J. P. Zheng, T. R. Jow, *J. Power Sources* **1996**, *62*, 155.
[301] V. Srinivasan, J. W. Weidner, *J. Power Sources* **2002**, *108*, 15.
[302] B. O. Park, C. D. Lokhande, H. S. Park, *J. Power Sources* **2004**, *134*, 148.
[303] J. P. Zheng, T. R. Jow, *J. Electrochem. Soc.* **1995**, *142*, L6.
[304] C. Lin, J. A. Ritter, B. N. Popov, *J. Electrochem. Soc.* **1998**, *145*, 4097.
[305] R. S. Jayashree, P. V. Kamath, *J. Mater. Chem.* **1999**, *9*, 961.
[306] L. Cao, F. Xu, Y. Y. Liang, H. L. Li, *Adv. Mater.* **2004**, *16*, 1853.
[307] C. C. Hu, T. W. Tsou, *Electrochem. Commun.* **2002**, *4*, 105.
[308] V. Gupta, T. Kusahara, H. Toyama, S. Supta, N. Miura, *Electrochem. Commun.* **2007**, *9*, 2315.
[309] W. J. Zhou, D. D. Zhao, M. W. Xu, C. L. Xu, H. L. Li, *Electrochim. Acta* **2008**, *53*, 7210.
[310] L. B. Kong, M. C. Liu, J. W. Lang, M. Liu, Y. C. Luo, L. Kang, *J. Solid State Electrochem.* **2011**, *15*, 571.
[311] T. Xue, C. L. Xu, D. D. Zhao, X. H. Li, H. L. Li, *J. Power Sources* **2007**, *164*, 953.
[312] K. R. Prasad, N. Miura, *J. Power Sources* **2004**, *135*, 354.
[313] L. Cao, L. B. Kong, Y. Y. Liang, H. L. Li, *Chem. Commun.* **2004**, *14*, 1646.
[314] C.-C. Hu, C.-Y. Hung, K.-H. Chang, Y.-L. Yang, *J. Power Sources* **2011**, *196*, 847.
[315] H. Q. Wang, G. F. Yang, Q. Y. Li, X. X. Zhong, F. P. Wang, Z. S. Li, Y. H. Li, *New J. Chem.* **2011**, *35*, 469.
[316] T. M. Benedetti, V. R. Gonçales, D. F. S. Petri, S. I. Córdoba de Torresi, R. M. Torresi, *J. Braz. Chem. Soc.* **2010**, *21*, 1704.
[317] D. D. Zhao, S. J. Bao, W. J. Zhou, H. L. Li, *Electrochem. Commun.* **2007**, *9*, 869.
[318] T. Y. Wei, C. H. Chen, H. C. Chien, S. Y. Lu, C. C. Hu, *Adv. Mater.* **2010**, *22*, 347.
[319] M.-S. Wu, Y.-A. Huang, C.-H. Yang, J.-J. Jow, *Int. J. Hydrog. Energy* **2007**, *32*, 4153.
[320] D. S. Kong, J. M. Wang, H. B. Shao, J. Q. Zhang, C. N. Cao, *J. Alloys Compd.* **2011**, *509*, 5611.
[321] Y. F. Yuan, X. H. Xia, J. B. Wu, J. L. Yang, Y. B. Chen, S. Y. Guo, *Electrochim. Acta* **2011**, *56*, 2627.
[322] J. B. Wu, Z. G. Li, Y. Lin, *Electrochim. Acta* **2011**, *56*, 2116.
[323] A. I. Inamdar, Y. S. Kim, S. M. Pawar, J. H. Kim, H. Ima, H. Kim, *J. Power Sources* **2011**, *196*, 2393.
[324] G. Hu, C. Li, H. Gong, *J. Power Sources* **2010**, *195*, 6977.
[325] X. Zhang, W. Shi, J. Zhu, W. Zhao, J. Ma, S. Mhaisalkar, T. L. Maria, Y. Yang, H. Zhang, H. H. Hng, Q. Yan, *Nano Res.* **2010**, *3*, 643.
[326] K. C. Liu, M. A. Anderson, *J. Electrochem. Soc.* **1996**, *143*, 124.
[327] K. W. Nam, K. B. Kim, *J. Electrochem. Soc.* **2002**, *149*, 346.
[328] X. H. Xia, J. P. Tu, X. L. Wang, C. D. Gu, X. B. Zhao, *J. Mater. Chem.* **2011**, *21*, 671.
[329] A. Rudge, I. Raistrick, S. Gottesfeld, J. P. Ferraris, *J. Power Sources* **1994**, *47*, 89.
[330] K. Naoi, S. Suematsu, A. Manago, *J. Electrochem. Soc.* **2000**, *147*, 420.
[331] A. Laforgue, P. Simon, J.-F. Fauvarque, *Synth. Met.* **2001**, *123*, 311.
[332] X. Yang, D. Wu, X. Chen, R. Fu, *J. Phys. Chem. C* **2010**, *114*, 8581.
[333] Y. Li, X. Zhao, Q. Xu, Q. Zhang, D. Chen, *Langmuir* **2011**, *27*, 6458.
[334] L. Z. Fan, Y. S. Hu, J. Maier, Ph. Adelhelm, B. Smarsly, M. Antonietti, *Adv. Funct. Mater.* **2007**, *17*, 3083.
[335] H. Wang, Q. Gao, J. Hu, *J. Power Sources* **2010**, *195*, 3017.
[336] F. Lufrano, P. Staiti, E. G. Calvo, E. J. Juárez-Pérez, J. A. Menéndez, A. Arenillas, *Int. J. Electrochem. Sci.* **2011**, *6*, 596.
[337] Y. Peng, Z. Chen, J. Wen, Q. Xiao, D.Weng, S. He, H. Geng, Y. Lu, *Nano Res.* **2011**, *4*, 216.
[338] J. Zhang, L. B. Kong, J. J. Cai, Y. C. Luo, L. Kang, *J. Solid State Electrochem.* **2010**, *14*, 2065.
[339] D. W. Wang, F. Li, H. M. Cheng, *J. Power Sources* **2008**, *185*, 1563.
[340] J. Zhang, L. B. Kong, J. J. Cai, H. Li, Y. C. Luo, L. Kang, *Micropor. Mesopor. Mater.* **2010**, *132*, 154.
[341] K. Naoi, P. Simon, *Electrochem. Soc. Interface* **2008**, *17*, 34.
[342] R. L. Cohen, J. H. Wernick, *Science* **1981**, *214*, 108.
[343] A. Zaluska, L. Zaluski, J. O. Stroem, *Appl. Phys.* **2001**, *A72*, 157.
[344] J. Chen, N. Kuriyama, H. Yuan, H. T. Takeshita, T. Sakai, *J. Am. Chem. Soc.* **2001**, *123*, 11813.
[345] P. Gao, M. Zhang, Z. Niu, Q. Xiao, *Chem. Commun.* **2007**, 5197.
[346] G. P. Dai, C. Liu, M. Liu, M. Z. Wang, H. M. Cheng, *Nano Lett.* **2002**, *5*, 503.
[347] K. Jurewicz, E. Frackowiak, F. Béguin, *Fuel Process. Technol.* **2002**, *415*, 77.
[348] K. Jurewicz, E. Frackowiak, F. Béguin, *Appl. Phys. A* **2004**, *78*, 981.
[349] J. B. Pang, J. E. Hampsey, Z. W. Wu, Q. Y. Hu, Y. F. Lu, *Appl. Phys. Lett.* **2004**, *85*, 4887.
[350] C. Vix-Guterl, E. Frackowiak, K. Jurewicz, M. Friebe, J. Parmentier, F. Béguin, *Carbon* **2005**, *43*, 1293.
[351] B. Fang, H. S. Zhou, I. Honma, *J. Phys. Chem. B* **2006**, *110*, 4875.
[352] N. N. ing Liu, L. W. Yin, L. Kang, X. Y. Zhao, C. X. Wang, L. Y. Zhang, D. Xiang, R. Gao, Y. X. Qi, N. Lun, *Int. J. Hydrogen Energy* **2010**, *35*, 12410.
[353] L. N. Ye, C. Z. Wu, W. Guo, Y. Xie, *Chem. Commun.* **2006**, 4738.
[354] H.-P. Liang, N. S. Lawrence, L.-J. Wan, L. Jiang, W. G. Song, T. G. J. Jones, *J. Phys. Chem. C* **2008**, *112*, 338.
[355] B. Z. Fang, M. Kim, J. H. Kim, J.-S. Yu, *Langmuir* **2008**, *24*, 12068.
[356] H. Zhang, X. Fu, Y. Chen, S. Yi, S. Li, Y. Zhu, L. Wang, *Physica B* **2004**, *352*, 66.
[357] Z. Yang, Y. Xia, X. Sun, R. Mokaya, *J. Phys. Chem. B* **2006**, *110*, 18424.
[358] Z. Yang, Y. Xia, R. Mokaya, *J. Am. Chem. Soc.* **2007**, *129*, 1673.

[359] A. F. Gross, J. J. Vajo, S. L. Van Atta, G. L. Olson, *J. Phys. Chem. C* **2008**, *112*, 5651.
[360] H. L. Wang, Q. M. Gao, J. Hu, Z. Chen, *Carbon* **2009**, *47*, 2259.
[361] H. C. Foley, *J. Microporous Mater.* **1995**, *4*, 407.
[362] M. Rzepka, P. Lamp, M. A. De la Casa-Lillo, *J. Phys. Chem. B* **1998**, *102*, 10894.
[363] M. A. De la Casa-Lillo, F. Lamari-Darkrim, D. Cazorla-Amoros, A. Linares-Solano, *J. Phys. Chem. B* **2002**, *106*, 10930.
[364] N. Texier-Mandoki, J. Dentzer, T. Piquero, S. Saadallah, P. David, C. Vix-Guterl, *Carbon* **2004**, *42*, 2744.
[365] S. Pincemina, R. Olivesa, X. Py, M. Christ, *Sol. Energy Mater. Sol. Cells* **2008**, *92*, 603.
[366] J. C. Y. Koh, R. L. Stevens, *J. Heat Transfer-Trans. ASME* **1976**, *97*, 309.
[367] R. Siegel, *Int. J. Heat Mass Tranf.* **1977**, *20*, 1087.
[368] J. Fukai, Y. Hamada, Y. Morozumi, O. Miyatake, *Int. J. Heat Mass Tranf.* **2002**, *45*, 4781.
[369] P. V. Padmanabhan, M. V. Krishna Murthy, *Int. J. Heat Mass Tranf.* **1986**, *29*, 1855.
[370] R. Velraj, R. V. Seeniraj, B. Hafner, C. Faber, K. Schwarzer, *Sol. Energy* **1997**, *60*, 281.
[371] M. Costa, D. Buddhi, A. Oliva, *Energy Conv. Manage.* **1998**, *39*, 319.
[372] R. Velraj, R. V. Seeniraj, B. Hafner, C. Faber, K. Schwarzer, *Sol. Energy* **1999**, *65*, 171.
[373] K. A. R. Ismail, C. L. F. Alves, M. S. Modesto, *Appl. Therm. Eng.* **2001**, *21*, 53.
[374] J. A. Weaver, R. Viskanta, *J. Heat Transfer-Trans. ASME* **1986**, *108*, 654.
[375] C. J. Hoogendoorn, G. C. J. Bart, *Sol. Energy* **1992**, *48*, 53.
[376] X. Tong, J. A. Khan, *Numer. Heat Tr. A* **1996**, *30*, 125.
[377] X. Py, R. Olives, S. Mauran, *Int. J. Heat Mass Tranf.* **2001**, *44*, 2727.
[378] J. P. Trelles, J. J. Dufly, *Appl. Therm. Eng.* **2003**, *23*, 1647.
[379] O. Mesalhy, K. Lafdi, A. Elgafy, K. Bowman, *Energy Conv. Manage.* **2005**, *46*, 847.
[380] S. Pincemin, R. Olives, X. Py, M. Christ, *Sol. Energy Mater. Sol. Cells* **2008**, *92*, 603.
[381] S. Pincemin, X. Py, R. Olives, M. Chris, O. Oettinger, *J. Sol. Energy Eng.* **2008**, *130*, 1.
[382] A. Siahpush, J. O'Brien, J. Crepeau, *J. Heat Transfer-Trans. ASME* **2008**, *130*, 1.
[383] I. Fernández, C. J. Renedo, S. Pérez, J. Carcedo, M. Mañana, *Int. Conf. Renewable Energies Power Quality (ICREPQ'11)*, Spain, **2010**.
[384] C. Y. Zhao, T. J. Lu, H. P. Hodson, *Int. J. Heat Mass Tranfer* **2004**, *47*, 2927.
[385] C. Y. Zhao, T. J. Lu, H. P. Hodson, *Int. J. Heat Mass Tranfer* **2005**, *48*, 2452.
[386] C. Y. Zhao, W. Lu, S. A. Tassou, *Int. J. Heat Mass Tranfer* **2006**, *49*, 2762.
[387] C. Y. Zhao, S. A. Tassou, T. J. Lu, *Int. J. Heat Mass Tranfer* **2008**, *51*, 929.
[388] C. Y. Zhao, W. Lu, S. A. Tassou, *J. Heat Transfer-Trans. ASME* **2009**, *131*, 121002.
[389] C. Y. Zhao, Z. G. Wu, *Sol. Energy Mater. Sol. Cells* **2011**, *95*, 636.
[390] Z. G. Wu, C. Y. Zhao, *Sol. Energy* **2011**, *85*, 1371.
[391] T. Nomura, N. Okinaka, T. Akiyama, *Mater. Chem. Phys.* **2009**, *115*, 846.
[392] M. D. Romero-Sánchez, J. M. Rodes, C. Guillem-López, A. M. López-Buendía, *18th CIB World Building Congress*, Salford, UK **2010**, p. 9.
[393] D. Katsourinis, M. Stamatiadou, M. Founti, M. D. Romero-Sánchez, A. López-Buendía, *18th CIB World Building Congress*, Salford, UK **2010**, p. 83.
[394] B. Zalba, J. M. Mar, L. F. Cabeza, H. Mehling, *Appl. Therm. Eng.* **2003**, *23*, 251.
[395] A. M. Khudhair, M. M. Farid, *Energy Convers. Manage.* **2004**, *45*, 263.
[396] M. M. Farid, A. M. Khudhair, S. A. K. Razack, S. Al-Hallaj, *Energy Convers. Manage.* **2004**, *45*, 1597.
[397] A. Gil, M. Medrano, I. Martorell, A. Lázaro, P. Dolado, B. Zalba, L.F. Cabeza, *Renew. Sust. Energy Rev.* **2010**, *14*, 56.
[398] D. K. Benson, R. W. Burrows, *US Patent 5.202.150*, **1993**.
[399] B. L. Su, C. Sanchez, Xiao-Yu Yang, *Hierarchically structured porous materials: from nanoscience to catalysis, biomedicine, optics and energy*, Wiley-VCH, Weinheim, Germany **2011**.
[400] a) Z. Y. Yuan, T. Z. Ren, B. L. Su, *Adv. Mater.* **2003**, *15*, 1462; b) W. Deng, M. W. Toepke, B. H. Shanks, *Adv. Funct. Mater.* **2003**, *13*, 61; c) Z. Y. Yuan, A. Vantomme, A. Leonard, B. L. Su, *Chem. Commun.* **2003**, 1558; d) A. Leonard, J. L. Blin, B. L. Su, *Chem. Commun.* **2003**, 2568; e) A. Collins, D. Carriazo, S. A. Davis, S. Mann, *Chem. Commun.* **2004**, 568; f) A. Leonard, B. L. Su, *Chem. Commun.* **2004**, 1674; g) T. Z. Ren, Z. Y. Yuan, B. L. Su, *Chem. Commun.* **2004**, 2730; h) Z. Y. Yuan, T. Z. Ren, A. Vantomme, B. L. Su, *Chem. Mater.* **2004**, *16*, 5096; i) T. Z. Ren, Z. Y. Yuan, B. L. Su, *Langmuir* **2004**, *20*, 1531; j) A. Vantomme, Z. Y. Yuan, B. L. Su, *New J. Chem.* **2004**, *28*, 1083; k) T. Z. Ren, Z. Y. Yuan, B. L. Su, *Colloids Surf. A* **2004**, *241*, 67; l) T. Z. Ren, Z. Y. Yuan, B. L. Su, *Chem. Phys. Lett.* **2004**, *388*, 46; m) W. Deng, B. H. Shanks, *Chem. Mater.* **2005**, *17*, 3092; n) B. L. Su, A. Leonard, Z. Y. Yuan, *C. R. Chimie* **2005**, *8*, 713; o) A. Leonard, B. L. Su, *Chimie Nouvelle* **2005**, *89*, 77; p) Z. Y. Yuan, T. Z. Ren, A. Azioune, J. J. Pireaux, B. L. Su, *Catal. Today* **2005**, *105*, 647; q) A. Leonard, A. Vantomme, C. Bouvy, N. Moniotte, P. Mariaulle, B. L. Su, *Nanopages* **2006**, *1*, 1; r) Z. Y. Yuan, B. L. Su, *J. Mater. Chem.* **2006**, *16*, 663; s) T. Z. Ren, Z. Y. Yuan, A. Azioune, J. J. Pireaux, B. L. Su, *Langmuir* **2006**, *22*, 3886; u) A. Vantomme, A. Leonard, Z. Y. Yuan, B. L. Su, *Colloids Surf. A* **2007**, *300*, 70; v) A. Leonard, B. L. Su, *Colloids Surf. A* **2007**, *300*, 129; w) J. L. Blin, A. Leonard, Z. Yuan, L. Gigot, A. Vantomme, A. Cheetham, B. L. Su, *Angew. Chem. Int. Ed.* **2003**, *42*, 2872.